COLD MODEL INVESTIGATIONS ON BEHAVIOUR OF SUBMERGED GAS JET IN STEEL MELT

by

SARBJIT SINGH

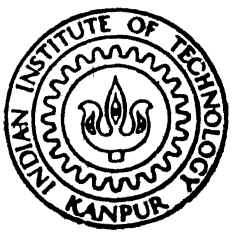

DEPARTMENT OF METALLURGICAL ENGINEERING

INDIAN INSTITUTE OF TECHNOLOGY, KANPUR

AUGUST 1988

COLD MODEL INVESTIGATIONS ON BEHAVIOUR OF SUBMERGED GAS JET IN STEEL MELT

A Thesis Submitted
In Partial Fulfilment of the Requirements
for the Degree of

MASTER OF TECHNOLOGY

by

SARBJIT SINGH

to the

DEPARTMENT OF METALLURGICAL ENGINEERING

INDIAN INSTITUTE OF TECHNOLOGY, KANPUR

AUGUST 1988

ME-1988-M-SIN-COL

CERTIFICATE

This is to certify that the present work entitled, "Cold Model Investigations on Behaviour of Submerged Gas Jets in Steel Melt" by Mr. Sarbjit Singh has been carried out under my supervision and that it has not been submitted elsewhere for a degree.

July 29, 1988.

(S.C. Koria)
Assistant Professor
Department of Metallurgical Engineering
Indian Institute of Technology
Kanpur

ACKNOWLEDGEMENTS

I express my sincere gratitude to my guide Dr. S.C. Koria for his assiduous guidance, constant encouragement and erudite suggestions throughout this endeavour. I am deeply indebted to him for his keen interest and concientious efforts.

Thanks also to Mr. U.S. Mishra for his excellent typing and Mr. V.P. Gupta for tracing and drawings.

-Sarbjit Singh
Author

CONTENTS

LIST OF TABLES

LIST OF FIGURES

NOMENCLATURE

d_o	diameter of nozzle (cm)
f	local bubble frequency
$\bar{f}$	local mean bubble frequency
$\bar{f}_{max}$	axial mean bubble frequency
$\bar{f}_{av.}$	average bubble frequency
g	acceleration due to gravity (m/sec^2)
H_o	height of the liquid bath
$\dot{Q}$	gas injection rate (NL/min.)
r	radial coordinate of plume (mm)
r_p	radius of plume (mm)
$r_{\bar{\varepsilon}\ max/2}$	half value radius of plume where $\bar{\varepsilon} = \frac{\bar{\varepsilon}\ max}{2}$
$r_{\bar{f}_{max/2}}$	half value radius of plume where $\bar{f} = \frac{\bar{f}_{max}}{2}$
$r_{p,\bar{\varepsilon}}$	plume radius based upon gas hold-up measurement
$r_{p\bar{f}}$	plume radius based upon bubble frequency measurement
u_g	velocity of gas in the plume (m/sec)
U_g	superficial velocity of gas in the plume (m/sec)
u_B	velocity of a single bubble in liquid bath cm/sec)
u_l	velocity of liquid in the plume (m/sec)
$\dot{V}_l$	circulating flow rate of liquid (m^3/sec)
Z	axial distance from nozzle

ρ_g	density of gas
ρ_l	density of liquid
ε	local gas hold-up
$\bar{\varepsilon}$	local mean gas hold-up
$\bar{\varepsilon}_{av.}$	average gas hold-up
$\bar{\varepsilon}_{max}$	axial gas hold-up.

ABSTRACT

In the present investigation, the behaviour of gas jet in liquid is studied by injecting air into water. Air is injected through the nozzle located at the centre of the base of the vessel. A self designed and developed electroresistivity probe is used to measure the properties of the bubble plume, such as gas hold-up, bubble frequency and plume radius. The signals obtained with the help of electroresistivity probe, are recorded on the storage oscilloscope screen. Because of the highly rotating and oscillating nature of the bubble plume, measurements of properties at any point in the liquid bath are made over a long time.

The above study has been organized in the following chapters:

Chapter 1 describes the general features of the submerged gas injection technique and the importance of gas hold-up and bubble plume radius. Literature review has been made about the information on gas hold-up and plume radius. Chapter 2, is about the design of experiment. The values of experimental variable i.e. bath height and gas injection rate have been calculated to simulate the model with steel melts.

Experimental program in Chapter 3 describes about the experimental set-up, measuring device and typical signals obtained on oscilloscope, experimental procedure has also been

given in this chapter. In Chapter 4, experimental results have been given and method of evaluation of parameters, i.e. local gas hold-up, local bubble frequency, local mean gas hold-up profiles, local mean bubble frequency profiles has been described.

Discussion of results has been done in Chapter 5. Gas hold-up and bubble frequency profiles have been correlated and compared with Gaussian profile and profiles proposed by other investigators.

Dimensionless correlations for axial gas hold-up and half value radius have been found out and compared with the correlation proposed by other investigators.

In Chapter 6, the conclusion of present investigation and suggestions for further work are enlisted.

CHAPTER 1

INTRODUCTION

1.1 General Features

The submerged injection of gas into molten bath has been practiced in both, the ferrous and nonferrous industries. In ferrous industry this practice is widely used for the pretreatment of hot metal, conversion of pig ironinto steel (combined blowing process) and treatment of liquid steel contained in ladles. In the nonferrous industry, typical examples of the processes employing submerged gas injection technique are copper converting of mattes and slag processing for the extraction of nonferrous metals[1].

The popularity of submerged gas injection technique for refining of molten metal is easy to understand. The jets are turbulent and provide efficient mixing of both the gas and liquid phases. Moreover, because the gas enters the liquid at a high flow rate and breaks up into a swarm of bubbles, the area of contact between the gas and the liquid is large. Both effects combine to produce a highly efficient reaction system, with respect to optimum utilization of agitation energy and turnover of refined molten metal at relatively low gas injection rates.

1.2 Theoretical Background

The success of submerged gas injection technique among other factors depends largely upon the behaviour of gas jet into liquid. Gas jet is main carrier of agitation energy into the bath for inert gas injection and also carrier of oxidation potential for refining purpose for reactive gas injection.

When a gas is made to flow through a submerged nozzle, the behaviour depends on gas flow rate. At low flow rates and discharge velocities (less than sonic value) bubbles are formed whereas at high gas flow rates and discharge velocities (greater than sonic value) a more or less continuous jet is formed[1-3]. It is well accepted that gas injection rates corresponding to bubbling mode are sufficient to generate the required mixing conditions in the bath[1-4]. The mixing conditions of the bath depends upon the properties of the plume such as gas hold-up and its radius generated by gas injection.

A gas stirred melt can be considered to consist of two regions, a single phase zone of recirculating liquid and a two phase zone of gas dispersed in liquid as shown in Fig. (1)[2]. This two phase zone of gas and liquid is called bubble plume zone[2] and its properties govern the recirculating rates of liquid in the single phase zone.

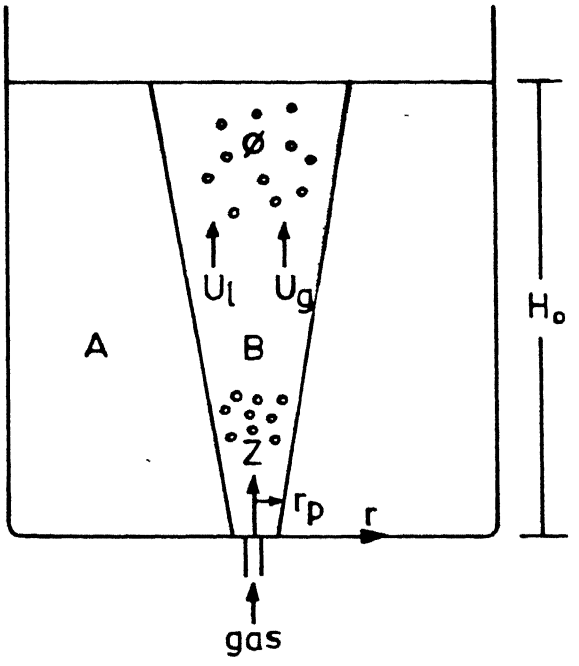

Gas stirred bath

A : Single phase zone of recirculating liquid

B : Two phase zone

Figure 1 : Gas Stirred Bath

The most important parameters characterizing the bubble plume are gas hold-up and plume radius. Both these parameters influence the liquid velocity and liquid circulating flow rate in the bath induced by gas injection. This can be shown by the following macroscopic mass balance.

The macroscopic mass balance for the gas phase is given by the following equation:[3]

$$r_p^2 \, \varepsilon_{av} \cdot \rho_g \, u_g = \rho_g \cdot V_g \qquad (1.1)$$

All the symbols and their meanings are given in nomenclature.

The volumetric flow rate, $\dot{V}_l$ of the liquid in the bubble plume is given by the following relation[3]:

$$\dot{V}_l = r_p^2 \, (1 - \varepsilon_{av}) \, u_l \qquad (1.2)$$

The liquid velocity, u_l in the eq. (1.2) is related with u_g and ε_{av} as follows[5]:

$$u_g - u_l = \frac{U_g}{\varepsilon_{av}} - u_l = \frac{u_B}{1 - \varepsilon_{av}} \qquad (1.3)$$

From the above presentation we note that gas hold up and plume radius are the two important parameters governing the liquid velocity and circulating flow rate of liquid induced by submerged gas injection. So the literature

review is restricted to the information available on gas hold-up and plume radius.

1.3 Literature Review

The distribution of gas and liquid in bubble plume zone has been measured by some investigators[6-8] using electro-resistivity probes. In these measurements gas hold-up and bubble frequency were measured. From the measured values of the above parameters the information on plume radius was derived.

Tacke et.al.[7] made measurements on gas bubble jets by injecting air, helium into water and nitrogen into mercury. Gas concentration in the bubble plume was measured by electroresistivity probe. They concluded from the measurements that radi l profiles of gas hold-up and bubble frequency are close to that represented by Gaussian function,[7]

$$\frac{\bar{\varepsilon}}{\bar{\varepsilon}_{max}} = \exp\left[-0.7\left(\frac{r}{r_{\bar{\varepsilon}_{max/2}}}\right)^2\right] \qquad (1.3)$$

and

$$\frac{\bar{f}}{\bar{f}_{max}} = \exp\left[-0.7\left(\frac{r}{r_{\bar{f}_{max/2}}}\right)^2\right] \qquad (1.4)$$

Tacke et.al. have also proposed dimensionless empirical correlations to calculate gas hold-up and plume radius. Accordin to them:

$$\bar{\varepsilon}_{max} = 50\left[\ 0.20(Z/d_o)\left(\frac{g\, d_o^5\, \rho_l}{Q^2 \cdot \rho_g}\right)^{0.3}\right]^{-\gamma} \qquad (1.5)$$

$$r_{\bar{\varepsilon}\ max/2} \cdot \left(\frac{g}{\dot{Q}^2}\right)^{1/5} = 0.42\left[\ 0.20(Z/d_o)\left(\frac{g\, d_c^{\varepsilon}\, \rho_l}{\dot{Q}^2 \cdot \rho_g}\right)^{0.30}\right]^{\beta}$$

(1.6)

The equation (1.5) is valid for the range $Z \geq Z_o$[7]. Here Z_o is the distance from the nozzle at which $\bar{\varepsilon}_{max}$ = 50 pct.[7] The value of exponent in this equation is 1.22 for air/water and 0.866 for nitrogen/mercury and helium/water systems.

Equation (1.6) gives the dimensionless empirical correlation for half plume radius. The value of exponent in this equation is 0.78 for the air/water and 0.56 for nitrogen/mercury and helium/water systems.

Castillejos et.al.[8] have also studied the development of air/water bubble plumes during upward injection into a ladle-shaped vessel. They measured distribution of gas fraction and bubble frequency by using a double-contact electroresistivity sensor. The gas injection rates involved were lower than those used by Tacke et.al. They derived from the measurement that the gas hold-up profiles were narrower than those represented by a Gaussian function (1.3). According to them, the radial gas hold-up distribution approximates the following function:

$$\frac{\bar{\varepsilon}}{\bar{\varepsilon}_{max}} = \exp\left[-0.7\left(\frac{r}{r_{\bar{\varepsilon}\,max/2}}\right)^{2.4}\right] \qquad (1.7)$$

Here we note, that the difference between the Gaussian function and the function proposed by Castillejos et.al. lies in the power of dimensionless radial term. Physically it would mean that the gas hold-up with respect to radial distance will decrease for a Gaussian profile slower than that for the function(1.7) at all axial distances downstream the nozzle.

Castillejos et.al. obtained the following expressions for the variation of the axial gas hold-up and half value radius with modified Froude number and vertical position

$$\bar{\varepsilon}_{max} = 293.77\left[\left(\frac{g\, d_o^5\,(\rho_l - \rho_g)}{\dot{Q}^2\,\rho_g}\right)^{0.269}\left(\frac{Z}{d_o}\right)^{0.993}\right]^{-1}$$

$$N \geq 4 \qquad (1.8)$$

$$r_{\bar{\varepsilon}\,max/2}\left(\frac{g}{\dot{Q}^2}\right)^{1/5} = 0.243\left[\left(\frac{g\, d_o^5\,(\rho_l - \rho_g)}{\dot{Q}^2\,\rho_g}\right)^{0.184}\left(\frac{Z}{d_o}\right)^{0.48}\right] \qquad (1.9)$$

and for the region of plume where $\bar{\varepsilon}_{max} > 70$ pct. the following expression holds for the variation of the axial gas hold-up.

$$\bar{\varepsilon}_{max} = 100\left[\left(\frac{g\, d_o^5(\rho_l - \rho_g)}{\dot{Q}^2\, g}\right)^{0.269}\left(\frac{Z}{d_o}\right)^{0.993}\right]^{-0.22}$$

$$N < 4 \qquad (1.10)$$

Ebneth et.al.[9] made measurements on local velocities in the water bath induced by bottom gas injection. They made use of the propeller type flow meter to measure local velocities. From the velocity profiles, they derived the following empirical equations for gas hold-up and plume radius:

$$\bar{\varepsilon}_{max}\ \lambda^2 = 0.58 \cdot Q^{0.50} \cdot Z^{-1.25} \qquad (1.11)$$

$$r_{1/2} = 0.38\ Q^{0.15} \cdot Z^{0.62} \qquad (1.12)$$

The value of λ, for water model measurements is 0.67.

Ebneth et.al.[9] observed that the plume axis is not static but slowly performs inclinations and rotations. They found the maximum angle of inclination 7.8^{o} and the mean value about 3.8^{o}. According to them, the angle grows with increasing gas flow rate and plume remains in correct vertical position during the first minute of gas discharge.

It may be mentioned here that no further information could be found in the open technical literature on behaviour of gas jets in liquid in terms of gas hold-up and plume radius.

1.4 Objectives of Present Investigation

From the literature survey presented above, it seems that not much work has been reported concerning the behaviour of gas bubble plumes in liquid.

The present work is an experimental study of air-water bubble plumes formed during upward gas injection in a vertical cylindrical vessel. The bubble plume was reported to be highly rotating with reference to its axis[9]. Therefore one of the objective of the present investigation is to measure the properties of the plume over a long time. This would result in recording the influence of rotation of the plume on the gas hold-up and bubble frequency at a fixed axial and radial location of the bath. For this purpose a sensor probe was developed and used in this investigation. The sensor probe was kept stationary in the bath.

Another purpose of investigation was to find dimensionless correlation between the down stream bubble plume properties and the upstream parameters.

CHAPTER 2

DESIGN OF EXPERIMENT

In the present investigation, the behaviour of gas jets in steel melts is studied by cold model simulation as adopted by many other investigators[3,7,8].

The model consist of cylindrical perspex vessel, 146 mm in diameter and 300 mm in height. The height of the model bath is determined by the value of the aspect ratio (1.2) of the steel bath of industrial laddles. The model bath height is 0.176 m.

Gas injection rate in the model is determined by the requirement of agitation energy for the purpose of submerged gas injection treatment. According to the Nashiva et.al. the optimum agitation energy is 800 watt/ton in order to realize the full potential of submerged gas injection in terms of the improved metallurgical characteristics of the process[10],

The agitation energy produced by submerged gas injection is given by

$$\dot{\varepsilon} = 6.18 \frac{\dot{Q}\ T_1}{M_1} \ln\ (1 + \frac{H_o}{1.46 \times 10^{-5} P_2}) + (1 - \frac{T_o}{T_1}) \qquad (2.1)$$

Substituting the value of $\dot{\varepsilon} = 800$ watt/ton,

in eq. 2.1 the model gas injection rate is determined as follows:

$$\dot{\varepsilon} = \frac{6.18 \times Q.298.15}{2.946 \times 10^{-3}} \ln \left(1 + \frac{0.176}{1.46 \times 10^{-5} \times 1.0123 \times 10^{5}}\right) \quad (2.2)$$

The solution of equation (2.2) gives the value model gas injection rate as 11.37 NL/min. Following the above value the gas injection rate is varied purposely in the range 2 NL/min. to 18 NL/min. in order to study the influence of gas injection rate on the properties of the plume.

CHAPTER 3

EXPERIMENTAL PROGRAM

3.1 Experimental Setup

The experimental apparatus employed in the study of air-water system is illustrated schematically in Fig. (2). It consisted of a cylindrical vessel made up of persplex glass. The dimensions of the vessel were 14.6 cms. in diameter and 30 cms. in height.

The nozzles used were of straight-bore type and were located at the center of the base of the vessel. The upper surface of the nozzle was kept in level with the vessel bottom. The lower end of the nozzle was connected to a gas supply. The gas flow rate was monitored using capiliary flow meter. To measure the gas hold-up, bubble frequency and plume radius, an electrical circuit consisting of electroresistivity probe and storage oscilloscope was employed. On top of the vessel, a holder and a graduated traversing system were mounted to rigidly hold the electroresistivity probe and allow accurate placement of the probe tip at any point in the bath.

3.2 Measuring Device

3.2.1 Electroresistivity Probe

The probe used in the study is shown in Fig. (3). A silver wire was used in this probe. This is because

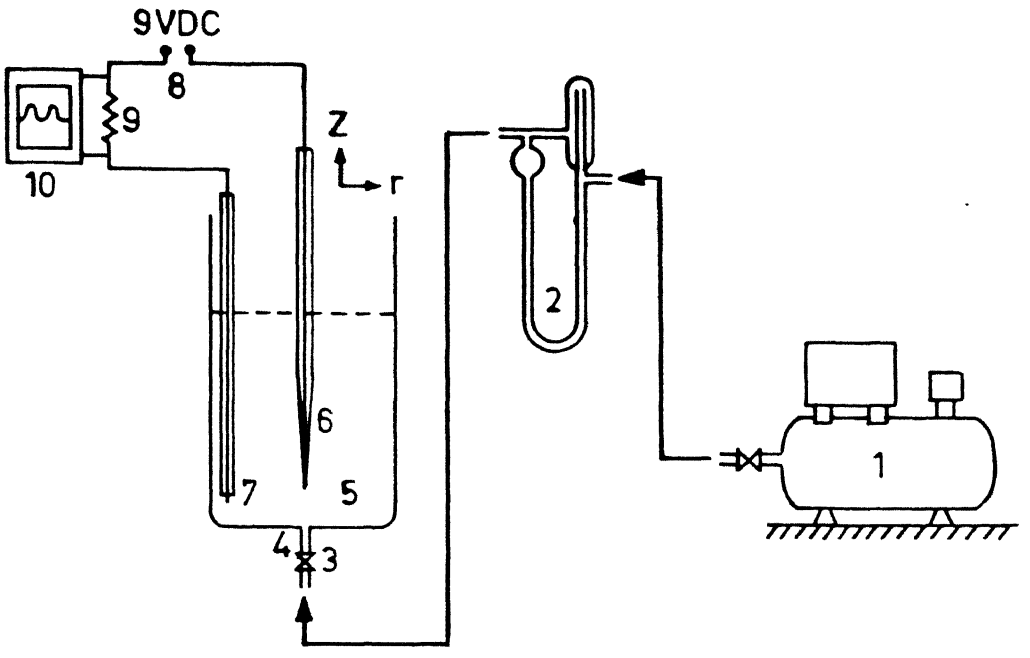

1. Air reservoir 2. Capillary flow meter 3. Valve
4 Nozzle 5. Water reservoir 6. Electroresistivity probe
7. Return electrode 8. 9VDC supply 9. Resistance
10. Storage oscilloscope.

Figure 2. Experimental Setup

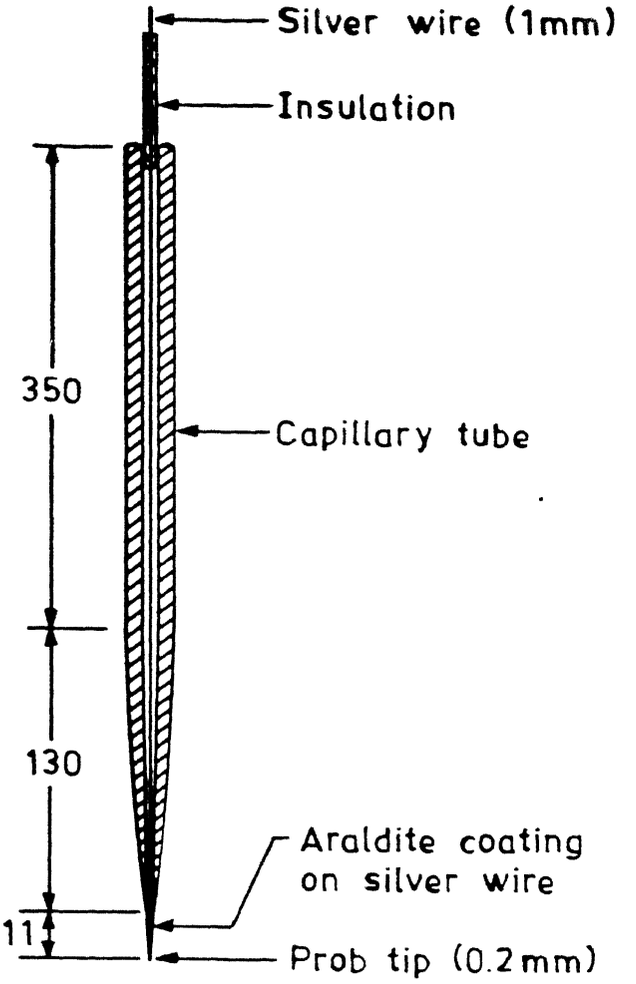

Dimensions in mm

Figure 3. Electroresistivity Probe

of the high electrical conductivity of the material. The diameter of the wire was 1 mm. One end of this wire was ground to 0.2 mm. diameter. This silver wire was introduced into a capillary tube. The 0.2 mm. diameter side of the wire was kept outside the capillary tube and was coated with araldite so as to make it insulator The tip of the wire was latter rubbed with emery paper to make it conducting.

3.2.2 Electrical Circuit

Electrical circuit is as shown in Fig. (2). Electrical circuit is established between the electroresistivity probe and the conducting liquid. Ordinary water already contains small amounts of sodium and calcium salts, which make it conducting and hence it forms a part of the electrical circuit. To maintain the resistivity, water from the same source was used. An insulating wire having its one end conducting was used as the counter electrode. 220V A.C. supply was converted into 9V D.C. supply by using eliminator. This supply was applied to the probe. A resistance of the order of 2 Ohm was also connected in the circuit. Storage oscilloscope was connected across this resistance.

3.2.3 Typical Signals and Their Evaluation

Typical real signals of the probe are shown in Fig. (4a) and Fig.(4b). The type of phase (liquid or gas) present at the tip of the probe is also shown. An ideal

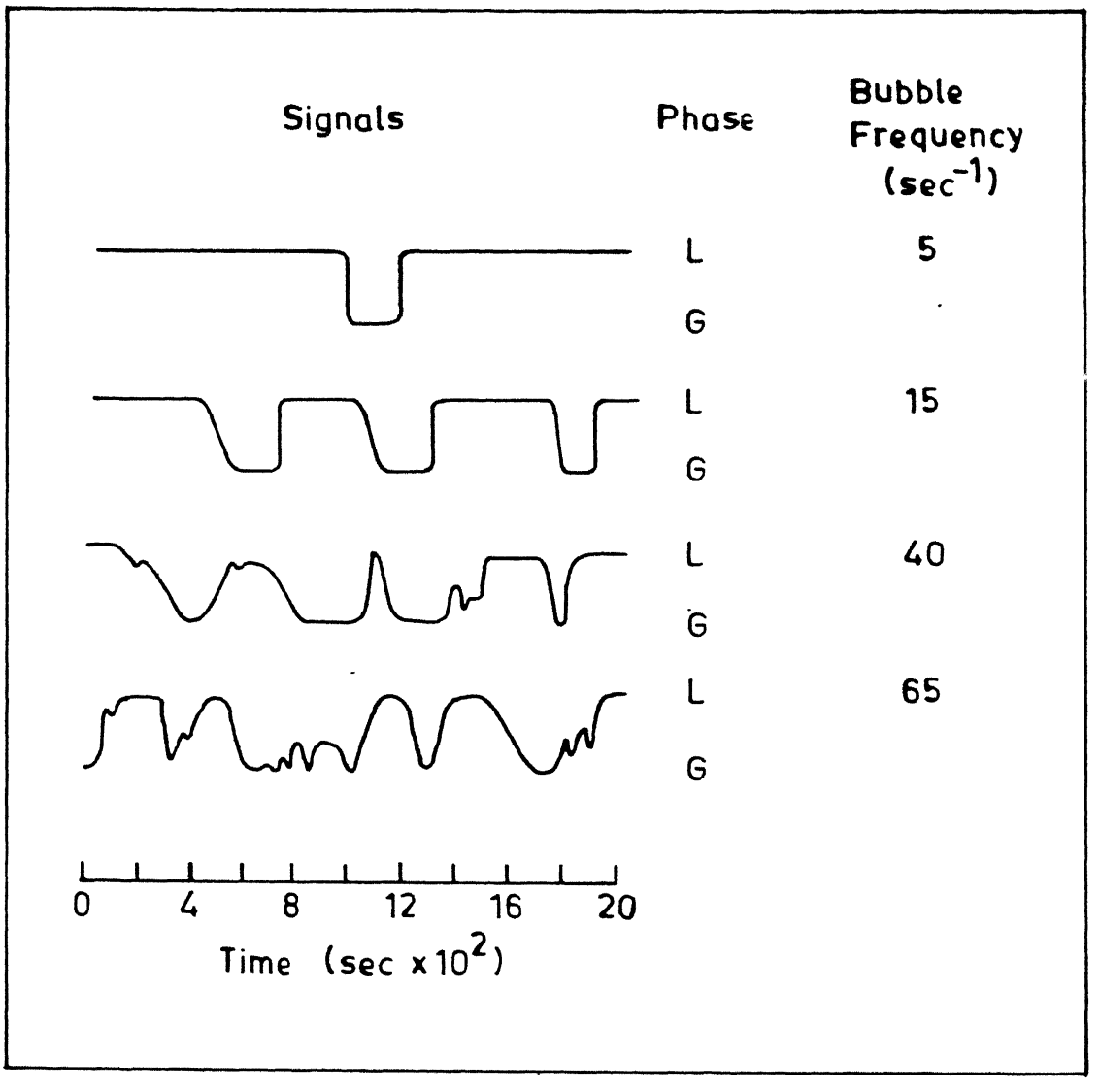

Figure 4. Typical response of the electroresistivity probe in terms of the signals obtained on the oscilloscope

(a) air/water system

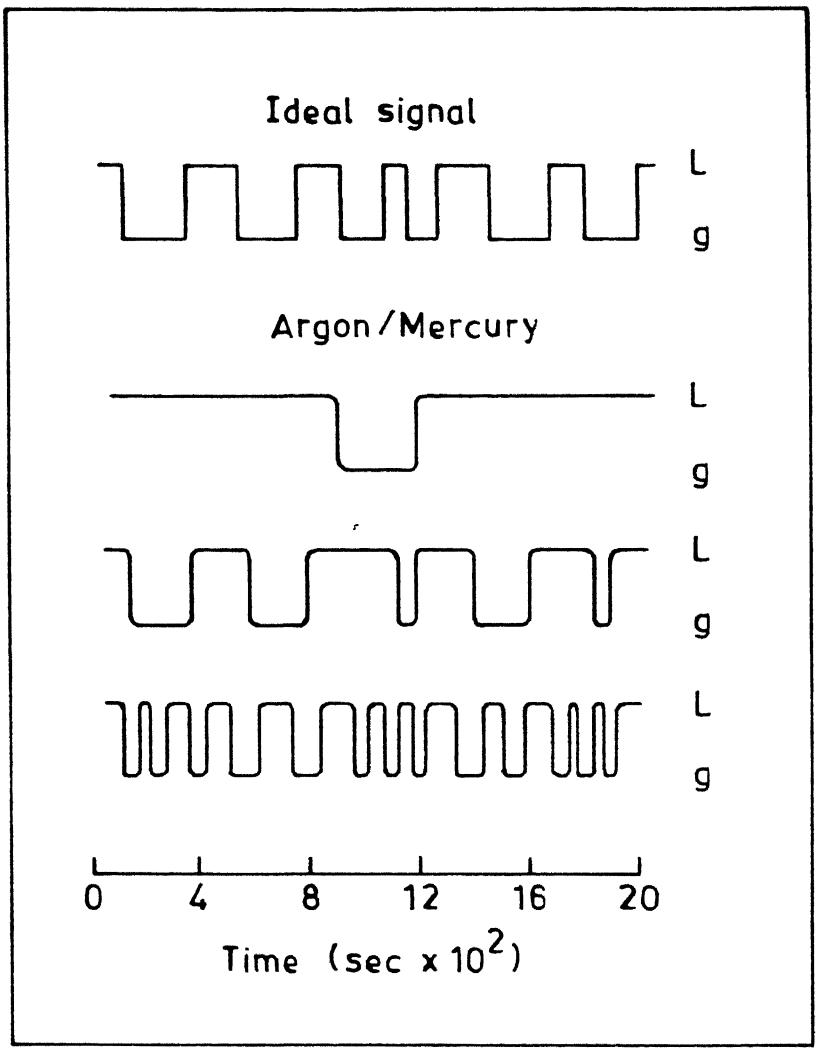

(b) Argon/mercury system

signal is represented by square wave as shown in Fig.(4b). The square wave appears due to the drop in voltage across the resistance. This is because of the breaking of the circuit, whenever gas is present at the tip of the probe.

An ideal signal is produced in the mercury due to the much shorter rise time. On the other hand signal is not ideal in water due to the higher rise time. The reason for higher rise time in water is its wetting behavior[7]. Rise time also increases when the tip of the probe is not sharp.

The first row in the Fig. (4a) shows the traces of single bubbles. As the flow rate is increased, the number of waves appearing in a particular interval of time increases. In the second row of the figure, the single bubbles can still be distinguished. When the flow rate is further increased, we observe the peaks which do not drop down to full voltage drop value or indents which do not go back to zero voltage. Such signals may be caused by bubbles just touching the probe or by pairs of bubbles following each other closely. These types of signals are shown in third row of the figure. The lowest row in Fig. (4a) shows measurements at a very high bubble frequency. However in mercury the signals are still very close to ideal as is shown in Fig. 4(b).

3.3 Calibration of Flow Meter

This is done by means of a wet-test flow meter. The results are given in Table 1. The calibration curve is shown in Fig. 5.

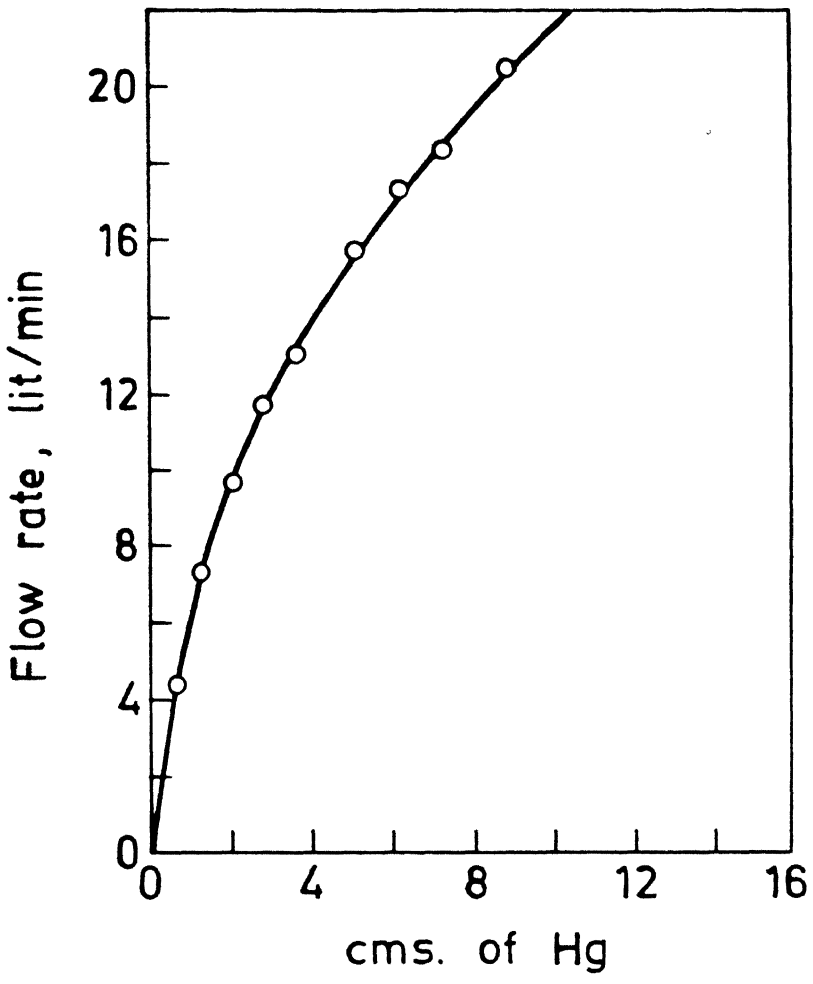

Figure 5. Calibration Curve for Flowmeter

3.4 Experimental Procedure

The position of the sensor is fixed in the vessel. Gas valve is opened so as to pass gas at a very low flow rate through the nozzle before filling up the vessel with the liquid. Now the vessel is filled with the liquid to the required depth. Before filling the vessel with liquid, gas valve is opened in order to avoid the liquid entrance into the nozzle. Now gas is passed at a fixed flow rate. The oscilloscope and D.C. power supply to the electro-resistivity probe circuit is switched on. After few minutes, the waves will start coming on the oscilloscope screen. The chart speed of the oscilloscope is adjusted so as to make the each wave distinguishable.Volts per division are also adjusted, and this value is kept constant in all the experiments.

There are 50 small division on the screen of the oscilloscope. In order to find out the bubble frequency, the number of times, the waves are formed within these 50 divisions, are counted. Knowing the chart speed of the oscilloscope, one can calculate the bubble frenquency. In order to find out gas hold-up, the number of divisions for which gas was present at the tip of the sensor are counted. The procedure for counting these divisions is shown in Fig. 6. Again from chart speed one can find out the time value corresponding to these divisions. So in this

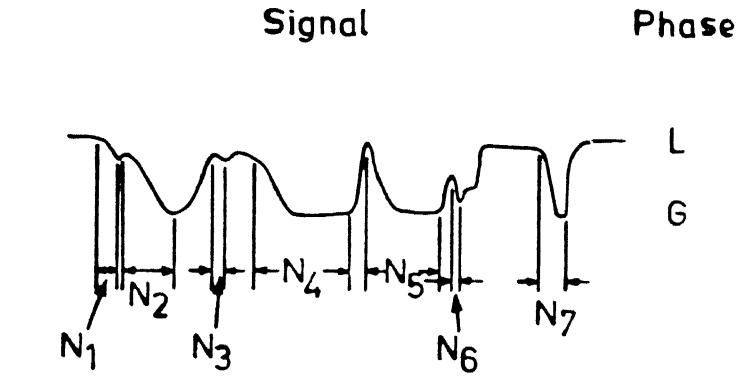

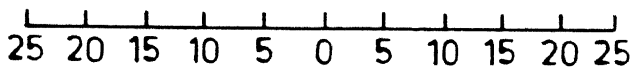

Number of divisions

$$\text{Gas hold-up, } \varepsilon = \frac{\sum_{i=1}^{7} Ni}{50}$$

Figure 6. Procedure to calculate gas hold-up from oscilloscope signal

way by knowing time for which gas was present at the tip of the sensor and time corresponding to the 50 small divisions, one can calculate the gas hold-up.

After every minute, the signal is stored and above mentioned readings for calculations of bubble frequency and gas hold-up are taken. At each position in the bath, 20 to 30 readings are taken. The sensor is moved from center to the radial direction. The readings are taken at 4 to 5 positions between the center and the periphery of the bubble plume zone.

Above procedure is repeated at four heights above the nozzle (Z = 5, 20, 50 and 100 mm).

3.5 Experimental Variables

The experimental variables studied were gas flow rate, nozzle diameter and the type of system. Gas flow rate ranging from 2 NL/min. to 18 NL/min. were used. Nozzles of straight bore diameters of 0.08, 0.12 and 0.24 cms. were used. Two systems i.e. air/water and argon/mercury were studied.

CHAPTER 4

EXPERIMENTAL RESULTS

All the experimental results obtained in this investigation are reported in Tables 2 and 3*. In Table 2 the experimental data for air/water (nozzle diameters: 0.12 and 0.24 cms.) and in Table 3 for argon/mercury (nozzle diameter: 0.08 cm.) systems are reported. First and second column of both the tables represent the radial position of the sensor probe and chart speed of the oscilloscope respectively. Third column enlists the data for bubble frequency calculations. Each value represents the number of waves developed per ten divisions, i.e. Σn on the oscilloscope screen. Each wave formed is due to a bubble striking the probe tip. At a particular radial position about 20-30 values have been taken. Each reading has been taken after a gap of approximately one minute.

The fourth column of the aforementioned tables enlists the data for gas hold-up evaluation. Each value represents the number of small divisions for which gas was present at the tip of the sensor probe per 50 divisions i.e. Σn . The data has been taken similar to that in case of bubble frequency data. i.e. at a particular radial position of the sensor, each value in fourth column has been taken after a gap of approximately one minute.

- -

* Appendix 1.

4.1 Evaluation of Local Gas Hold-up

The local gas hold-up is determined as follows:

$$\Sigma = \frac{\text{Total number of small divisions on oscilloscope screen for which gas was present at probe tip}}{\text{Total number of small divisions on oscilloscope screen}}$$

$$= \frac{\Sigma n}{50} \qquad (4.1)$$

The values of gas hold-up calculated by Eq. (4.1) are plotted against time of measurement in Figs. 7 to 14. Consider Fig. 7 for the purpose of illustration. This figure is for nozzle diameter: 0.24 cm; Gas injection rate 13.2 NL/min., and system: air/water. Local gas hold-up values are plotted against time of measurement for different radial positions and constant axial position of the sensor probe. Such a representation will show the dynamic nature of the gas bubble plume.

The graph shows that the value of local gas hold-up at any radial position of sensor probe is not a single value but it continues to oscillate. (In fact one should obtain a single value of gas hold-up for any radial axial probe location because the upstream parameters i.e. nozzle diameter, gas injection rate generating the bubble plume are constant). Similar observations can be made in Figs. 8-14 for air/water and argon/mercury systems at other constant upstream parameters.

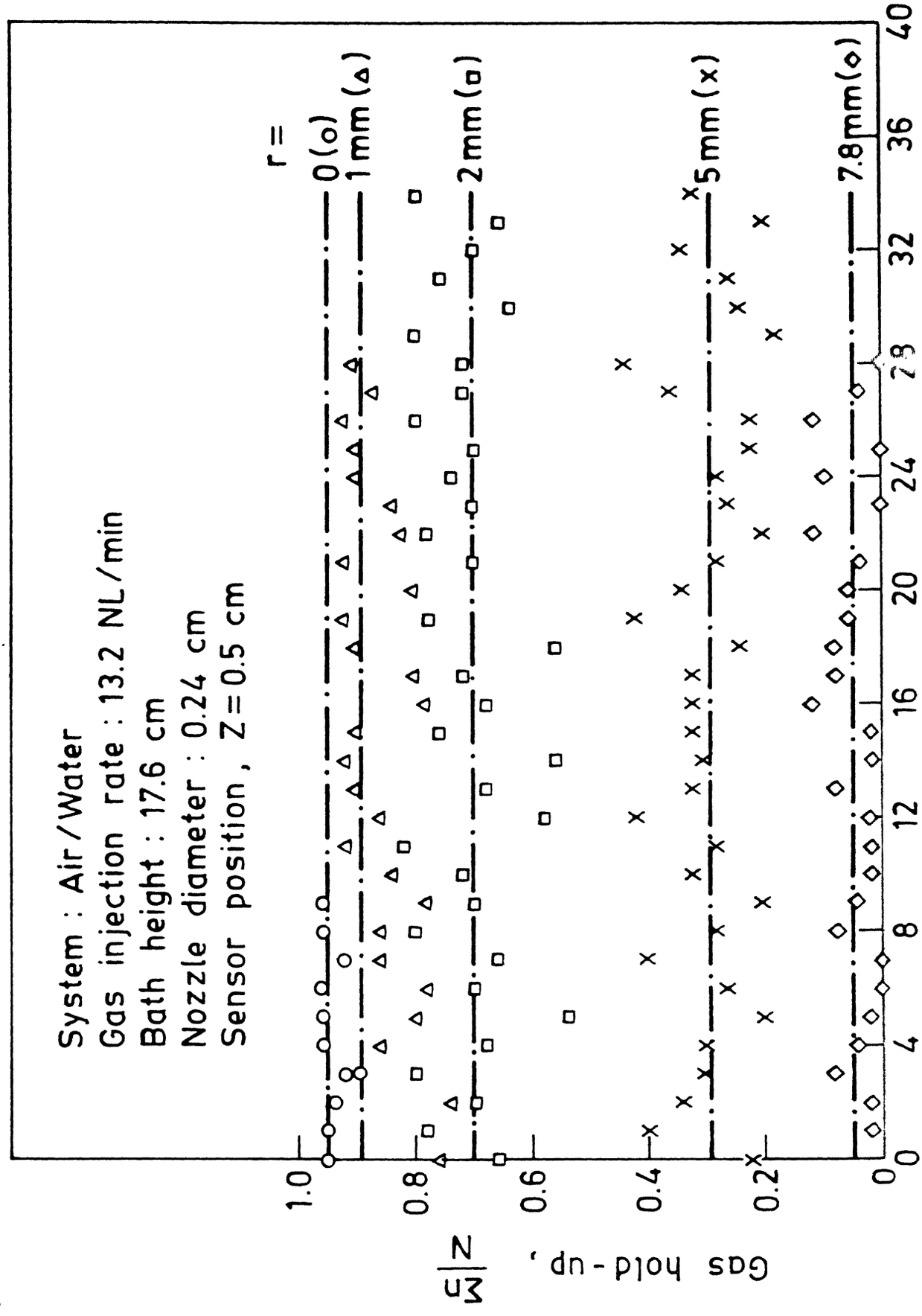

Figure 7. Variation of local gas hold-up against time of measurement

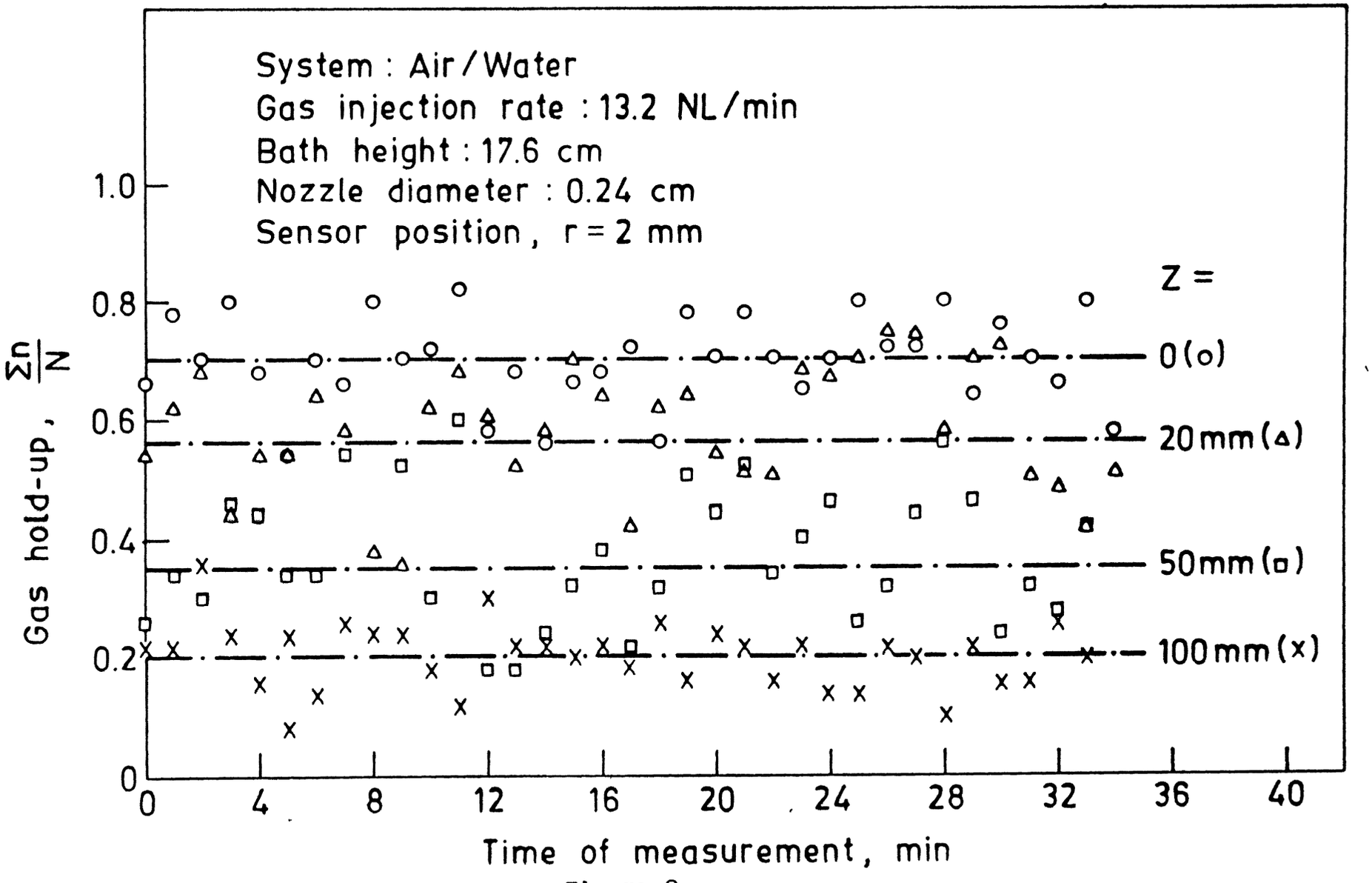

Figure 8

Variation of local gas hold-up against time of measurement

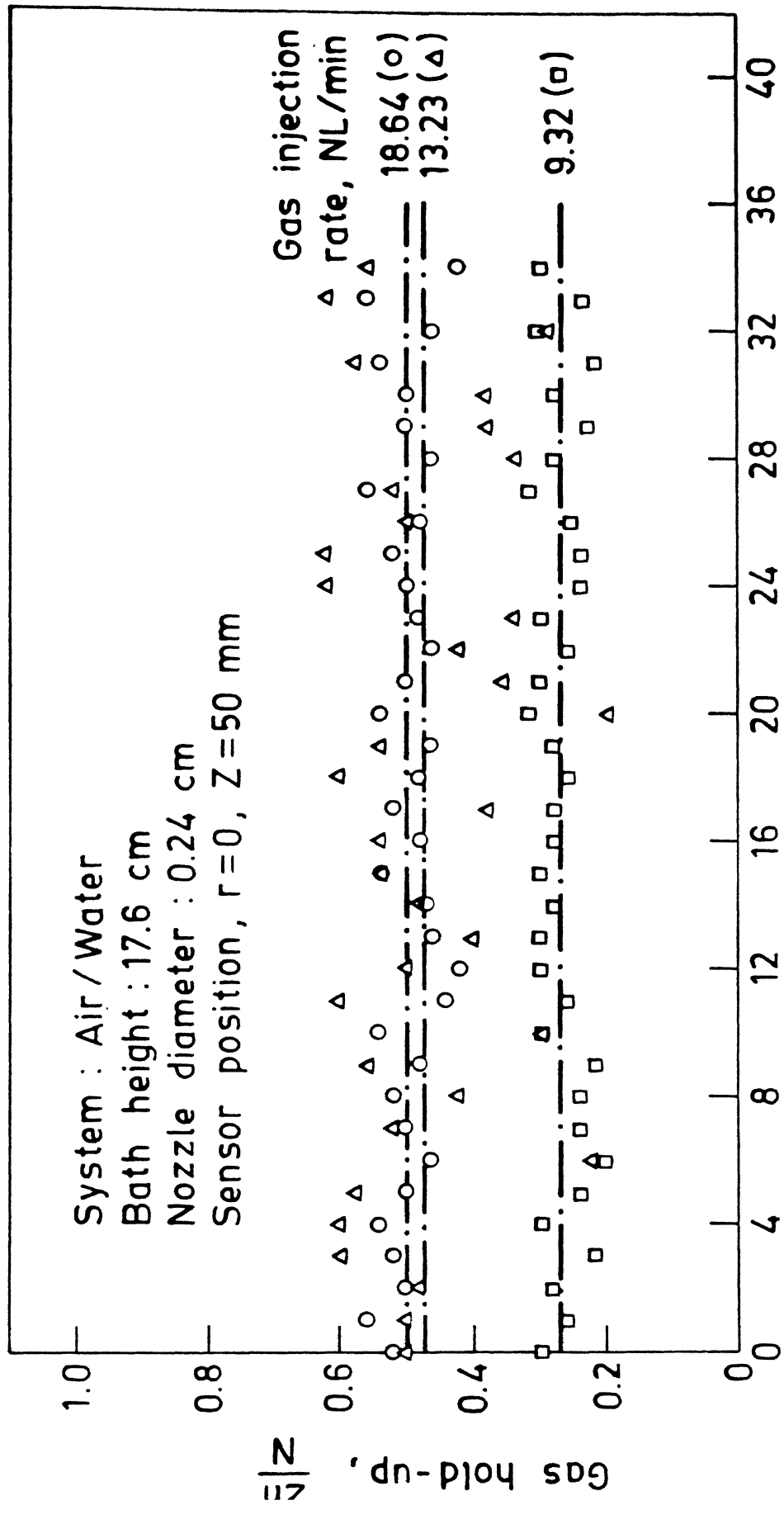

Figure 9

Variation of local gas hold-up against time of measurement

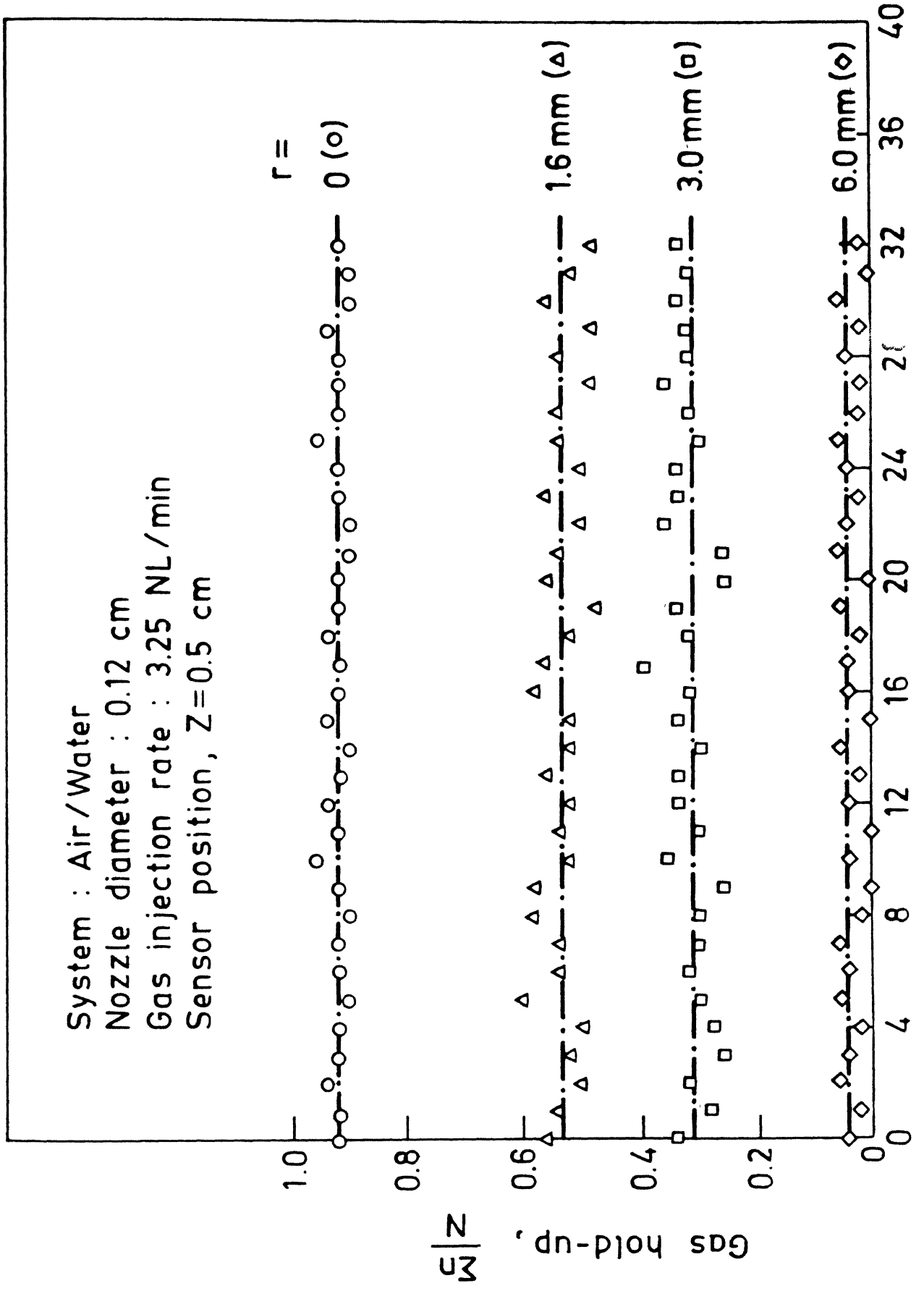

Variation of local gas hold-up against time of measurement

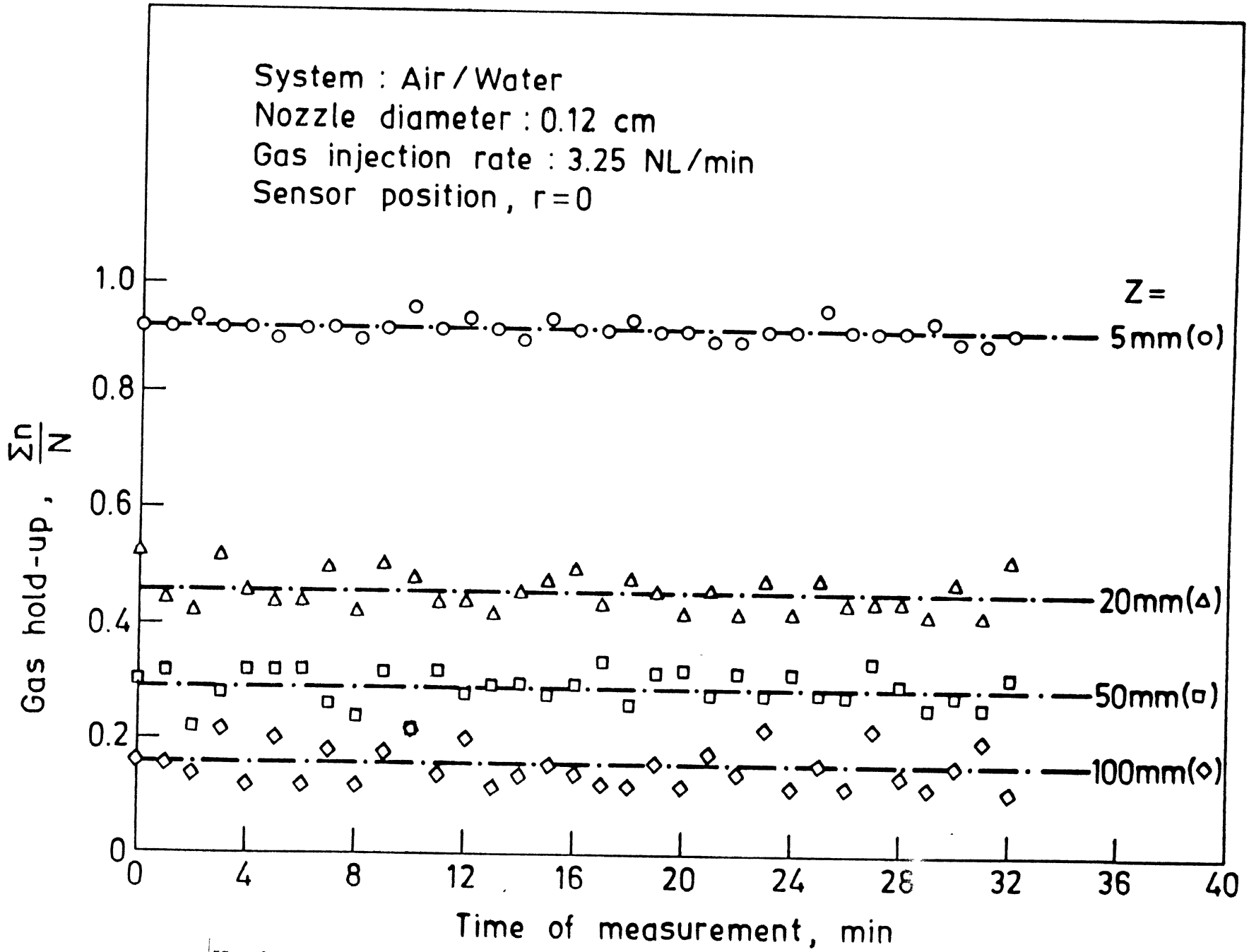

Variation of local gas hold-up against time of measurement

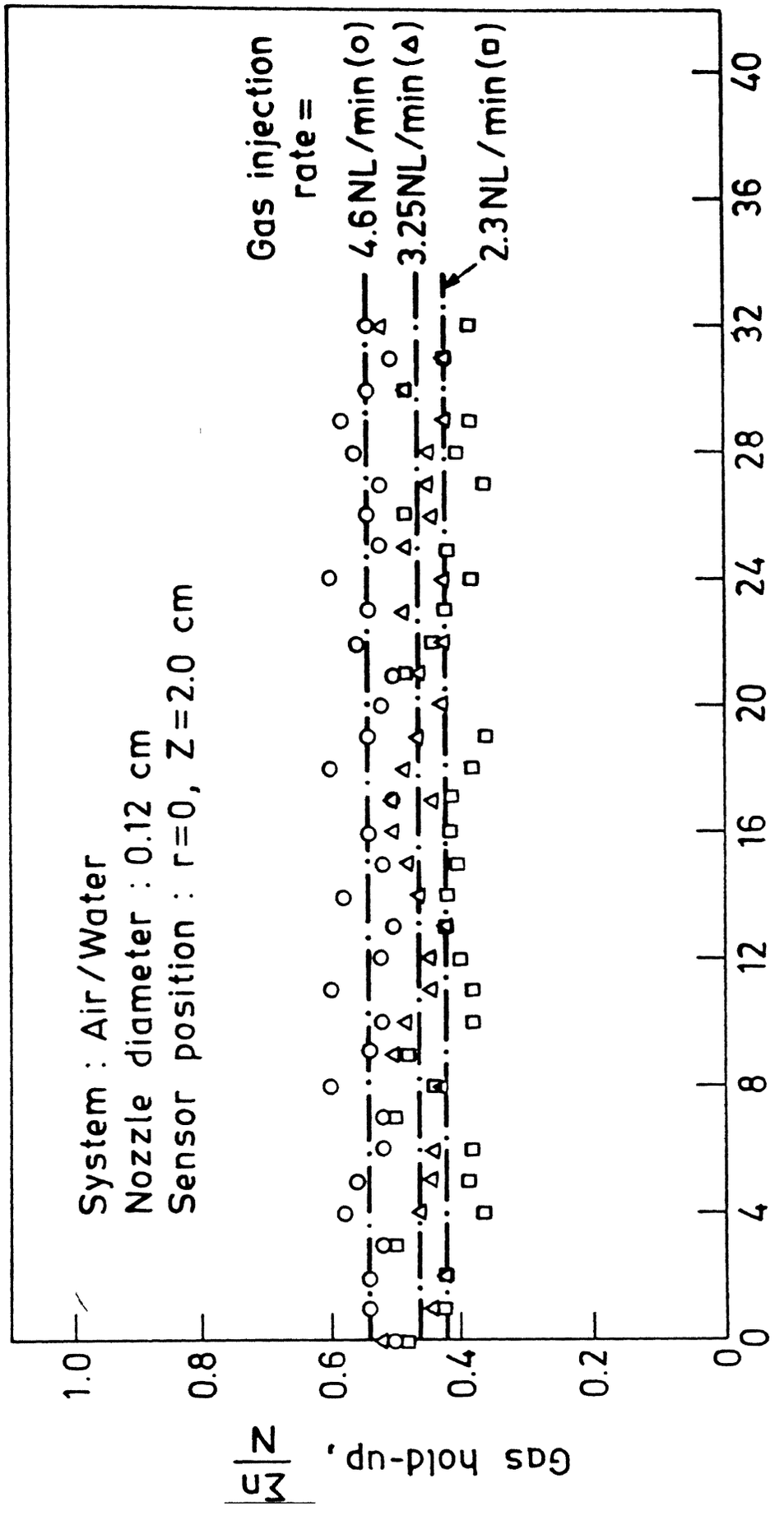

Figure 12

Variation of local gas hold-up against time of measurement

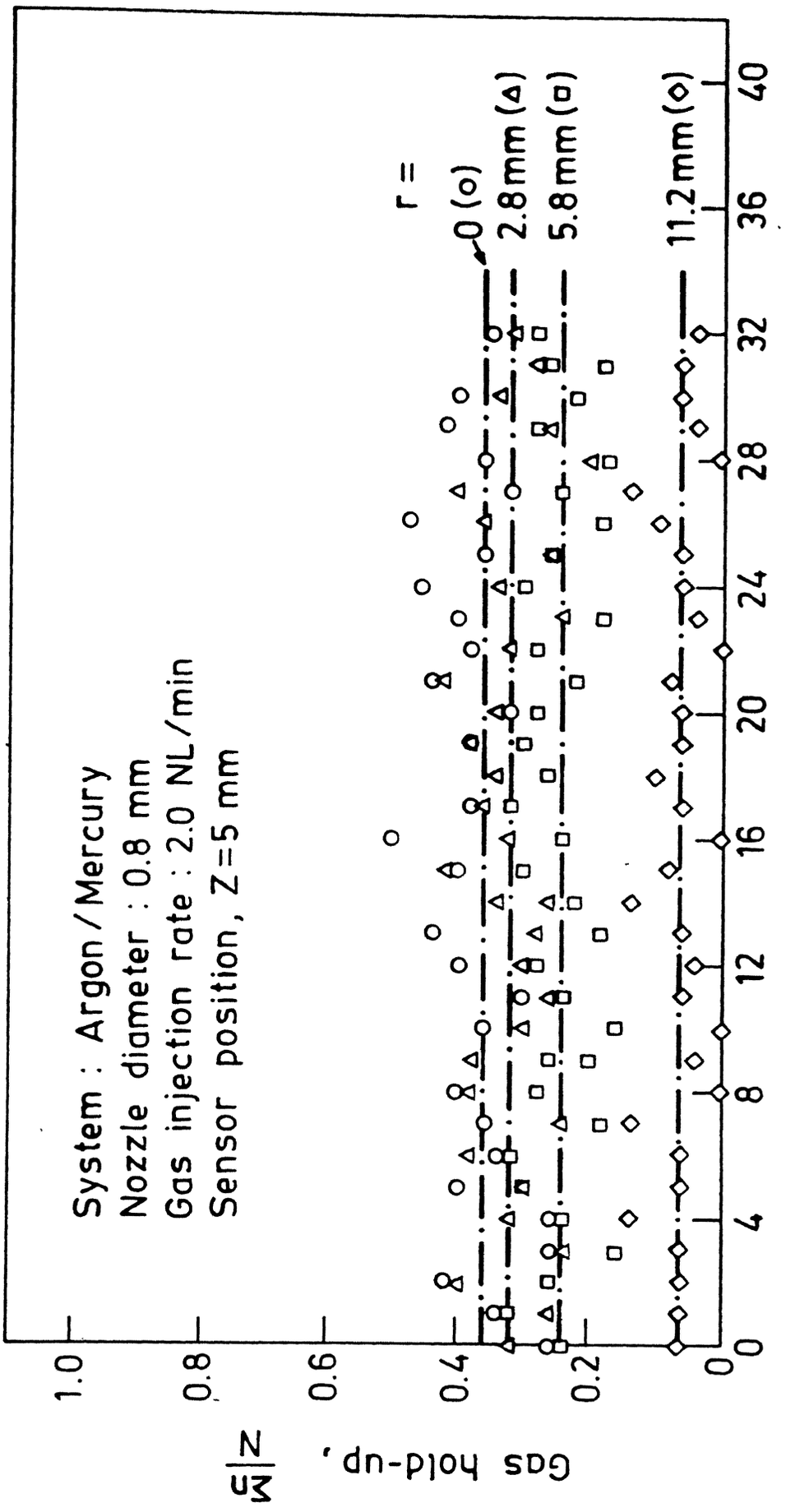

Figure 13

Variation of local gas hold-up against time of measurement

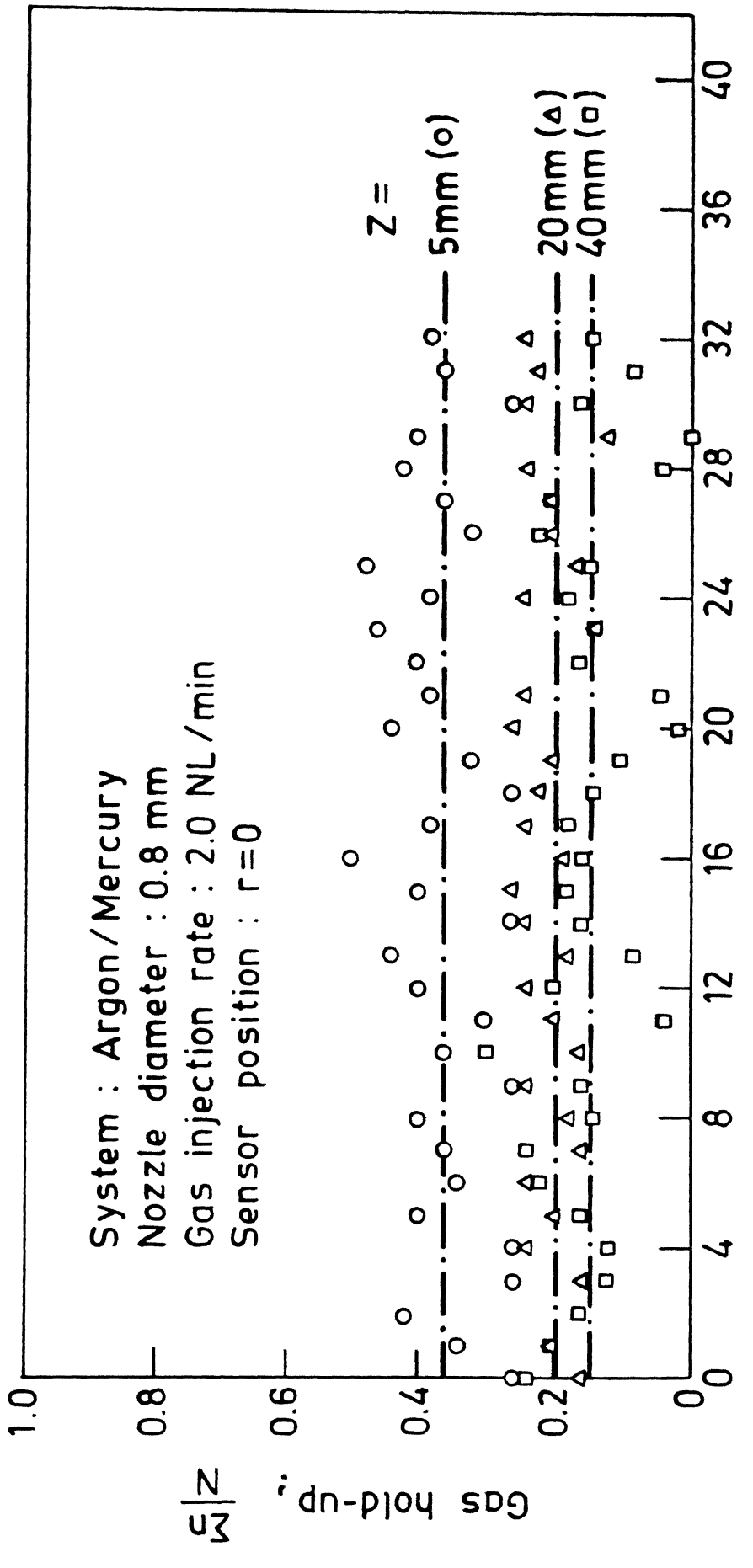

Figure 14

Variation of local gas hold-up against time of measurement

The fluctuation in gas hold-up for any combination of upstream parameters is due to the oscillatory motion of the gas bubble plume. Visual observations have indicated that the axis of the gas bubble plume was highly rotating (In the separate experiments this rotation was measured by stop watch and also by the sensor. The approximate number of rotation was found to be 33 revolutions/min. with reference to the observation made at the bath surface). Since the sensor probe location was stationary but the axis of the bubble plume was oscillating, therefore, it is obvious that the local gas hold-up will not have a single constant value but will have different values depending on the position of the axis of the gas bubble plume. Figures 7-14 confirm the above view.

So in order to represent all these values (taken for 30-35 min. at a particular position of sensor probe) by a single value of gas hold-up, an arithmetic mean value has been calculated. These are shown by broken lines in the figures 7-14.

4.2 Evaluation of Local Frequency

The local bubble frequency is calculated by the following formula:

$$f = \frac{\text{Number of waves developed per 10 divisions on oscilloscope screen}}{\text{Chart speed of oscilloscope in mS/div.}} \times 100$$

$$= \frac{\Sigma n}{\text{Chart speed of oscilloscope in ms/div.}} \times 100$$

Table (2) and Table (3) [Column -3] enlists all the data for calculations of f. Similar type of plots as reported in Figures 7-14, were also obtained for bubble frequency. The method of evaluation of mean value of local bubble frequency is similar to the one described in section 4.1.

4.3 Local Mean Gas Hold-up Profiles

Table (4) enlists the mean value of local gas hold-up determined from Figures 7-14.

In Figures 15-19, local mean gas hold-up ($\bar{\varepsilon}$) is plotted against radial distance for different nozzle diameters, gas injection rates, and axial distances for the systems air/water and argon/mercury. In the figures, the radial position r = 0 represents the axis of the nozzle (this is also the axis of the vessel). The profiles in all the figures are symmetrical with reference to r = 0 axis. In all the figures, it can be seen that the shape of the radial profiles is similar and is independent of the experimental variables. However, the local gas hold-up depends upon the gas injection rate and axial position of the sensor.

The measurements reveal the continuous spread of the gas within the plume, the profiles become flatter and wider down stream from the gas injecting nozzle. (For example see Fig. 15 for radial profiles at Z = 2 cms, solid line and Z = 10 cms, broken line for any gas injection rate. Other figures also show a similar observation).

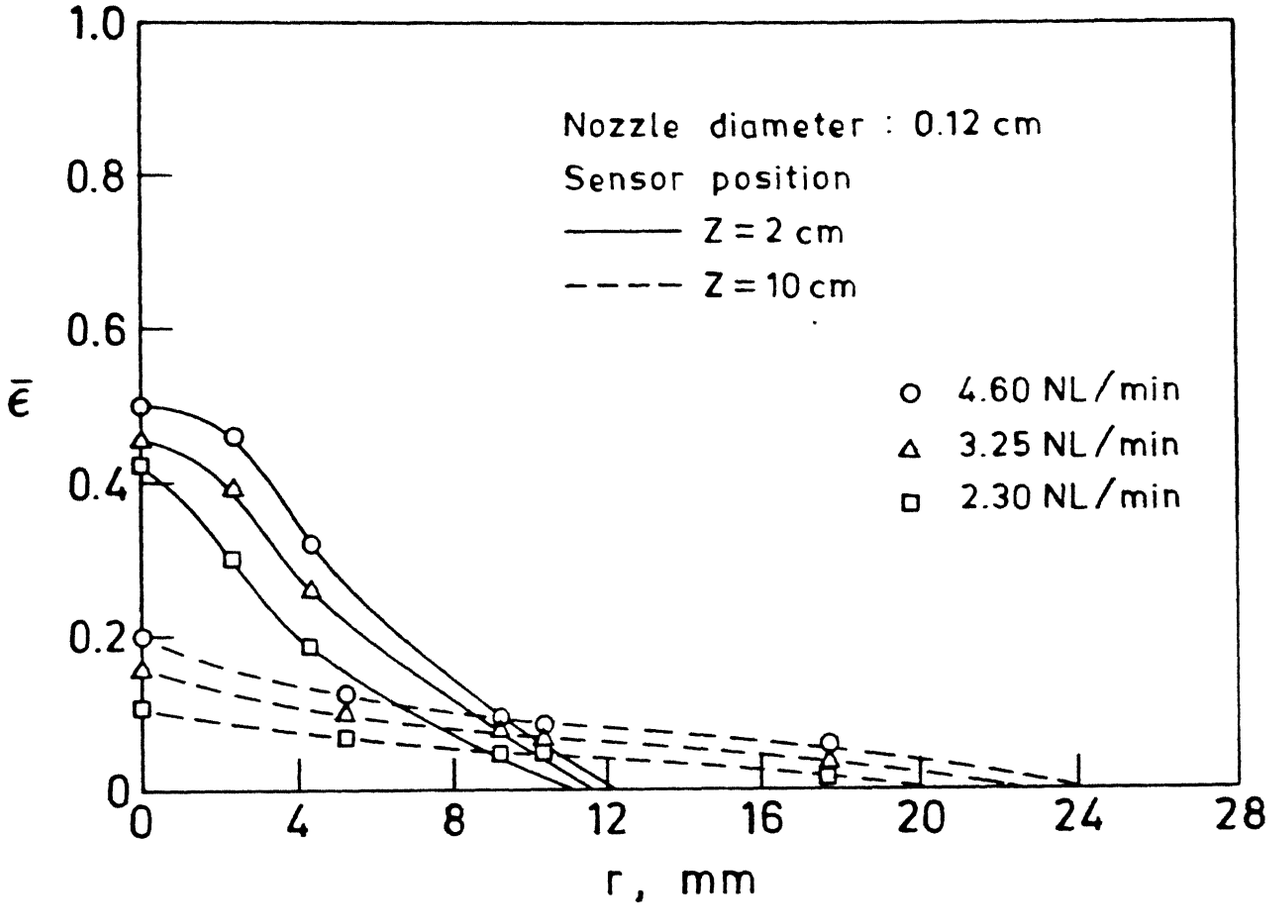

Figure 15. Variation of local mean gas hold-up against radial distance

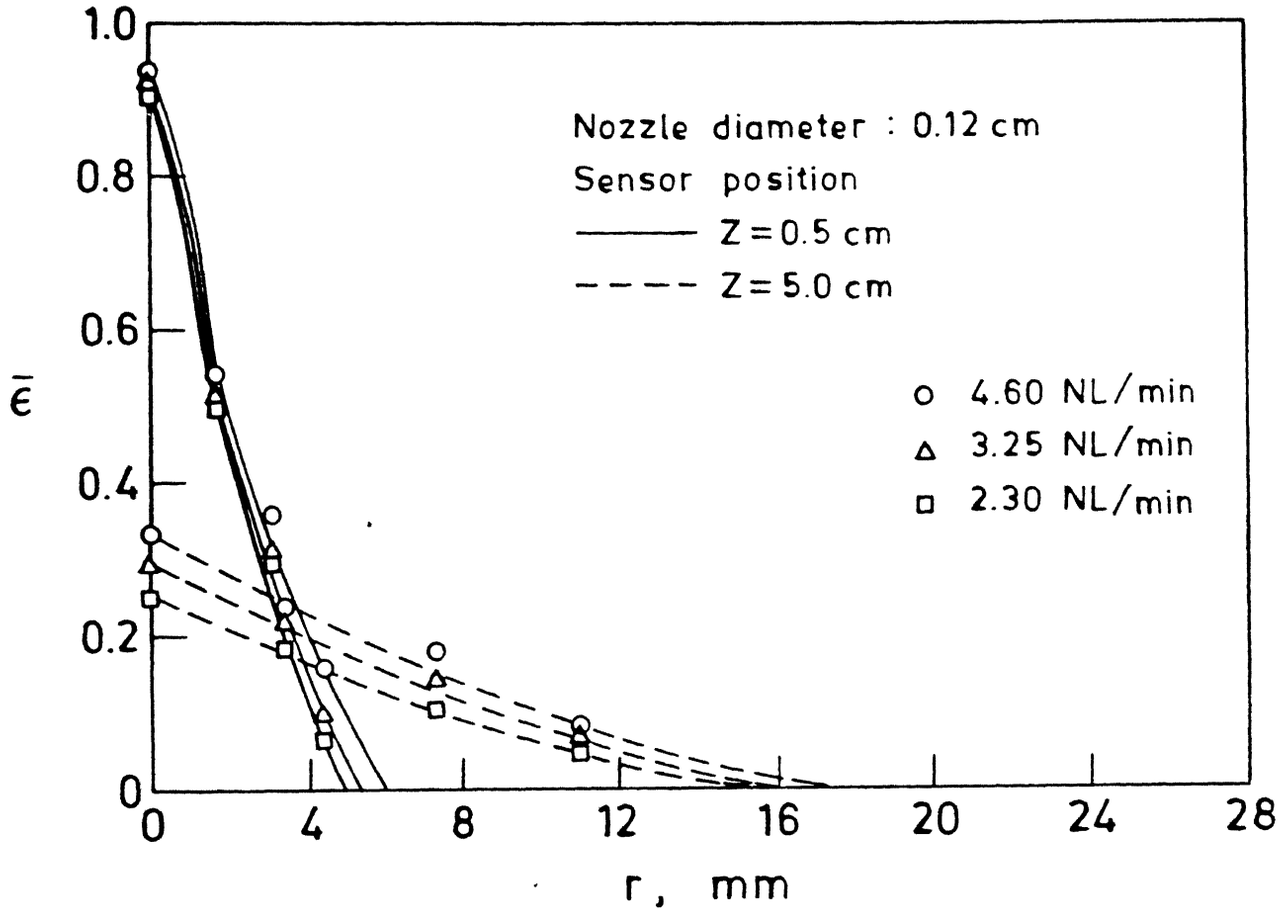

Figure 16

Variation of local mean gas hold-up against radial distance

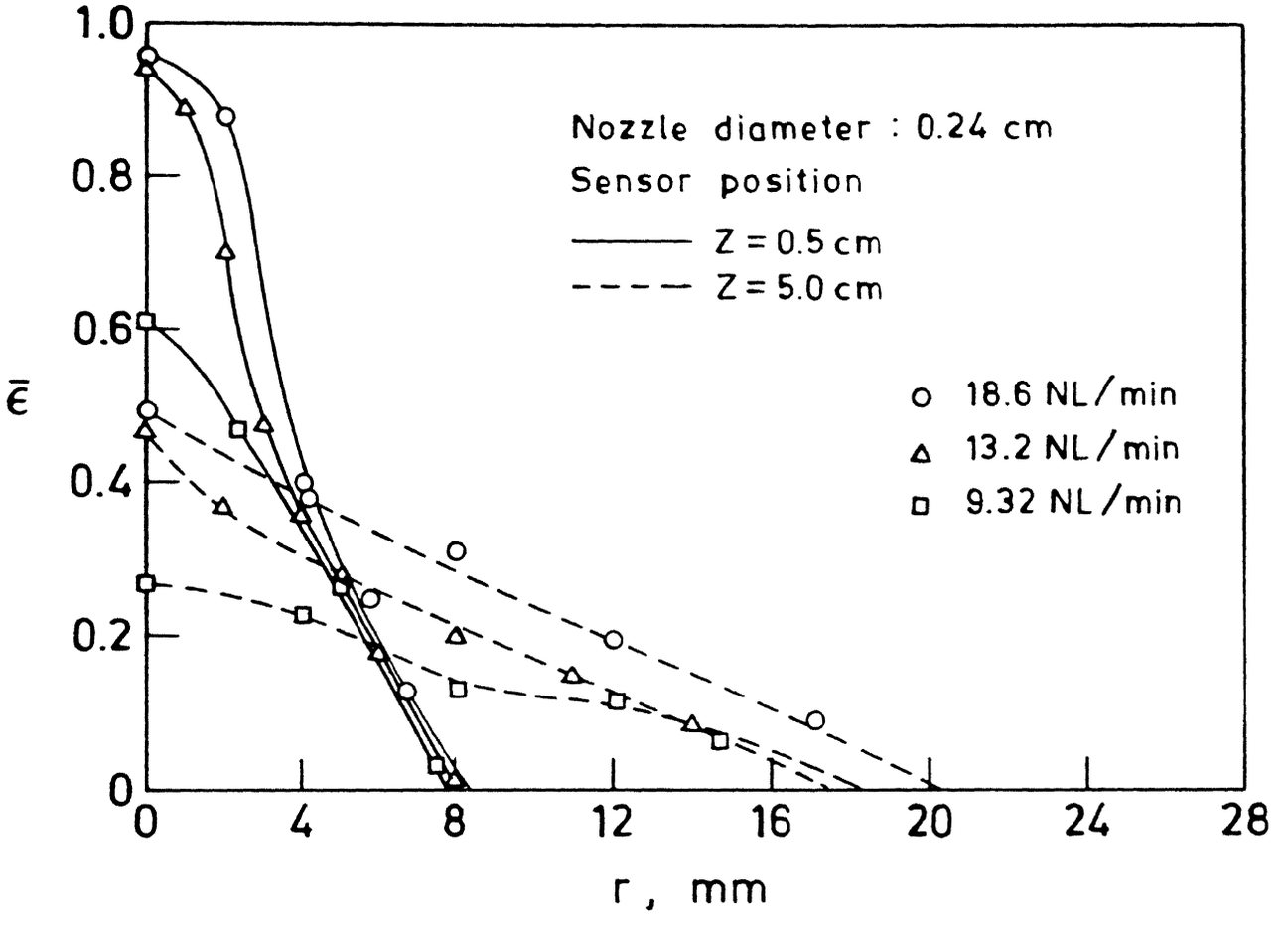

Figure 17

Variation of local mean gas hold-up against radial distance

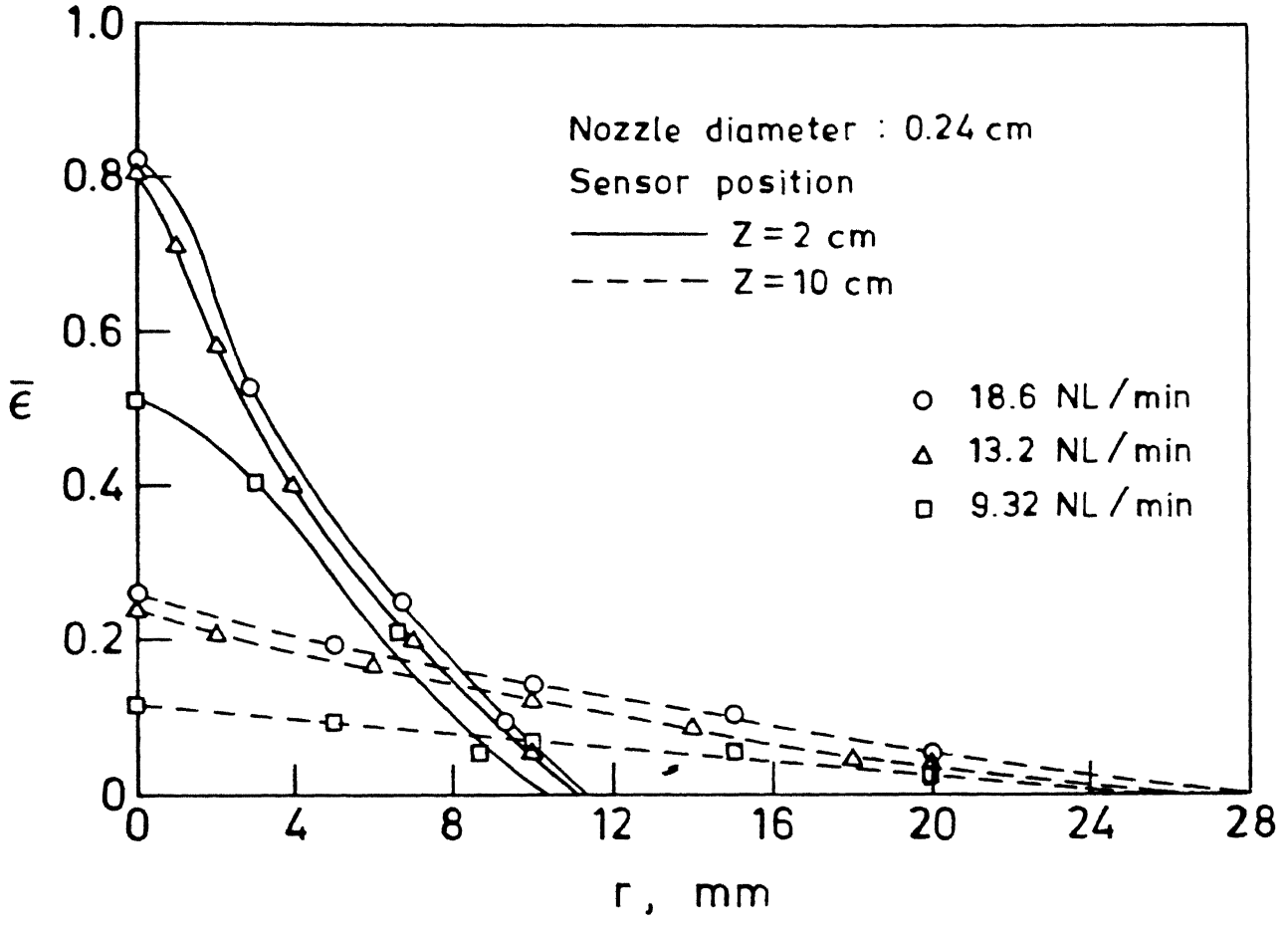

Figure 18

Variation of local mean gas hold-up against radial distance

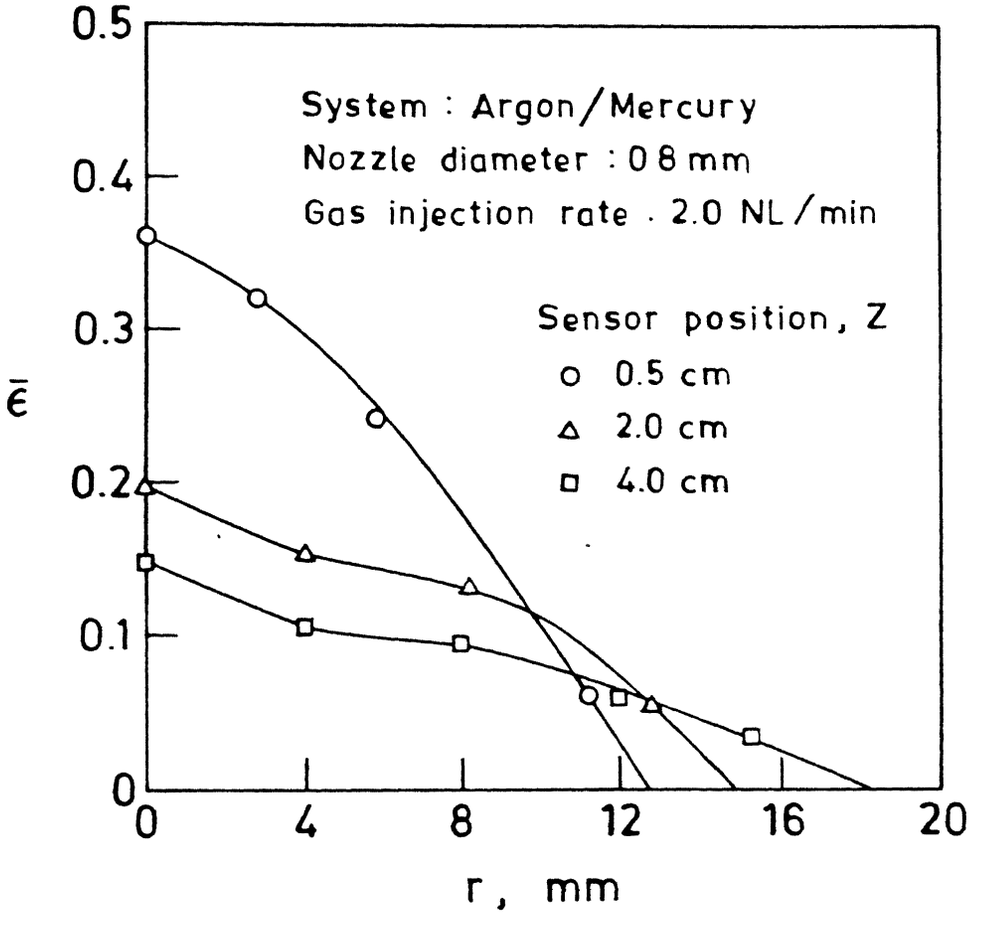

Figure 19

Variation of local mean gas hold-up against radial distance

4.4 Local Mean Bubble Frequency Profiles

Figures 20-24 show the local mean bubble frequency plotted against the radial distance, for different gas injection rates, nozzle diameters and sensor positions.

The frequency profiles are also similar in shape as those of gas hold-up profiles.

4.5 Estimation of $\bar{\varepsilon}_{max}$ and $r_{p,\varepsilon}$

$\bar{\varepsilon}_{max}$ is the axial value of local mean gas hold-up. Plume radius for any axial location is defined as the radial distance from the axis of the plume where the value of local mean gas hold-up becomes approximately equal to zero. The values of $\bar{\varepsilon}_{max}$ and $r_{p,\varepsilon}$ are estimated from the $\bar{\varepsilon}$ vs. r plots. Table (5) enlists the values aof these two parameters. The variation of $\bar{\varepsilon}_{max}$ and $r_{p,\varepsilon}$ with gas injection parameter is presented in detail in the discussion section.

4.6 Estimation of $\bar{f}_{max}$ and $r_{p,f}$

$\bar{f}_{max}$ is the axial value of local mean bubble frequency . Plume radius, $r_{p,f}$ for any axial location is the radial distance from the axis of the plume, where $\bar{f}$ becomes approximately equal to zero. The values of $\bar{f}_{max}$ and $r_{p,f}$ are estimated from the $\bar{f}$-r plots and are given in Table (5).

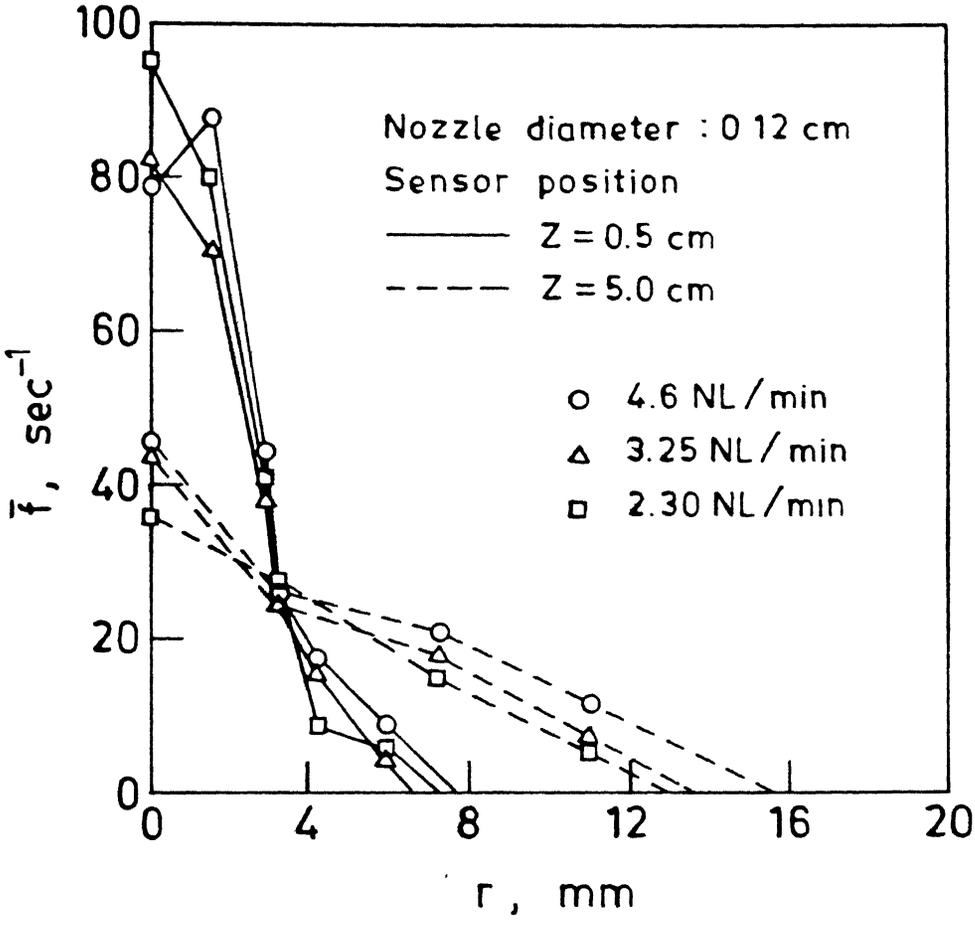

Figure 2[illegible]. Variation of local mean bubble frequency vs. radial distance

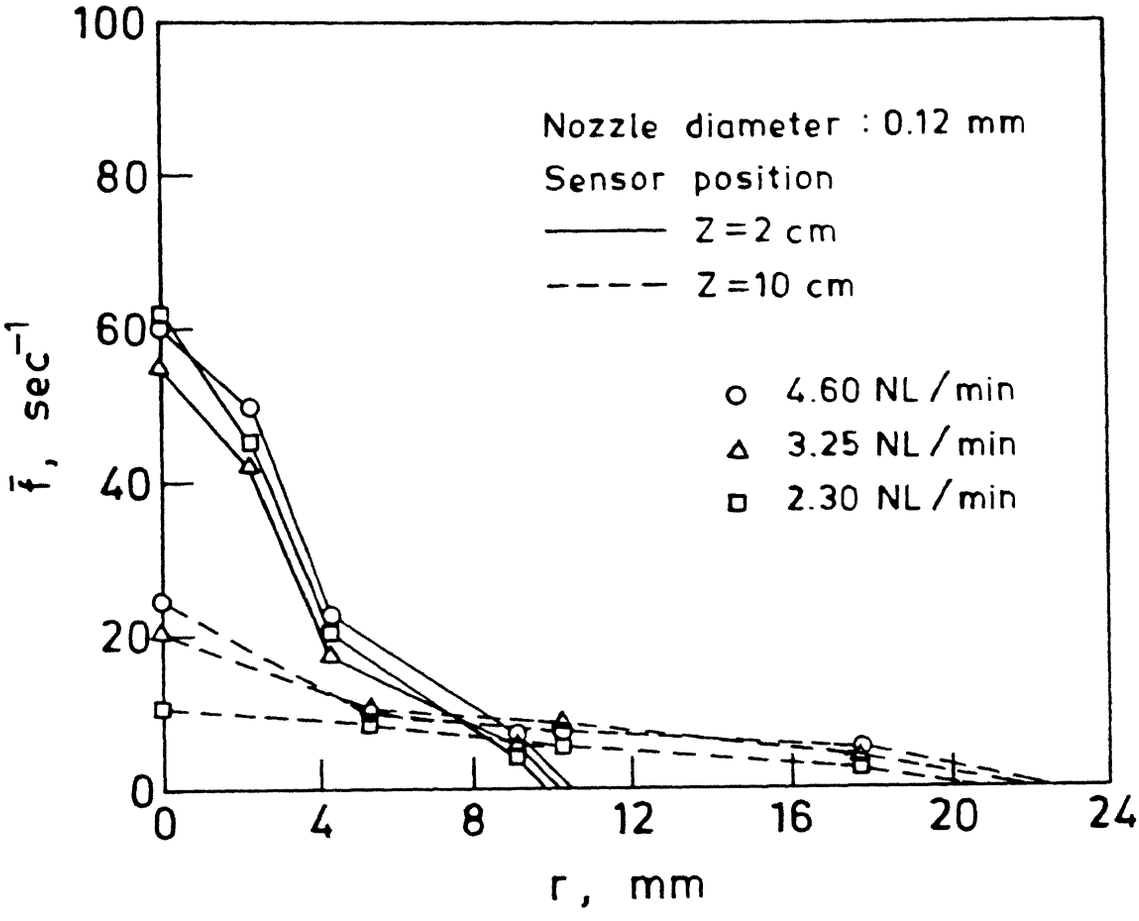

Figure 21

Variation of local mean bubble frequency vs. radial distance

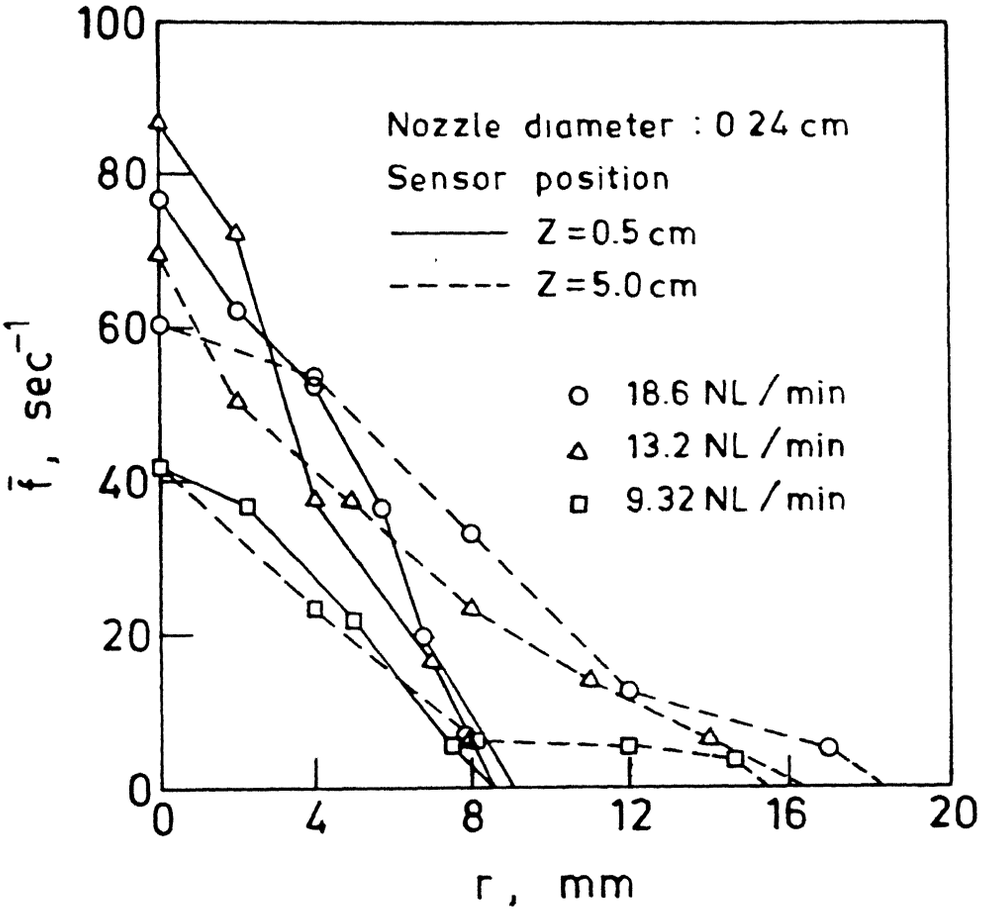

Figure 22

Variation of local mean bubble frequency vs. radial distance

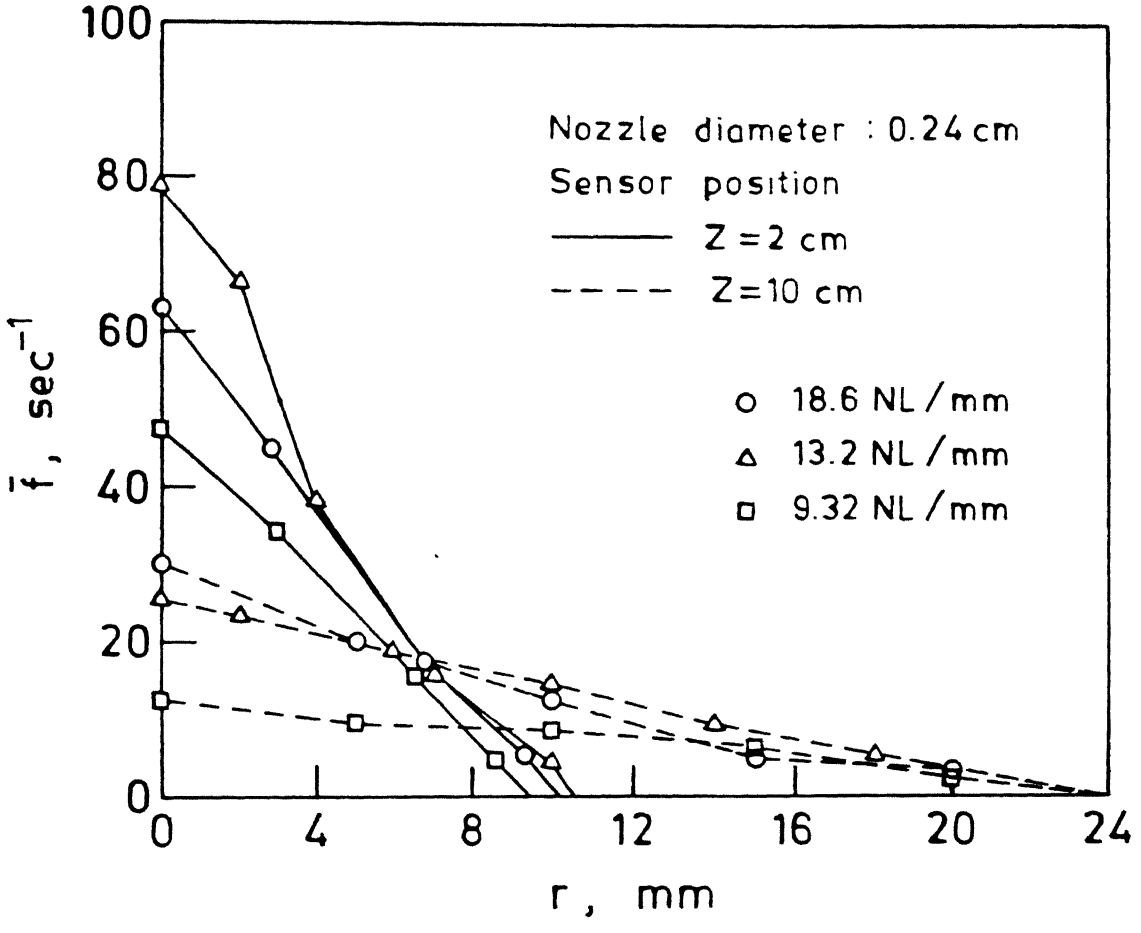

Figure 23

Variation of local mean bubble frequency vs. radial distance

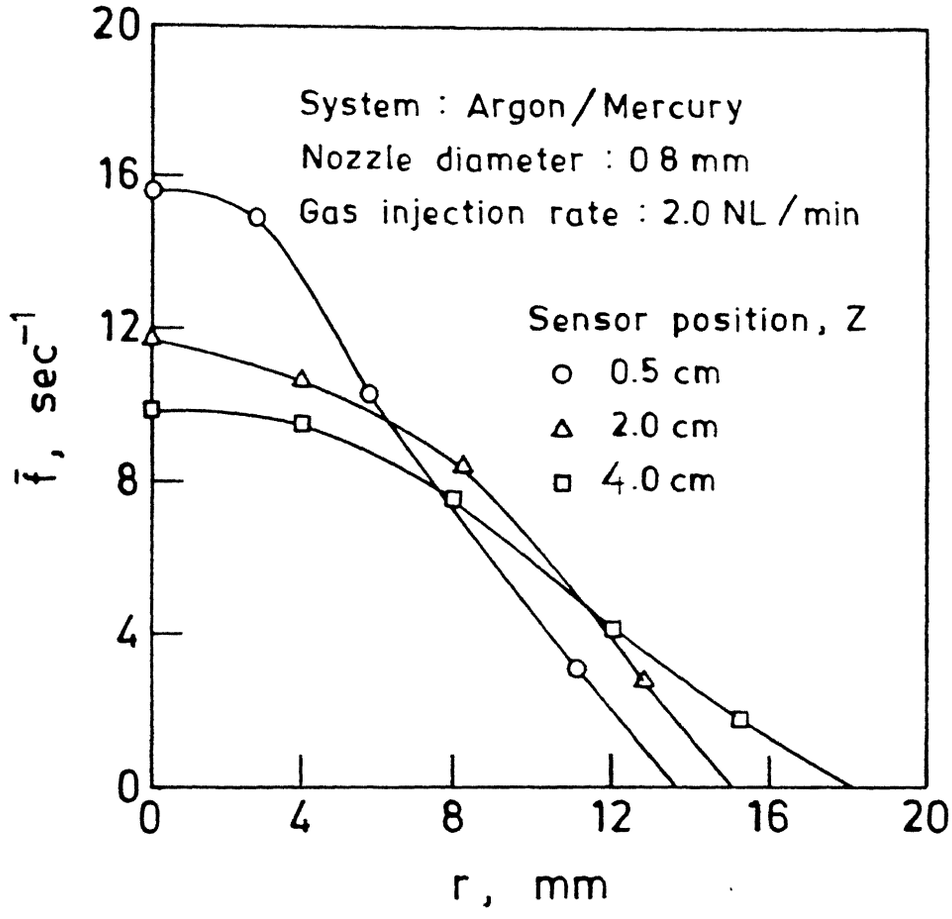

Figure 24

Variation of local mean bubble frequency vs. radial distance

4.7 Variation of $\bar{\varepsilon}_{max}$ and $r_{\bar{\varepsilon}_{max/2}}$

The variations of $\bar{\varepsilon}_{max}$ and $r_{\bar{\varepsilon}\ max/2}$ against Z are shown in Figures 25 and 26. The experimental variables are given in the respective figures. Figure 25 shows the experimental decrease of $\bar{\varepsilon}_{max}$ with increase in Z at all gas injection rates and nozzle diameters employed in this investigation.

The decrease in $\bar{\varepsilon}_{max}$ with Z is due to the flattening of the $\bar{\varepsilon}$ - r profiles. This is due to the law of conservation of mass of gas.

Figure 26 shows the increase in half value radius with Z at all gas injection rates and nozzle diameters.

The lines in Figures 25 and 26 are drawn to show the trend of experimental results.

4.8 Angle Measurement

In order to measure cone angle of the gas bubble plume, the values of $r_{p,}$ have been plotted against Z, for the two nozzle diameters and different gas injection rates in figure 27. The experimental points have been joined with the help of smooth curves so as to assess the outer profile of the plume.

The cone angle has been calculated by drawing a straight line passing through the experimental points and

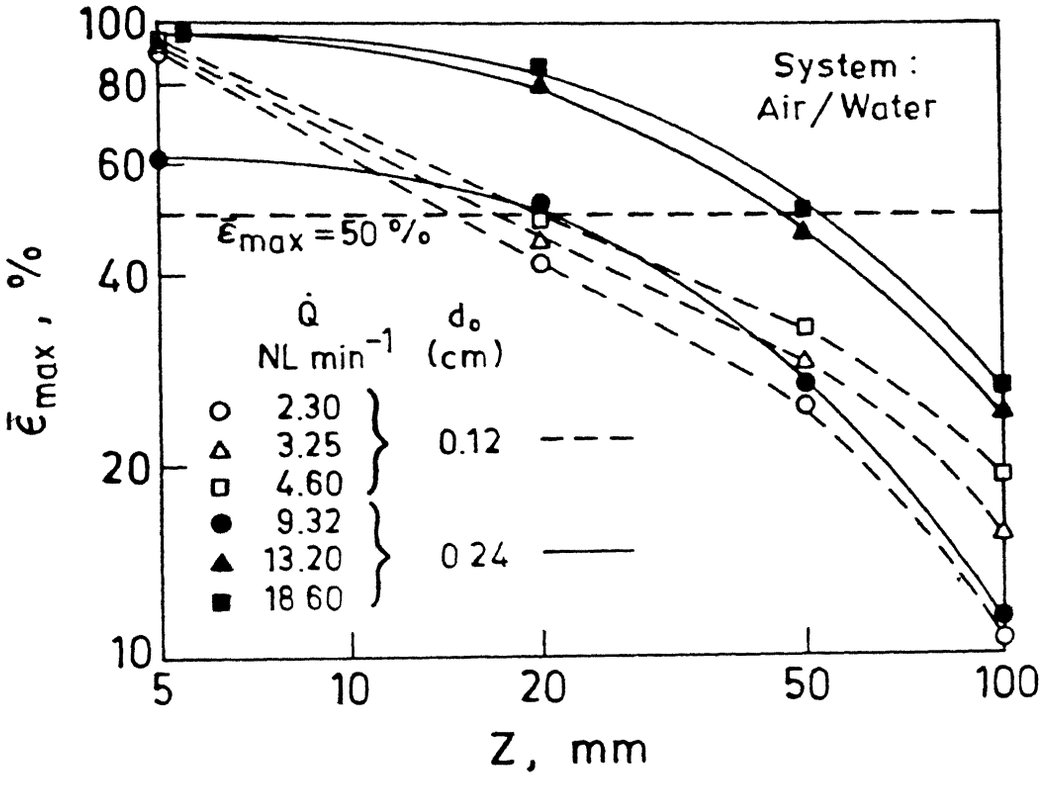

Figure 25. Variation of $\bar{\epsilon}_{max}$ with Z

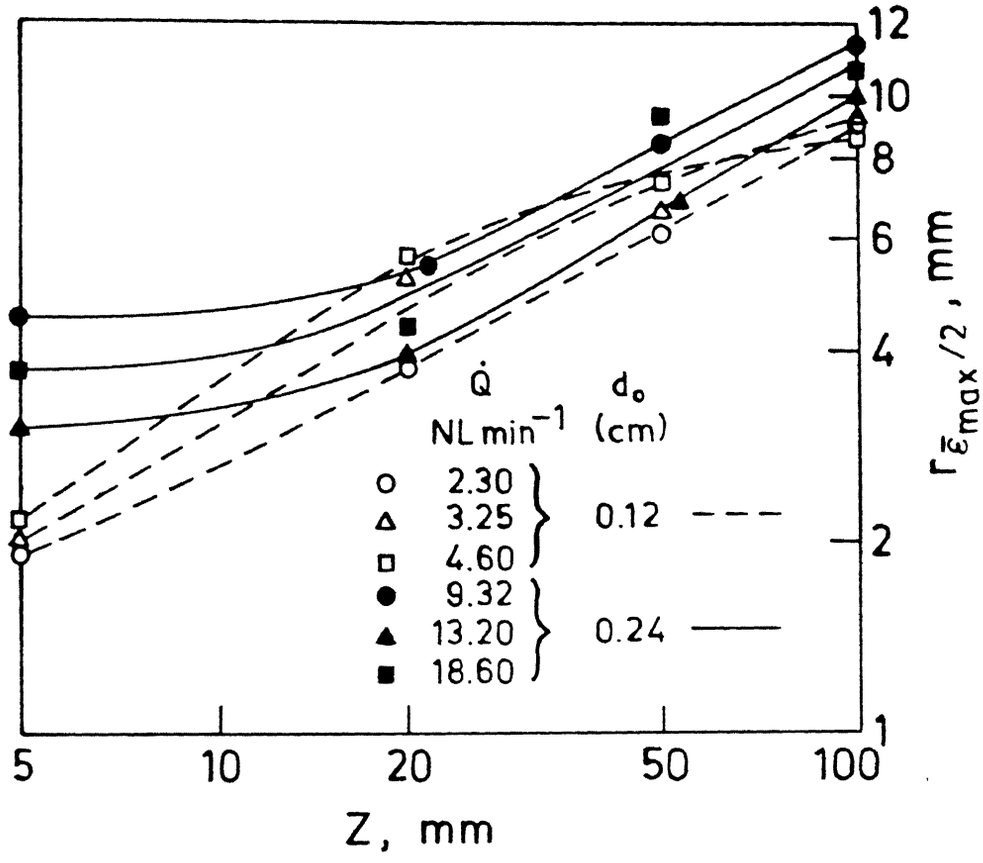

Figure 26. Variation of $r_{\bar{\varepsilon}\ max/2}$ with Z

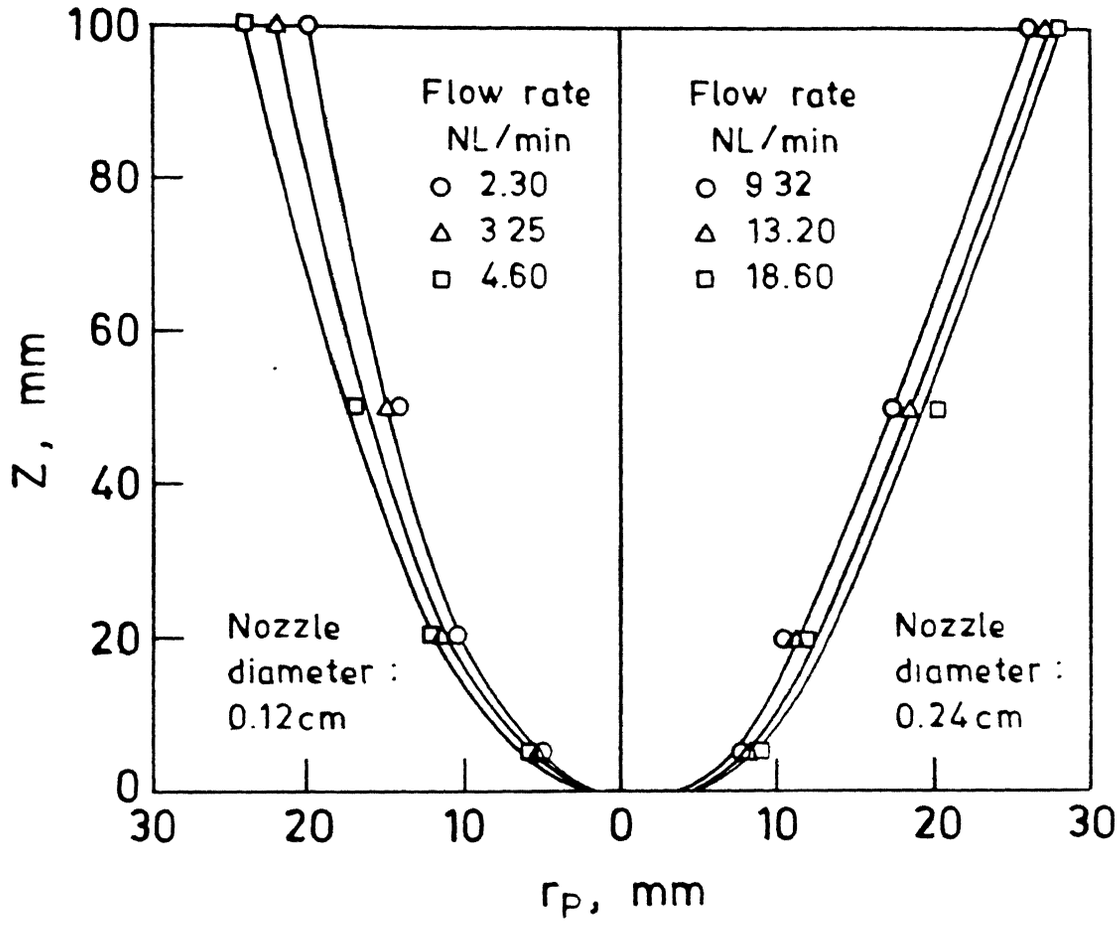

Figure 27. Variation of plume radius ($r_{p,\varepsilon}$) against axial distance

measuring its inclination with the Z axis. The cone angle calculated for nozzle diameters of 0.12 cm and 0.24 cm are 17.4^{o} and 20.6^{o} respectively for the air/water system.

CHAPTER 5

DISCUSSION

The different aspects of the behaviour of the gas bubble plumes are discussed below.

5.1 Similarity of the Profile

5.1.1 Gas Hold-up Profiles

The similarity of the gas hold-up profiles in successive sections of the plume becomes evident when the profiles are normalized by plotting the ratio of the local gas hold up, $\bar{\varepsilon}$, to the maximum value, $\bar{\varepsilon}_{max}$ against the reduced radial distance $r/r_{\bar{\varepsilon}\ max/2}$[7]. The distance $r_{\bar{\varepsilon}\ max/2}$ is the half value radius where the value of $\bar{\varepsilon}$ becomes, 50% of its respective maximum value, at the axis of the plume[7].

The normalized gas hold-up profiles at different axial distances are shown in Figure 28 for nozzle diameter 0.12 cm and in Figure 29 for nozzle diameter 0.24 cm. The similarity of cross-sectional profiles is observed over the entire plume height, Under all the condition studied, the experimental reduced gas hold-up distribution isapproximated by the following function:

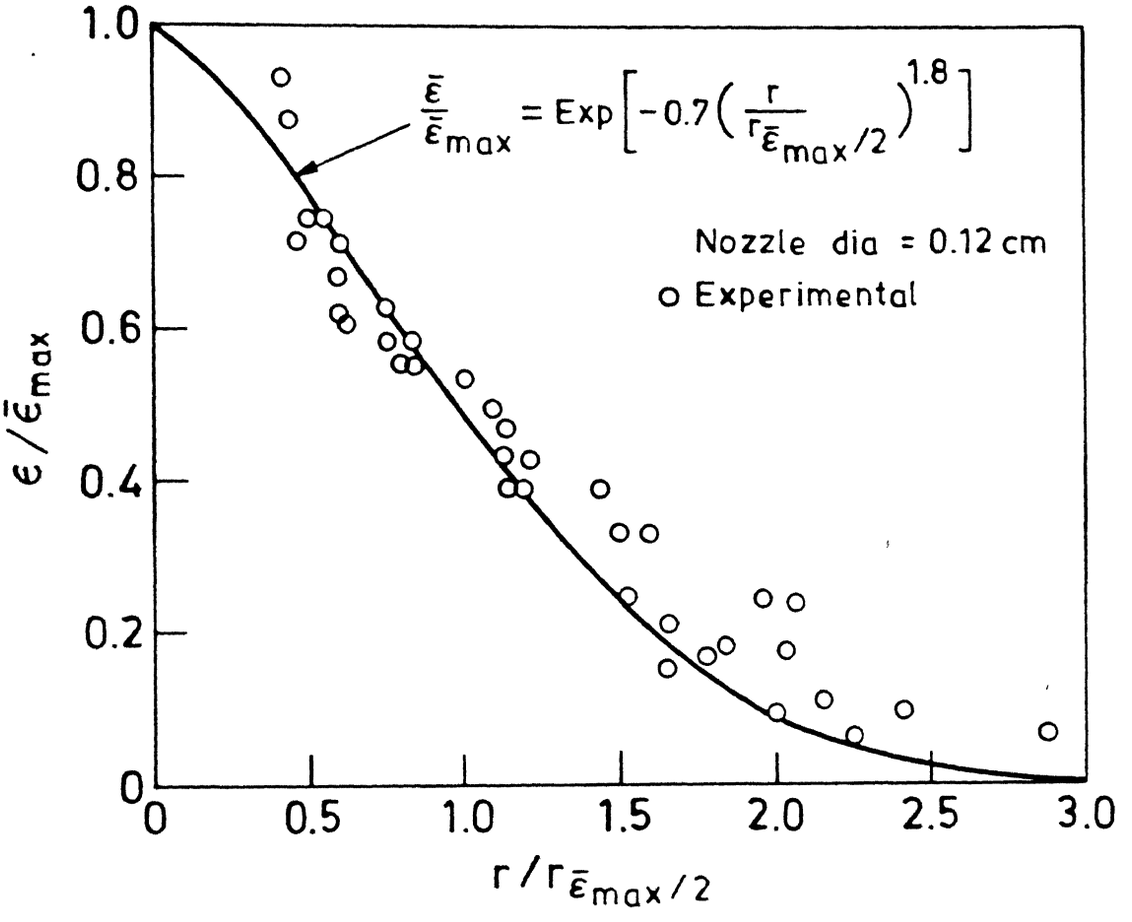

Figure 28. Normalized radial gas hold-up profiles at different axial distances from the nozzle in air-water plumes

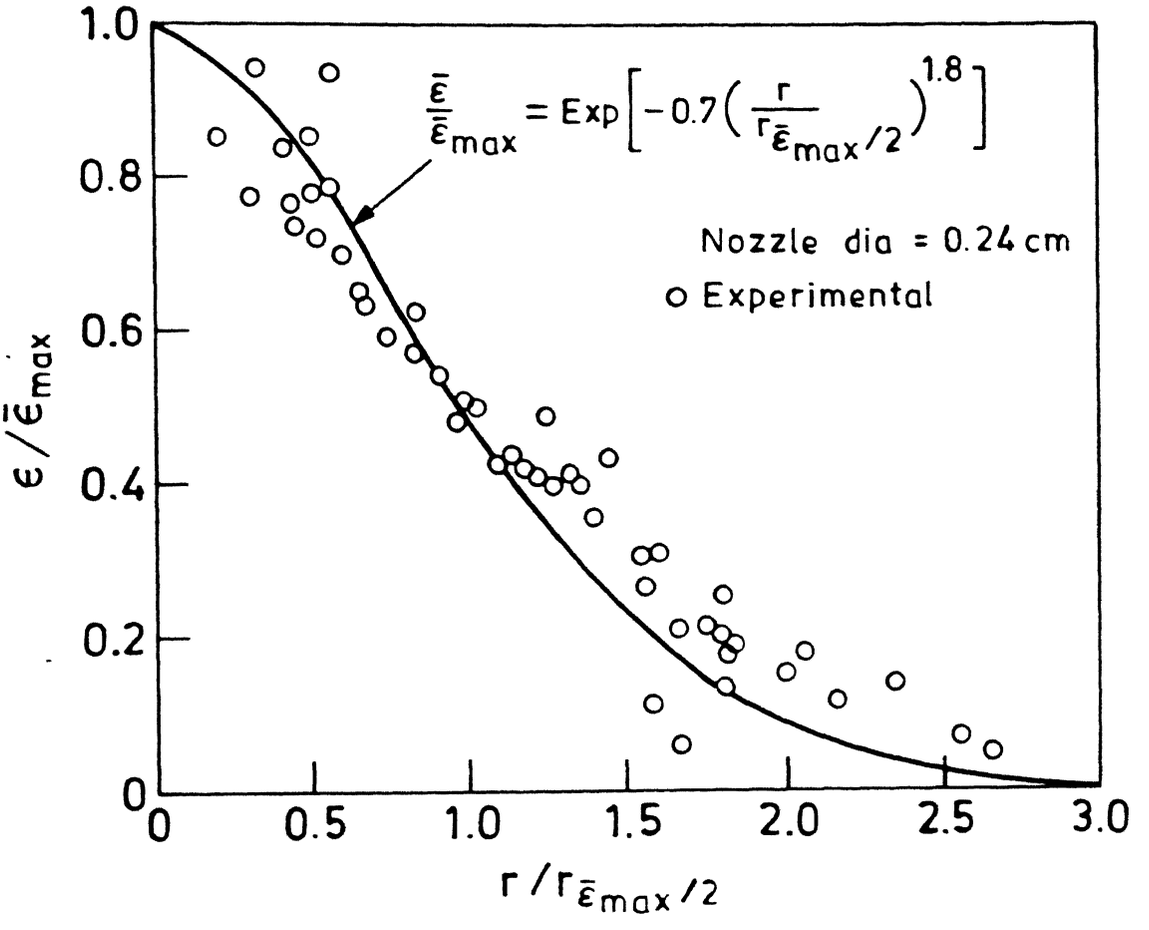

Figure 29

Normalized radial gas hold-up profiles at different axial distances from the nozzle in air/water plumes

$$\frac{\bar{\varepsilon}}{\bar{\varepsilon}_{max}} = \exp\left[-0.7\ (r/r_{\bar{\varepsilon}\ max/2})^{1.8}\right] \qquad (5.1)$$

The solid line in the Figures 26 and 27 represents the above function. It can be seen in both the figures that the function (5.1) yields a satisfactory agreement with the experimental data over the entire plume.

The function (5.1) indicates that the normallized gas hold-up profiles obtained in the investigation are some what broader than those represented by a Gaussian function[7].

5.1.2 Gas Bubble Frequency Profile

In Figures 30 and 31, the normallized gas bubble frequency ($\bar{f}/\bar{f}_{max}$) is plotted against reduced radial distance ($r/r_{\bar{f}\ max/2}$, $r_{\bar{f}\ max/2}$ is the half value radius at which the value of $\bar{f}$ becomes 50% of its maximum value at the axis of the plume. The solid lines represents the function:

$$\frac{\bar{f}}{\bar{f}_{max}} = \exp\left[-0.7\ (r/r_{\bar{f}\ max/2})^{1.8}\right] \qquad (5.2)$$

The experimental results are in good agreement with the function (5.2). The normallized gas bubble frequency profiles

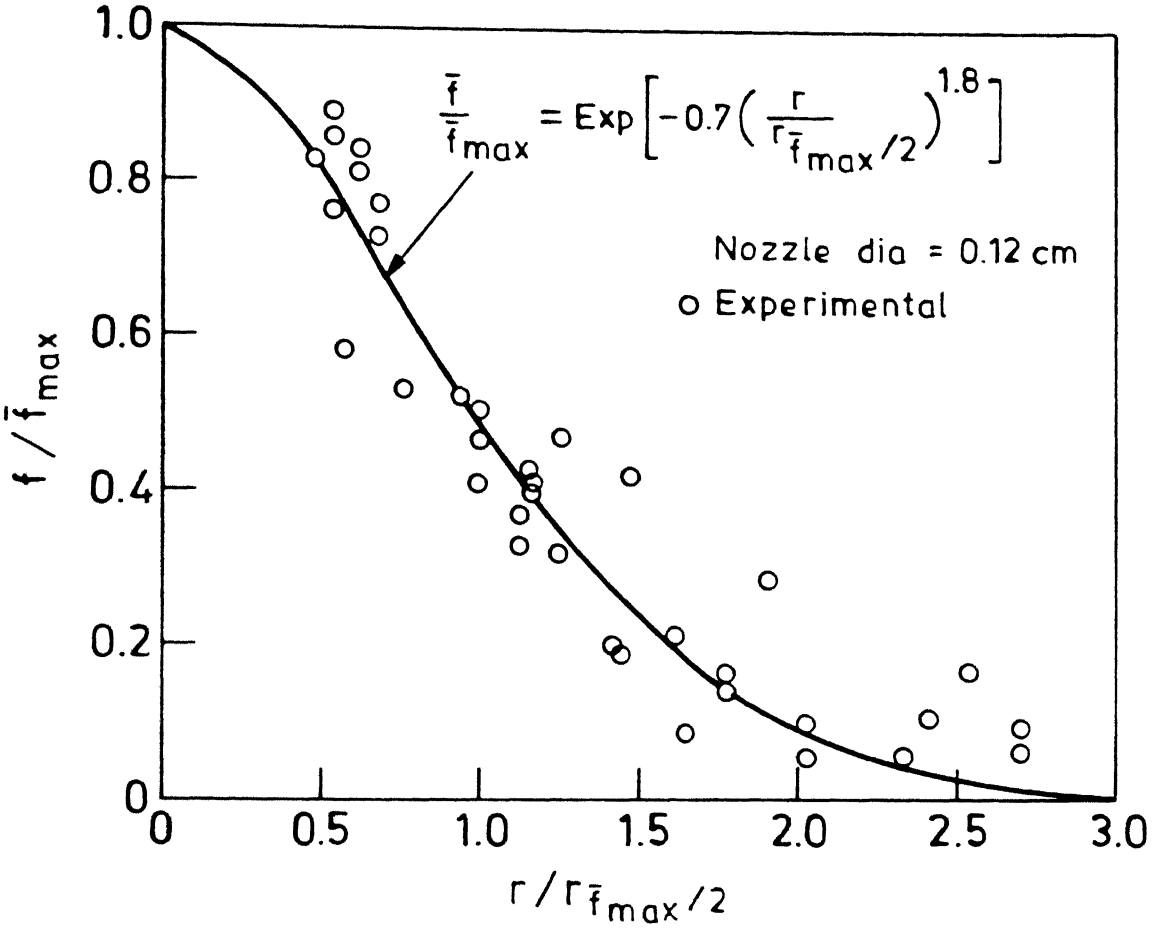

Figure 30. Normalized radial bubble frequency profiles at different axial distances from the nozzle in air/water plumes

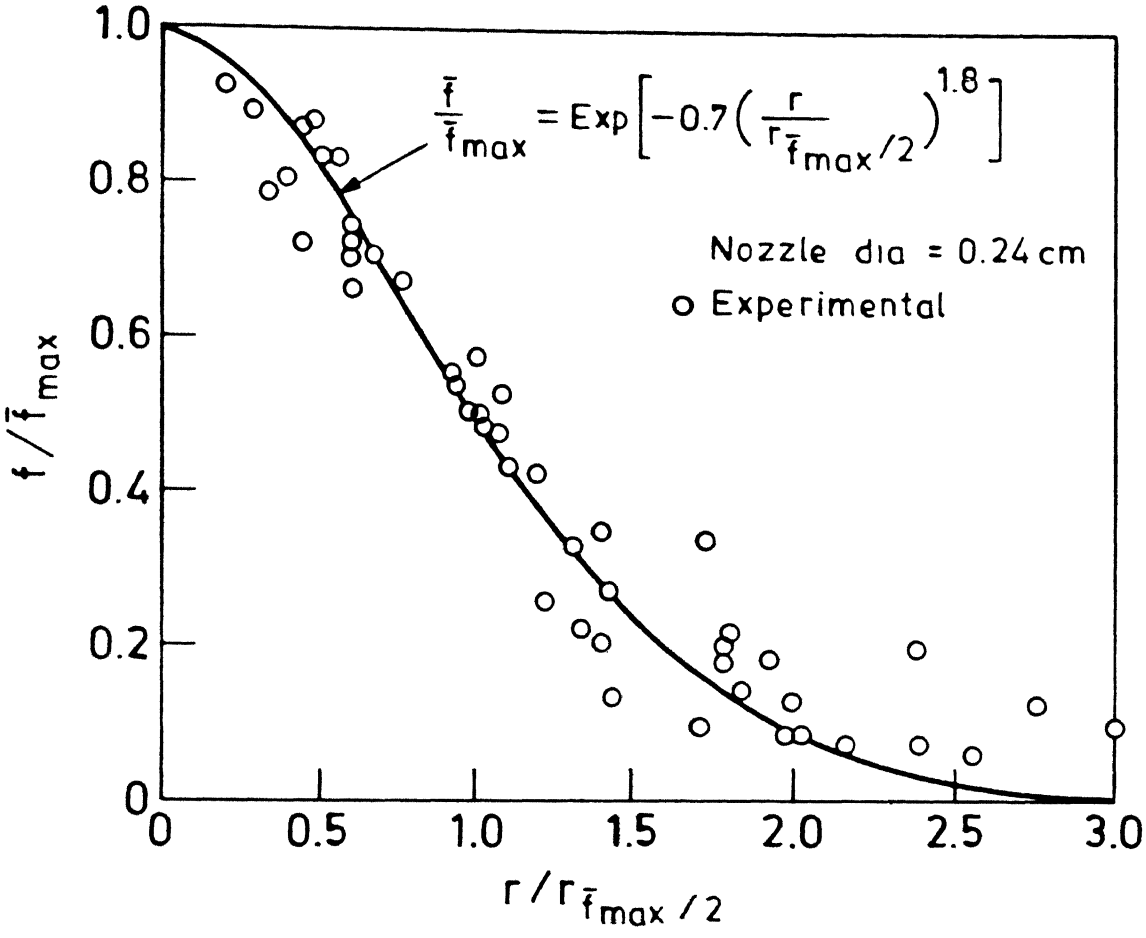

Figure 31

Normalized radial bubble frequency profiles at different axial distances from the nozzle in air/water plumes

are also some what broader than Gaussian profile[7].

5.2 Dimensionless Correlations

In order to obtain the correlation for $\bar{\varepsilon}_{max}$, and $r_{\bar{\varepsilon}\ max/2}$, an axial position, Z_o is defined as that position where $\bar{\varepsilon}$ is 50 pct.[7] According to Tacke et.al. this axial position characterizes the penetration depth or the extension of the gas core of the jet[7]. The values of Z have been found out from the Figure (25). In Figure (32), Z_o/d_o values have been plotted against the modified Froude number, $(\dot{Q}^2_g/g\ d_o^5 \rho_l)$. Following relation have been found between these two dimensionless parameters:

$$\frac{Z_o}{d_o} = 3.61 \left(\frac{\dot{Q}^2 \cdot \rho_g}{g\ d_o^5 \rho_l}\right)^{0.30} \qquad (5.3)$$

The actual value of pre-exponent is 3.60656 and that of exponent is 0.30404.

Figure (33) shows the plot between the plume half radius at Z_o, $r_{\bar{\varepsilon}\ max/2}(Z_o)$ and $(\dot{Q}^2/g)^{1/5}$. Following relation has been calculated:

$$r_{\bar{\varepsilon}\ max/2}(Z_o) = 0.32\ [(\dot{Q}^2/g)^{1/5}]^{0.97} \qquad (5.4)$$

The actual value of preexponent is 0.320659 and that of exponent is 0.96786.

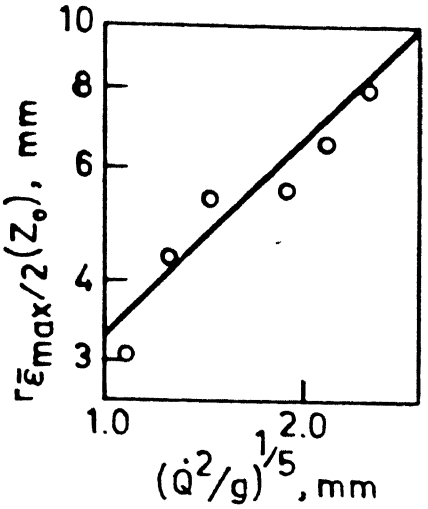

—— $r_{\bar{\varepsilon}max/2}(Z_o) = 0.32\left[\left(\frac{\dot{Q}^2}{g}\right)^{1/5}\right]^{0.97}$

o Experimental

Figure 33. Variation of $r_{\bar{\varepsilon}\ max/2}(Z_o)$ against $(\dot{Q}^2/g)^{1/5}$

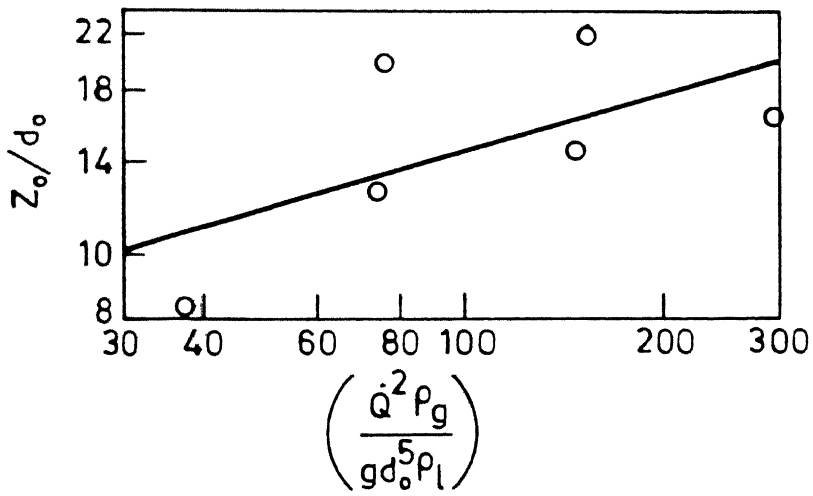

—— $Z_o/d_o = 3.61\left(\frac{\dot{Q}^2\rho_g}{gd_o^5\rho_l}\right)^{0.30}$

o Experimental

Figure 32. Variation of Z_o/d_o against $\left(\frac{\dot{Q}^2\rho_g}{g\,d_o^5\,\rho_l}\right)$

5.2.1 Correlations for $\bar{\varepsilon}_{max}$ and $r_{\bar{\varepsilon}_{max/2}}$

The equation (5.3) is transformed as follows:

$$\frac{Z}{Z_o} = 0.2772 \left(\frac{Z}{d_o}\right)\left(\frac{g\, d_o^5\, \rho_l}{Q^2\, \rho_g}\right)^{0.30404} \qquad (5.5)$$

In Figure (34), $\bar{\varepsilon}_{max}$ values have been plotted against Z/Z_o and following correlations have been found by least-square analysis method:

$$\bar{\varepsilon}_{max} = 0.51\ (Z/Z_o)^{-0.68} \qquad (5.6)$$

The actual value of pre-exponent is 0.5066 and that of exponent is 0.6847. By combining equations (5.5) and (5.6) we obtain,

$$\bar{\varepsilon}_{max} = 0.51\left[\ 0.28\ \left(\frac{Z}{d_o}\right)\ \left(\frac{g\, d_o^5 \rho_l}{Q^2\, \rho_g}\right)^{0.30}\ \right]^{-0.68} \qquad (5.7)$$

The equation (5.7) is plotted in Figure (35) along with all the experimental points derived in this investigation The plot suggests that the equation (5.7) represents satisfactorily the measured results on axial gas hold-up. The scatter of the experimental values is attributed to the experimental problems encountered during the measurement. (These problems include the influence of oscillatory motion of

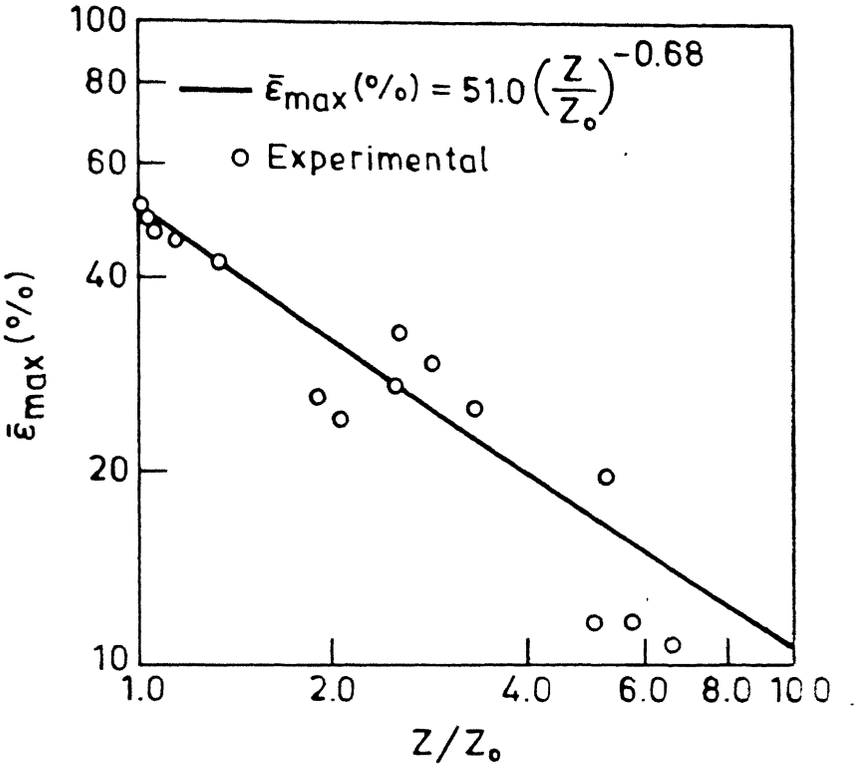

Figure 34. Variation of $\bar{\varepsilon}_{max}$ against Z/Z_o

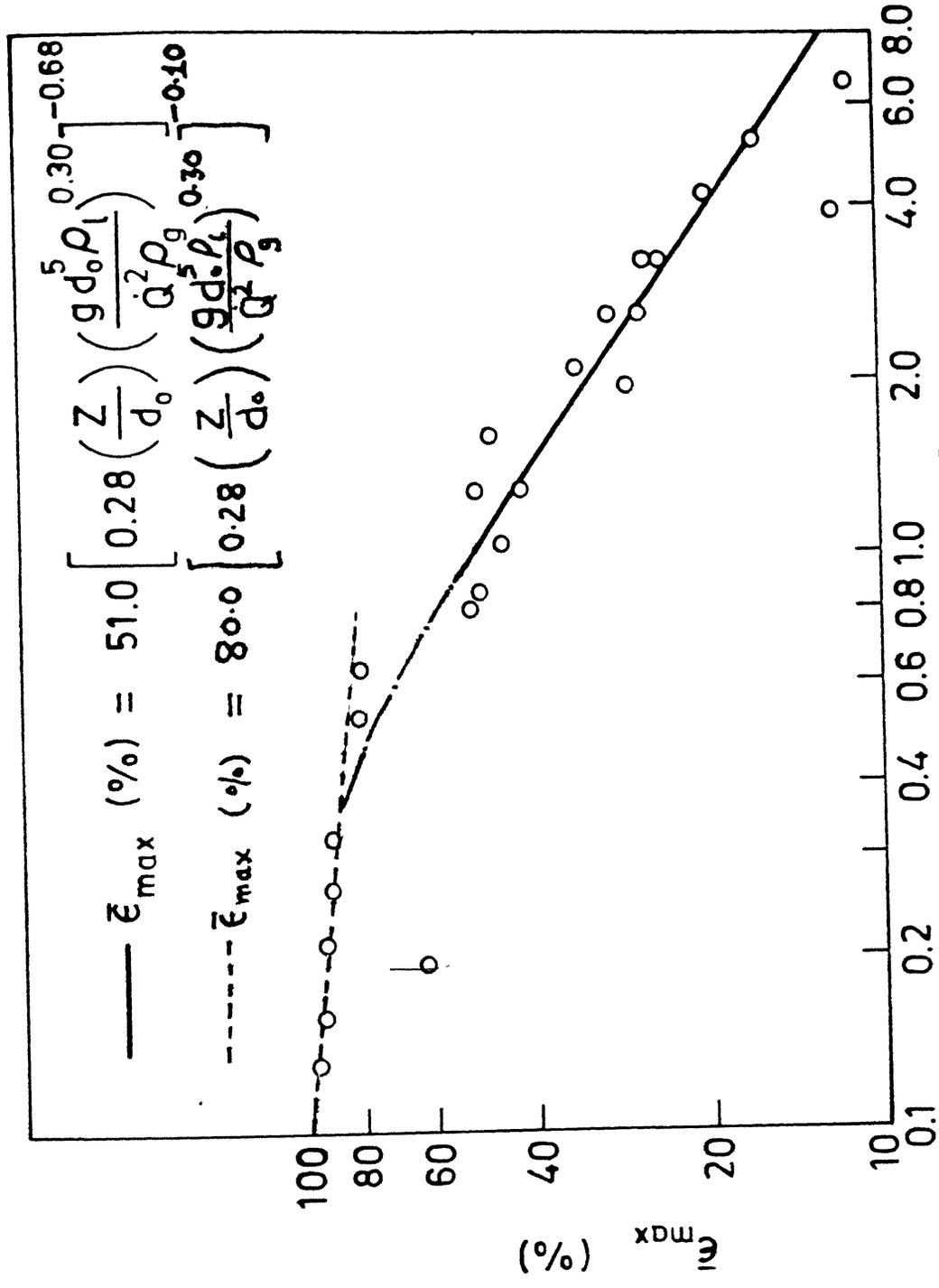

Figure 35. Axial gas concentration as a function of dimensionless distance

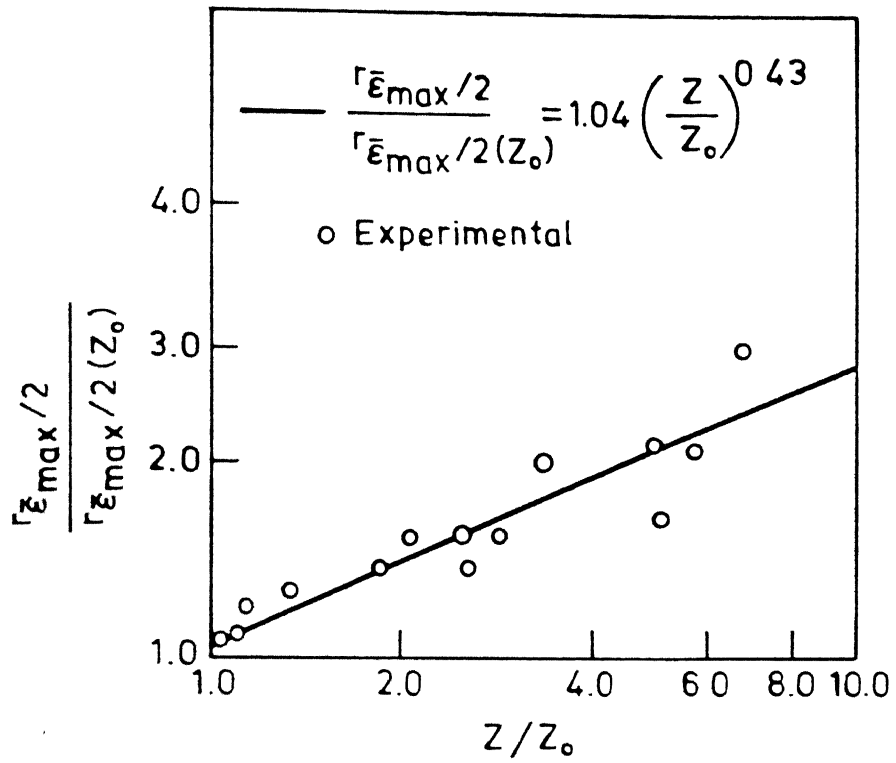

Figure 36. Variation of the ratio $r_{\bar{\varepsilon}\,max/2}$ / $r_{\bar{\varepsilon}\,max/2}$ (Z_o) against Z/Z_o

the plume on the gas holdup and use of stationary probe for measuring the properties of dynamical nature of the plume).

The Figure (36) shows the plot between ($r_{\bar{\varepsilon}\,max/2}/r_{\bar{\varepsilon}\,max/2}(Z_o)$) and ($Z/Z_o$). Following empirical correlation have been obtained by least-square analysis:

$$\frac{r_{\bar{\varepsilon}\,max/2}}{r_{\bar{\varepsilon}\,max/2}(Z_o)} = 1.04\,(Z/Z_o)^{0.43} \qquad (5.8)$$

The actual values of pre-exponent is 1.04473 and that of exponent is 0.431786.

Now substituting the value of $r_{\bar{\varepsilon}\,max/2}(Z_o)$ from equation (5.4) into equation (5.8), we obtain the following dimensionless correlation for half value radius:

$$r_{\bar{\varepsilon}\,max/2}\left(\frac{g}{Q^2}\right)^{1/5} = 0.335\left[0.28\,(Z/d_o)\left(\frac{g\,d_o^5\,\rho_l}{Q^2\,\rho_g}\right)^{0.30}\right]^{0.43} \qquad (5.9)$$

Equation (5.9) is plotted in Figure (37) along with the experimentally derived values of the half value radius. The equation (5.9) explains satisfactorily the experimental results.

Tacke et al. and Castillezose et.al. have measured axial gas hold-up and half radius by electroresistivity probes.

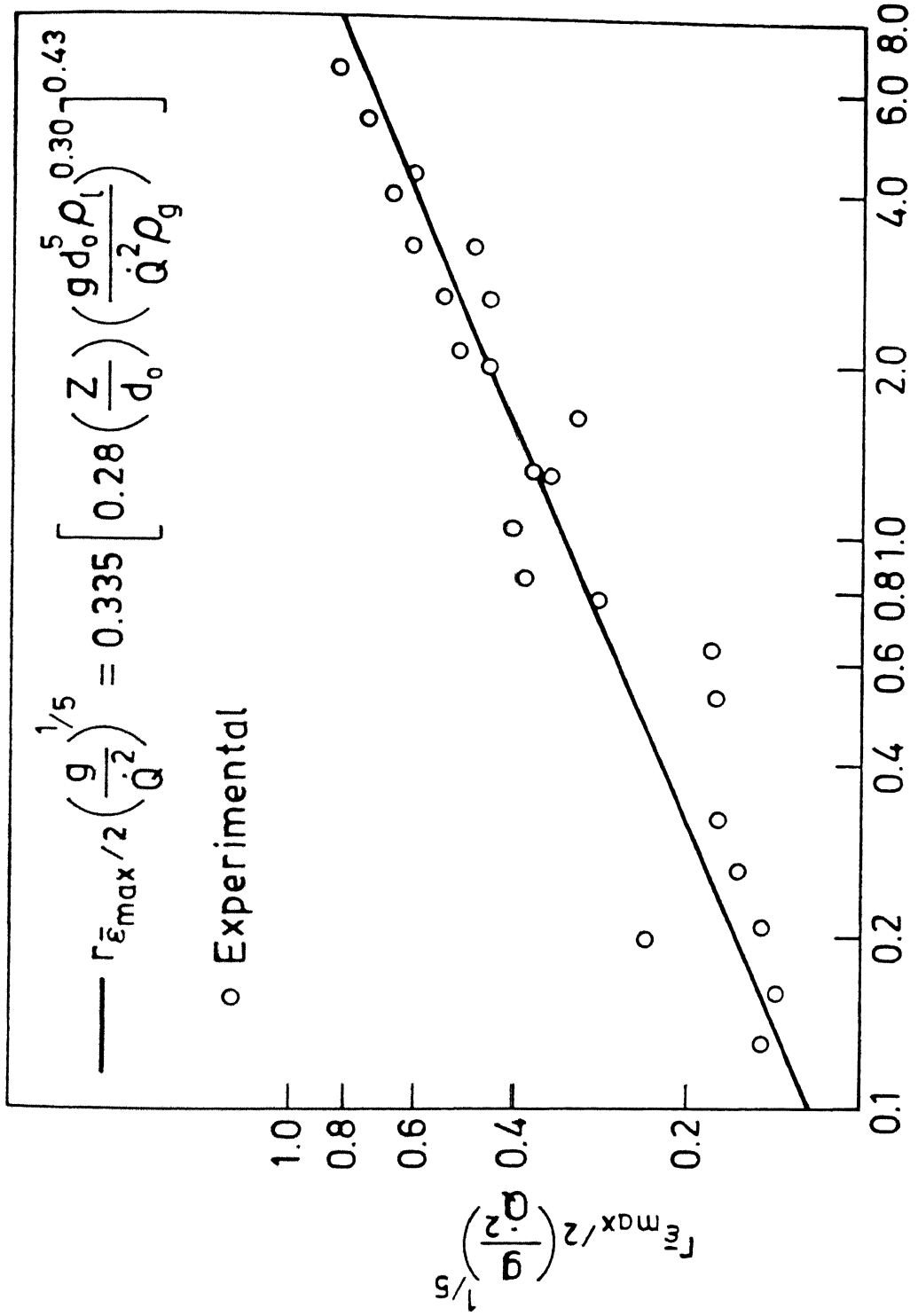

Figure 37. Dimensionless half radius as a function of dimensionless distance

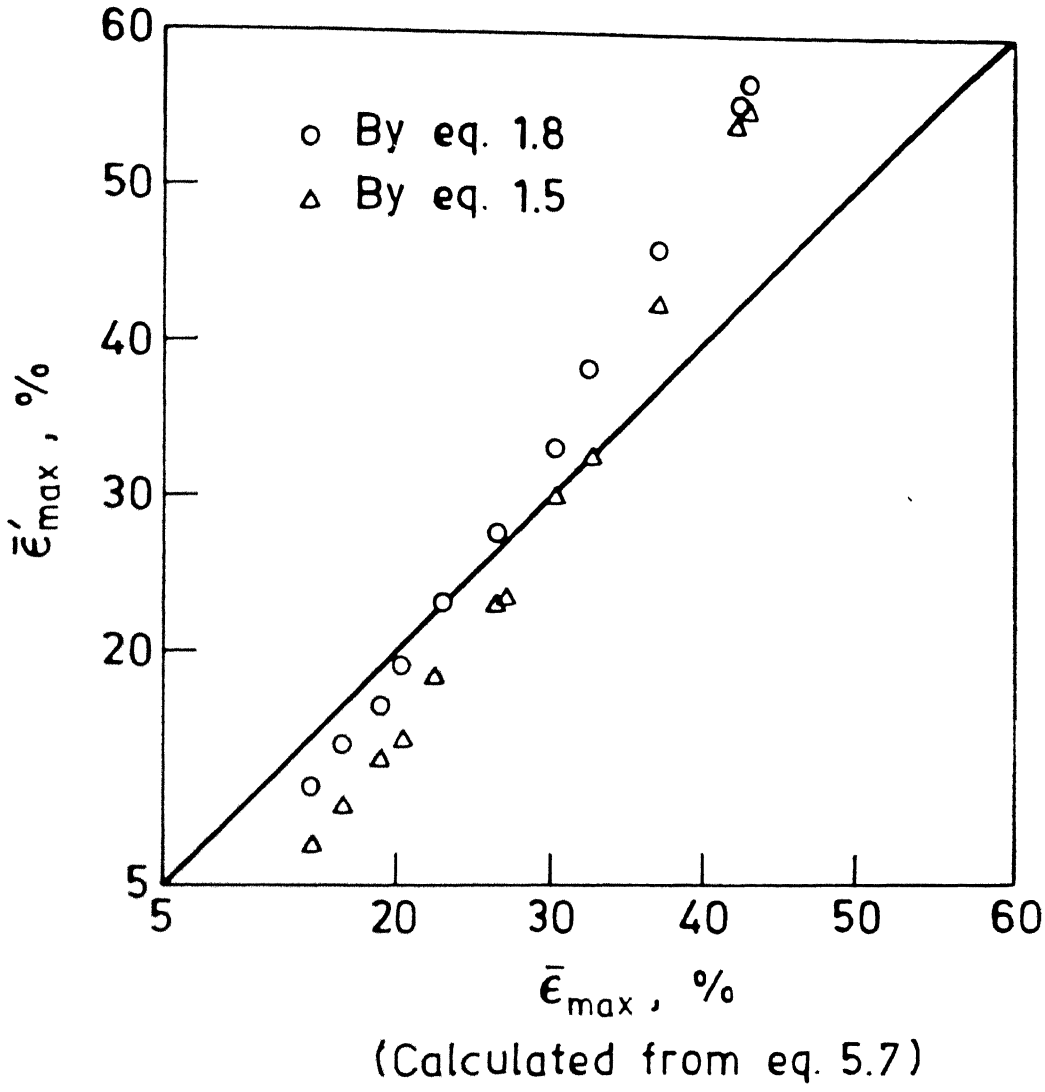

Figure 38. Comparison of calculated values of $\bar{\epsilon}_{max}$ using different equations

From the experimental results they arrived the equations which are given in the literature review (see equations (1.5), (1.6), (1.8) and (1.9)).

In Fig. (38) the calculated values of $\bar{\varepsilon}_{max}$ by equations[(1.5) and (1.8)] Literature equations are compared with those calculated by equation (5.7), derived in present investigation. The values of $\bar{\varepsilon}_{max}$ have been compared upto 50% value (because the values predicted by literature equations above, this limit was more than 100%, which is not physible). This figure shows that below 30% $\bar{\varepsilon}_{max}$, the values calculated by eqn. (1.8) are very close to those calculated by eqn. (5.7) and values calculated from equation (1.5) are somewhat lower. At higher values of $\bar{\varepsilon}_{max}$ than 30%, the values predicted by the equations (1.5) and (1.8) are considerably higher than those predicted by equation (5.7).

Figure (39) compares the values of $r_{\bar{\varepsilon}\ max/2}$ calculated by equations (1.6), (1.9) (literature equations) with those calculated by equation (5.9). The figure shows that below 1 cm. value of $r_{\bar{\varepsilon}\ max/2}$, the values calculated by all the three equations are very close. But for higher values of $r_{\bar{\varepsilon}\ max/2}$ than 1 cm, the values predicted by equation (1.6) are considerably higher.

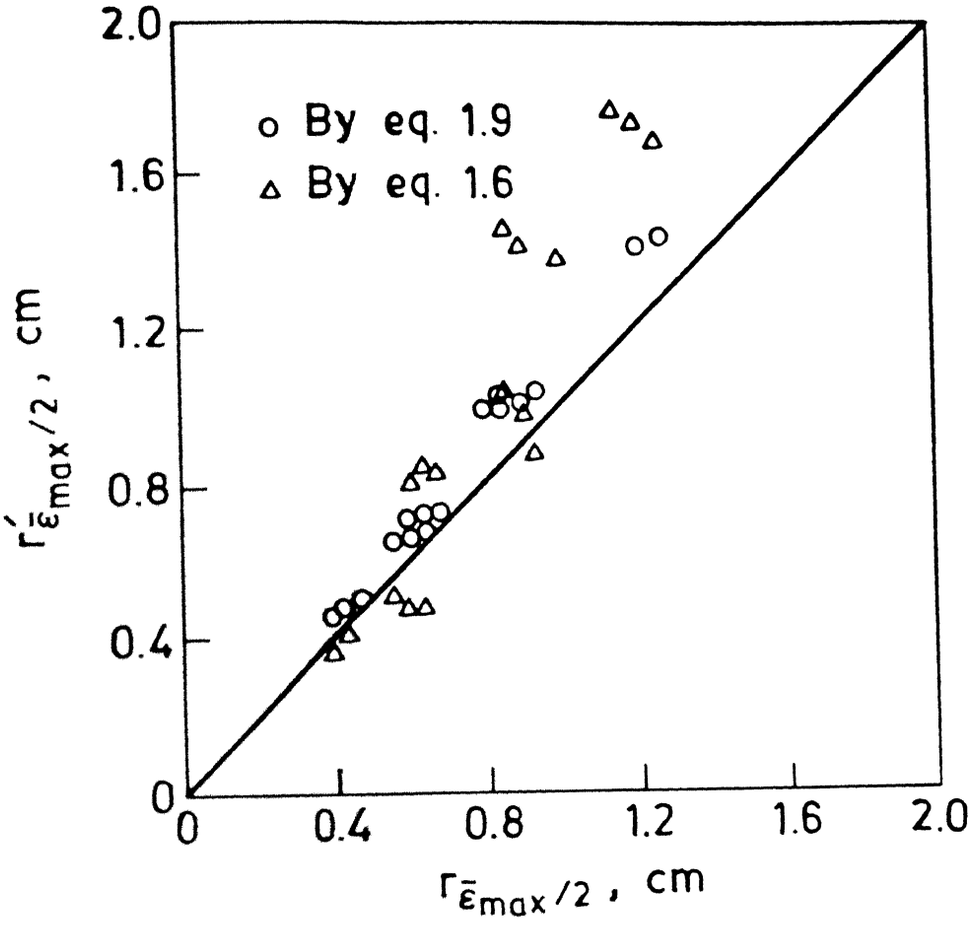

Figure 39. Comparison of half radius calculated by different equations

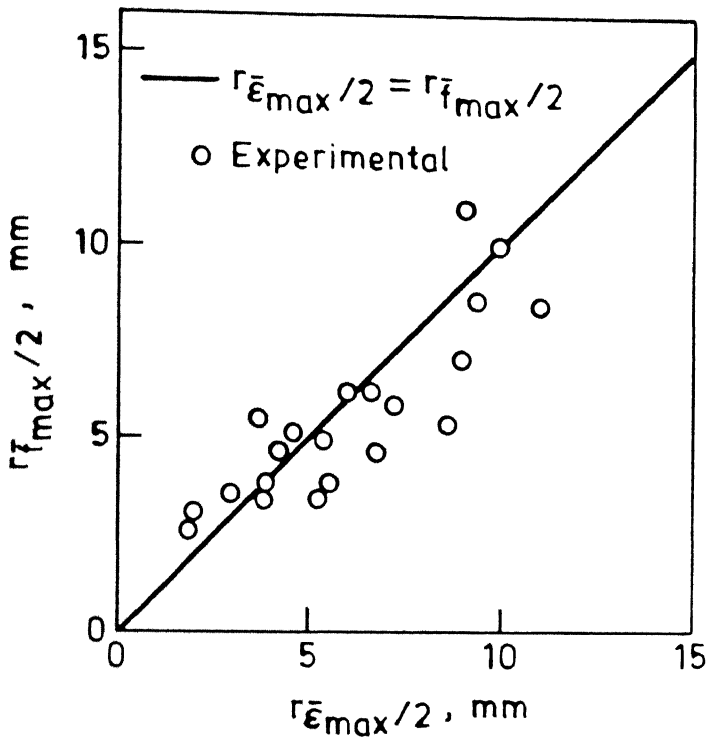

Figure 40. Comparison of $r_{\bar{f}_{max/2}}$ with $r_{\bar{\varepsilon}\ max/2}$. The line is drawn at 45°.

The comparison of the values of $\bar{\varepsilon}_{max}$ and $r_{\bar{\varepsilon}\ max/2}$ predicted by literature equations also show in the above figures that these two equations also do not predict the same values of these parameter. This is possibly due to the dynamic nature of the plume and measurement technique utilizing the stationary probe. More work is needed to predict the quantitative behaviour of the dynamic nature of the plume.

5.3 Comparison of $r_{\bar{\varepsilon}\ max/2}$ with $r_{\bar{f}_{max/2}}$

Figure 40 shows the values of $r_{\bar{\varepsilon}\ max/2}$ plotted against $r_{\bar{f}_{max/2}}$. The solid line is drawn at 45^{o}. The plot suggest that the both values are however, half radius by frequency measurement appears to be some what lower than those determined by gas hold-up measurement in some cases. Here no experimental data is available to confirm the validity of above findings.

5.4 Prediction of u_g, u_l and $\dot{V}_l$

In order to determine these properties it is necessary to determine, the average gas hold-up at any axial distance of the plume.

5.4.1 Average Gas Hold-up

The average gas hold-up, $\bar{\varepsilon}_{av.}$ is defined by the following formula:

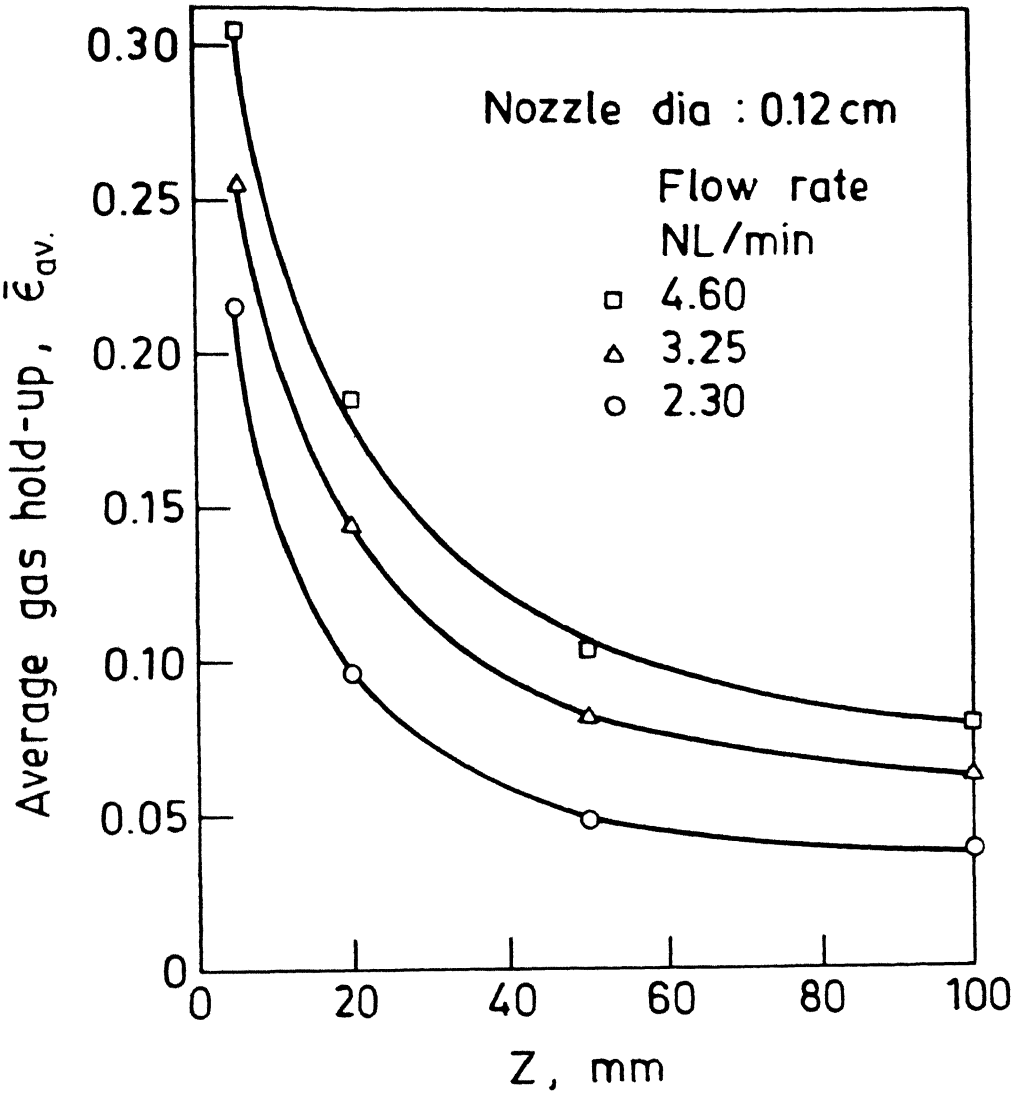

Figure 41. Plot of average gas hold-up vs. Z for nozzle diameter 0.12 cm. and 0.24 cm.

$$\bar{\varepsilon}_{av.} = \frac{\int_0^{r_p} 2\, r.\bar{\varepsilon}(r).dr}{\pi r_p^2} \qquad (5.10)$$

$\bar{\varepsilon}_{av.}$ can also be expressed as follows:

$$\bar{\varepsilon}_{av.} = \frac{\sum_{i=1}^{N} A_i \bar{\varepsilon}_i}{\sum_{i=1}^{N} A_i} \qquad (5.11)$$

Here $\bar{\varepsilon}_1$, $\bar{\varepsilon}_2$..... $\bar{\varepsilon}_N$ are local mean gas hold-up at $r = r_1, r_2....r_N$. In eq. (5.11) $\sum_{i=1}^{N} A_i \bar{\varepsilon}_i$ represents the area under the curve $\bar{\varepsilon}$ vs. r and $\sum_{i=1}^{N} A_i$ represents the total cross-sectional area of the plume (i.e. πr_p^2). The value of $\bar{\varepsilon}_{av.}$ can be calculated by finding out the area under the plots of $\bar{\varepsilon}$ vs. r. The results are tabulated in Table (5).

Average gas hold-up $\bar{\varepsilon}_{av.}$ vs. Z plots for different experimental variables have been shown in Figures 41 and 42. Figure (41) shows the relationship between $\bar{\varepsilon}_{av.}$ and Z for nozzle diameter of 0.12 cm. It is clear from this graph, that at smaller distances from the nozzle, there is a rapid decrease in the value of average gas hold-up, but at larger distances from the nozzle, the curves assumed an asymptotic nature. This graph also shows the effect of flow rate on the average gas hold-up parameter.

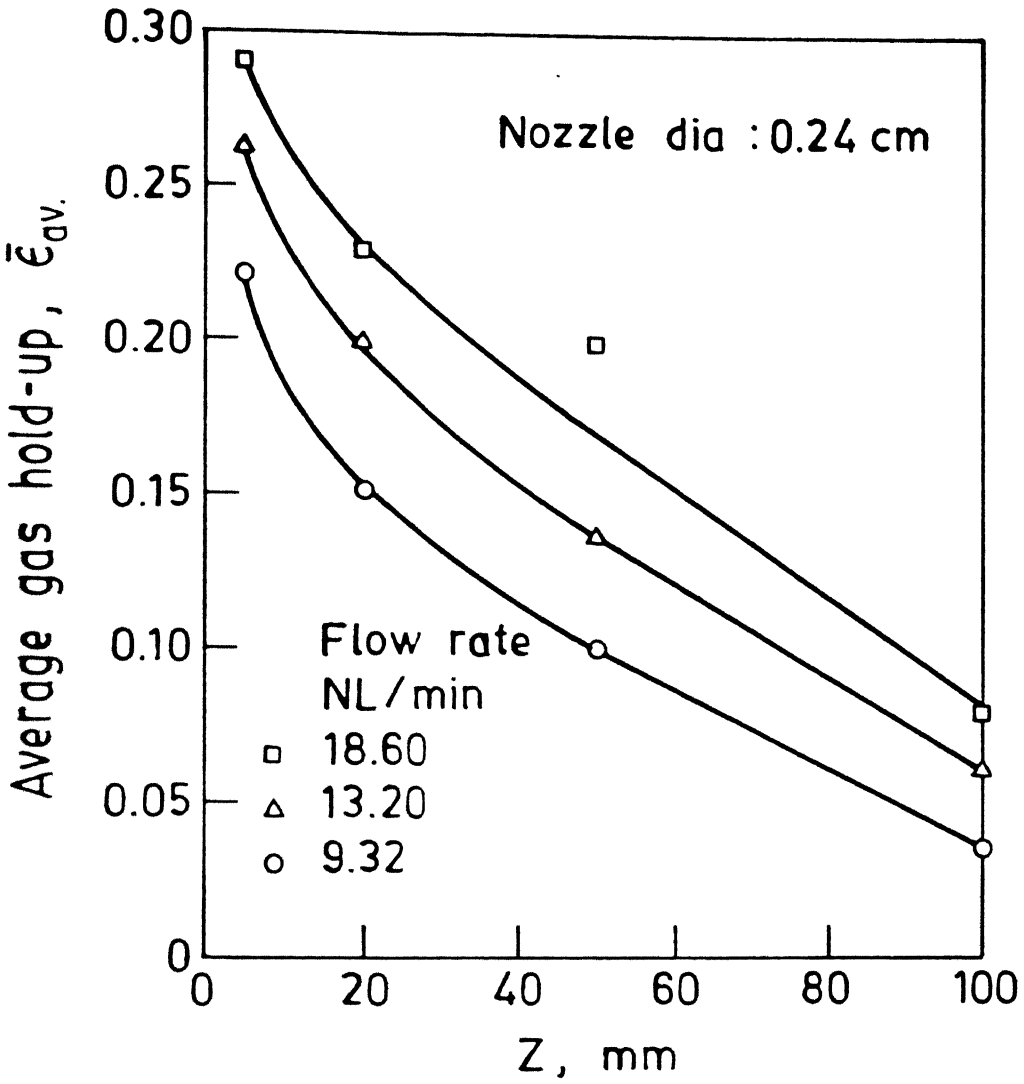
Nozzle dia : 0.24 cm
Average gas hold-up, $\bar{\epsilon}_{av.}$
0.30
0.25
0.20
0.15
0.10
0.05
0
Flow rate
NL/min
18.60
13.20
9.32
0
20
40
60
80
100
Z, mm

Figure 42

Figure (42) shows the plot between same parameters as above but for a nozzle diameter of 0.24 cm.

5.4.2 Calculations of u_g and u_l

The velocity of gas in the bubble plume zone i.e. u_g is related with plume radius, average gas hold-up and gas injection rate by following macroscopic mass balance of gas

$$\pi r_p^2 \quad \bar{\varepsilon}_{av.} \; \rho_g \cdot u_g = \rho_g \cdot \dot{Q} \qquad (1.1)$$

The relationship between u_g, u_l and $\bar{\varepsilon}_{av.}$ is given by the following equation:

$$u_g - u_l = \frac{U_g}{\bar{\varepsilon}_{av.}} = u_l = \frac{u_B}{1 - \bar{\varepsilon}_{av.}} \qquad (1.3)$$

Here u_B, the velocity of a single bubble in the liquid bath and for its calculations following equations used[5)]

$$u_B = \sqrt{0.5 \; d_B \cdot g} \qquad (5.10)$$

The bubble diameter d_B is estimated from the following correlation[5)]

$$d_B = 0.091 \left(\frac{\sigma}{\rho_l}\right)^{1/2} U_g^{0.44} \qquad (5.11)$$

Here U_g is superficial gas velocity in the plume, defined as

$$U_g = \frac{\dot{Q}}{\pi r_p^2} \qquad (5.12)$$

U_g and u_l have been calculated by using the equations (1.1), (1.3) and (5.10) to (5.12), and are enlisted in Table (6).

5.4.3 Calculations of $\dot{V}_l$

The volumetric circulating flow rate $\dot{V}_L$ of liquid in plume is obtained from the following equation:

$$\dot{V}_l = \pi r_p^2 \ (1 - \bar{\varepsilon}_{av.}) \ u_l \qquad (1.2)$$

Sano et.al. have given following relation to calculate circulating flow rate of liquid:

$$\dot{V}_l' = 1.17 \ (\dot{V}_{GM} \cdot g \cdot H_o \cdot A_p^2)^{0.339} \qquad (5.13)$$

where

$\dot{V}_{GM}$: gas flow rate at liquid temperature and logarithmic mean pressure P_m

P_m : $(P_1 - P_2)/\ln(P_1/P_2)$

P_1 : $P_2 + \rho_l \ g \cdot H_o$

P_2 : atmospheric pressure.

The volumetric circulating flow rate of water in plume zone have been calculated by using equations (1.2) and (5.13) and have been compared in figure (43). In this figure solid line is drawn at 45^o. The scattering of data on both sides of the solid line, shows that the values calculated by the two equations are comparable.

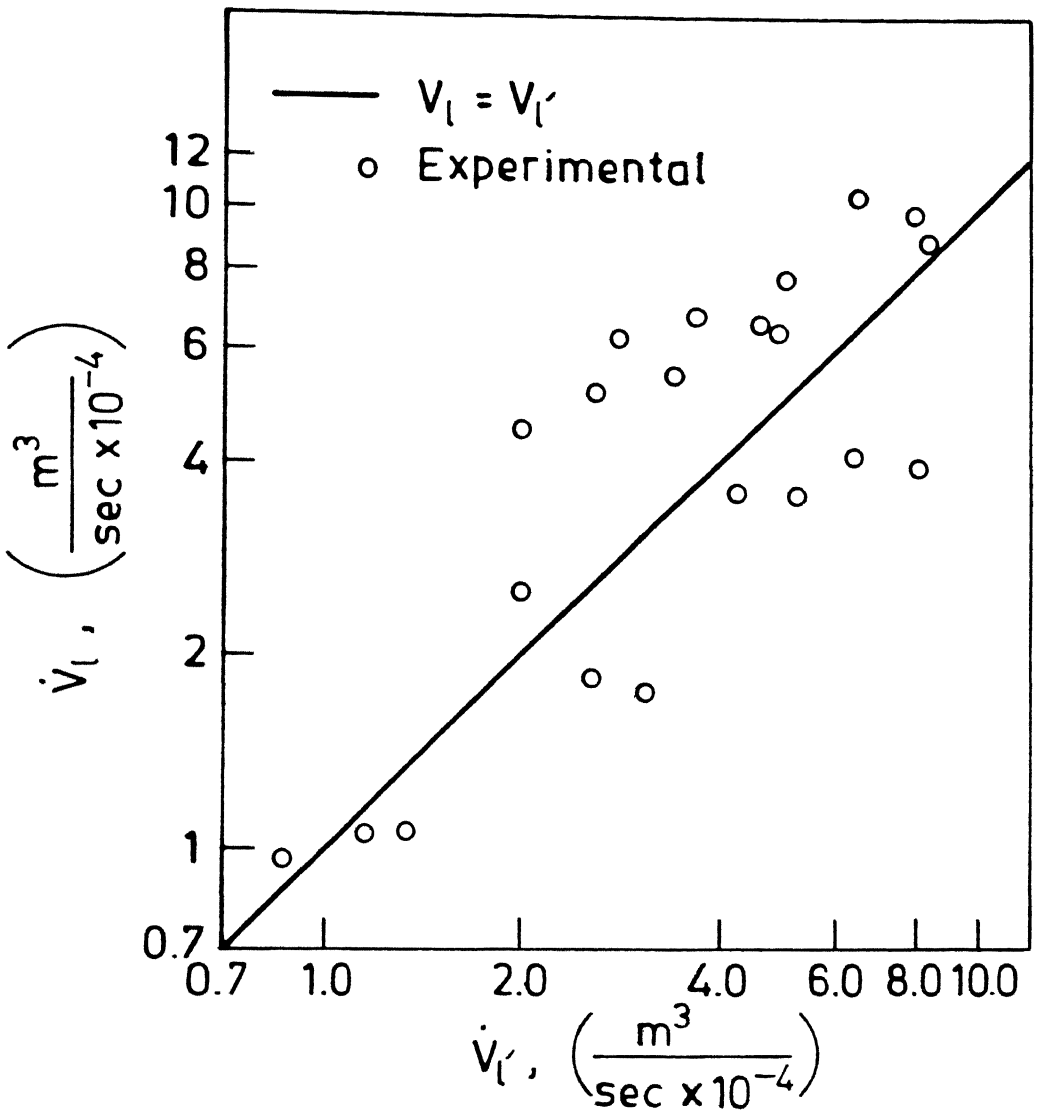

Figure 43. Comparison between volume circulating flow rate of liquid calculated by using $\varepsilon_{av.}$ $(\dot{V}_l)$ and that calculated by using gas injection rate $(\dot{V}_l)$.

CHAPTER 6

CONCLUSIONS

An experimental study was carried out to study the properties of gas bubble plume generated in the liquid by injecting gas through the bottom of a cold model bath. A self designed electroresistivity sensor probe was employed to determine the gas hold-up, bubble frequency and radius of the plume as a function of gas injection parameters for axial and radial location of the sensor probe. The sensor probe was stationary. The following conclusion are derived:

(1) Local gas hold-up and bubble frequency was found to vary at a fixed radial and axial location of the sensor probe for the constant upstream gas injection parameters within the range of present investigation. This phenomena was due to the oscillating motion of the axis of the bubble plume.

(2) The gas hold-up and bubble frequency profiles were successfully correlated by the following fraction

$$Y = \exp\left[-0.7 \left(\frac{r}{r_{1/2}}\right)^{1.8}\right]$$

where for, $Y = \bar{\varepsilon} / \bar{\varepsilon}_{max}$, $r_{1/2} = r_{\bar{\varepsilon}\ max/2}$

and for, $Y = \bar{f}/\bar{f}_{max}$, $r_{1/2} = r_{\bar{f}_{max}/2}$.

This function was found to valid at all downstream axial distances and upstream gas injection parameters.

(3) The cone angle of the bubble plume was measured and found to be 17.4^{o}. for 0.12 cm diameter nozzle and 20.6^{o} for 0.24 cm nozzle diameter.

(4) Axial gas hold-up and half plume radius were successfully correlated with the Froude number and downstream axial distance.

(5) From the results obtained on plume radius and gas hold-up, calculations were made for circulating flow rate of liquid, liquid velocity and gas velocity in the plume.

Suggestions for Further Work

Further the work may be done along the following lines:

(1) It is suggested to measure the properties of the plume in other systems like argon/mercury, helium/mercury and helium/water.

(2) A direct measurement on liquid and gas velocities is also worthwhile to undertake.

(3) It is suggested that more than one sensor probe should be used in order to take readings simultaneously at various locations in the bath.

REFERENCES

1. G.G. Richards, J.K. Brimacombe and G.W. Toop, Met. Trans., Vol. 16B, Sept. 1985, pp. 513-549.

2. Masamichi Sano and Kazumi Mori, Trans. Iron and Steel, Japan, 23 (1983).

3. Masamichi Sano, Hiroshi Makino, Yasuhisa Ozawa and Kazumi Mori, Transactions, ISIJ, Vol. 26, 1986.

4. K.W. Lange, International Materials Review, Vol. 33 (1988), 2, 33-89.

5. D.J. Nicklin, Chem. Eng. Sci., 17 (1962), 693.

6. M. Sano and K. Mori, Trans. ISIJ, 20, (1980), 675.

7. K.H. Tacke, H.G. Schubert, D.J. Weber and K.Schwerdtfeger, Met. Trans., 16B (1985), 263.

8. A.H. Castillejos, J.K. Brimacombe, Met. Trans., 18B (1987), 659.

9. Gunter Ebneth and Wolfganj Pluschkell, Steel Research, 56 (1985), 10, pp. 513-518.

10. Hajime Nashiwa, Susumu Yamaguchi, Mitsunobu Sato, Koji Idea and Minoru Ishi Kawa, 65th Steelmaking Conference Proceedings, Vol. 65, Pittsburgh Meeting, March 28-31, 1982, page 282-286.

11. Y. Sahai and R.I.L. Guthrie, Met. Trans., Vol. 13B, (1982), 193.

APPENDIX 1

TABLES

Table 1 : Calibration Data for the Flowmeter

S.No.	cm. of Hg.	Time for flow of 10 lit gas (sec)	Flow rate lit./min.
1	0.6	139.5	4.3
2	1.3	82.3	7.3
3	2.1	62.5	9.6
4	2.9	51.7	11.6
5	3.7	46.1	13.0
6	5.2	38.2	15.7
7	6.3	34.9	17.2
8	7.3	32.8	18.3
9	8.9	29.4	20.4

TABLE:2
SYSTEM : AIR/WATER
Nozzle Diameter : Ø.24cm

r (mm)	Chart speed ms/div.	No. of waves developed per ten div. on oscilloscope	No. of small div. for which gas is present at the tip of probe per fifty small div.
		FLOW RATE : 9.32NL/MIN	
		Z= Ø.5 cm	
Ø	2Ø	9-6-9-9-8-8-9-8-8-7-8-8 9-11-7-1Ø-7-9-8-1Ø-9-8-8-7-9-11-8-7-9-8	31-28-31-28-31-35-29-31-28-3Ø-31-32-29-31-32-28-27-33-3Ø-28-32-3Ø-29-3Ø-28-32-31-29-28-31-
2.3	2Ø	12-7-8-8-7-8-9-9-6-8-6-6-7-8-7-6-7-8-8-6-6-6-8-6-6-7-6-9-7-7	22-28-23-17-26-28-23-22-28-23-24-27-23-27-24-21-22-28-24-26-21-24-2Ø-19-18-23-24-21-23-22
5.1	5Ø	11-11-11-9-13-4-1Ø-9-9-1Ø-1Ø-11-9-13-12-11 13-9-11-1Ø-9-1Ø-9-1Ø-11-9-9-13-9-11-	14-14-15-12-14-14-13-14-13-14-12-14-11-13-12-14-1Ø-15-14-14-12-13-15-14-14-14-13-14-15-13-
7.5	1ØØ	7-4-8-5-6-6-6-7-5-7-5-5-3-4-5-5-8-6-7-7-3-7-5-7-5-5-8-6-5-7-	2-1-4-1-2-1-2-Ø-2-2-3-3-2-1-2-2-1-4-Ø-Ø-1-2-2-Ø-3-1-2-Ø-2-1
		Z = 2.Ø cm	
Ø	2Ø	1Ø-8-8-8-8-9-1Ø-9-1Ø-13-12-12-8-8-1Ø-8-8-1Ø-8-8-9-12-13-8-8-1Ø-12-9-1Ø-1Ø-	24-26-25-25-27-25-27-27-27-27-25-27-27-26-24-24-26-24-27-27-27-24-28-27-26-26-23-26-
3.Ø	2Ø	6-1Ø-6-6-8-8-8-6-5-8-6-1Ø-6-6-5-7-7-6-6-6-8-9-6-6-8-8-7-8-6-7-	23-23-25-25-24-22-17-26-16-18-19-18-19-16-19-2Ø-15-2Ø-24-21-2Ø-17-18-21-18-23-18-21-21-
6.6	5Ø	1Ø-9-8-8-7-6-8-7-8-8-6-6-9-8-7-8-9-1Ø-9-8-9-8-7-9-6-8-8-7-9-6-	1Ø-9-13-7-8-11-13-9-11-9-13-8-9-7-13-14-11-13-13-8-1Ø-9-8-9-1Ø-11-13-11-12-13-
8.6	1ØØ	6-3-3-8-4-3-3-3-6-8-7-5-4-3-3-6-4-5-4-5-5-3-6-5-4-7-4-3-6-3-	7-2-4-4-3-1-2-4-2-6-1-2-2-2-2-2-2-2-3-4-3-4-2-2-2-7-1-2-2-3-
		Z = 5.Ø cm	
Ø	2Ø	7-8-9-8-1Ø-16-8-1Ø-9-11-6-7-11-8-7-9-12-7-9-11-7-8-8-11-8-6-9-7-6-7	15-13-14-11-12-15-12-15-12 1Ø-12-11-14-12-15-15-14-15-14-14-13-14-16-15-13-15 12-12-13-16

4.1 5Ø	14-9-8-13-12-13-8-9-13 12-9-13-14-9-1Ø-11-14-13 11-13-11-9-12-13-11-13 11-13-13-11	12-1Ø-1Ø-1Ø-13-12-12-13-13 13-13-12-12-9-12-12-12-1Ø 11-12-1Ø-13-9-12-13-9-12- 11-13-1Ø-
8.1 5Ø	4-4-4-2-2-4-2-2-1-4-3-4- 5-4-4-2-2-4-1-4-2-3-4-2- 4-2-2-3-4-4-	1Ø-6-8-4-6-7-8-4-1Ø-5-4- 9-1Ø-1Ø6-2-8-8-3-6-9-8-6 3-4-5-7-7-1Ø-2
12.1 1ØØ	5-4-1-5-5-6-6-7-5-5-3-7- 5-5-6-7-2-4-5-7-11-4-5-6 5-5-1-7-6-5-	7-5-5-6-3-5-8-11-6-6-2-7- 7-8-7-4-3-6-4-8-4-6-8-5-4- 7-4-9-5-7
14.7 1ØØ	3-4-5-1-5-4-5-4-4-3-5-2- 3-6-3-3-8-5-2-4-1-1-2-5- 1-3-3-5-3-1-6	2-6-3-1-6-4-3-4-2-2-4-1-2- 3-2-1-8-6-2-2-Ø-5-Ø-2-4-3 3-3-Ø-4-3

Z = 1Ø.Ø cm

Ø 5Ø	7-7-5-3-4-6-6-8-8-6-4-4 9-6-9-7-5-7-7-7-5-4-6-7 5-5-8-6-7-6-	6-6-7-5-5-8-7-7-6-5-3-4- 8-4-7-4-4-7-4-6-5-6-7-7- 4-5-8-7-5-6
5.1 5Ø	6-6-6-3-4-6-6-3-4-7-6-7 5-5-3-3-3-4-5-5-5-2-8-6 4-4-6-3-5-4-	6-6-7-3-6-4-3-4-6-8-4-5- 7-7-2-7-3-2-4-4-6-4-3-5 5-6-3-5-6
1Ø.1 1ØØ	12-16-5-12-1Ø-8-6-1Ø-1Ø- 6-9-8-9-6-12-1Ø-12-9-4-6 7-7-8-6-12-7-6-11-7-9	5-7-4-4-4-3-2-4-3-3-3-3- 3-2-5-5-4-3-2-2-3-4-3-3- 5-3-3-5-4-3
15.1 1ØØ	7-6-6-7-1Ø-9-4-5-7-4-6-8 6-8-8-4-5-6-2-5-6-9-7-5- 4-5-7-6-5-6-	2-3-3-3-3-4-2-2-3-3-2-4-3 3-3-1-2-5-3-4-1-2-2-3-3-2 4-2-3-3
2Ø.1 1ØØ	1-3-Ø-2-2-2-2-3-2-2-4-2 2-2-5-4-3-4-3-4-2-4-3-Ø 6-3-4-2-4-2	1-Ø-Ø-2-2-Ø-1-1-1-1-2-2-1 1-3-2-1-2-1-1-1-2-1-Ø-Ø-3 2-1-2-Ø

FLOW RATE: 13.2 NL/MIN

Z = Ø.5 cm

Ø 1Ø	9-8-8-14-1Ø-8-6-1Ø-8- 9-7-1Ø-8-7-1Ø-9-9-8-9 8-12-7-9-8-9-9-8-8-9	47.5-47.5-47-46-48-48-48- 46-48-48-47-47-47.5-48-47 48-47-46-47.5-48-47-48-47 48-48.5-47-48-47-48-47
1.Ø 1Ø	7-5-1Ø-6-8-9-11-6-8-9 9-11-5-1Ø-6-3-5-13-12 17-5-11-5-8-6-7-7-8-9-8	38-47-37-45-43-4Ø-39-43- 43-39-42-46-43-45-46-45 39-4Ø-45-46-4Ø-46-41-42 45-45-46-47-44-45
2.Ø 1Ø	8-7-6-6-8-5-7-5-8-9-9 5-8-1Ø-12-6-8-11-3-6- 6-7-6-8-8-6-6-7-7-8	33-27-32-32-27-29-27-28 32-29-29-28-29-32-3Ø-33 28-31-33-26-28-29-3Ø-33 31-29-34-29-31-33
4.Ø 2Ø	6-7-8-7-6-1Ø-7-6-9-9 8-9-7-7-8-9-1Ø-7-9-8 7-9-8-1Ø-6-1Ø-8-7-6-5	25-26-21-22-18-23-23-18 13-22-23-19-21-2Ø-18-17 19-17-18-17-17-21-22-2Ø 14-18-21-22-19-14
7.Ø 2Ø	4-4-4-2-2-4-4-3-4-3-2 5-3-2-3-4-3-3-3-2-4-3- 3-2-4-3-3-3-4-3-	8-8-6-6-5-6-7-9-8-7-7-8 4-7-6-7-4-5-4-9-8-7-8-4 9-5-7-6-8-4
7.84 2Ø	4-1-1-2-2-1-Ø-Ø-2-1-1-	4-1-1-4-2-1-Ø-Ø-4-2-1-1

		1-1-1-1-1-3-2-1-2-1-2- 3-Ø-2-Ø-1-2-Ø-1	1-4-1-1-6-4-4-3-3-2-6-Ø 5-Ø-6-2-Ø-2
		Z = 2.Ø cm	
Ø	1Ø	9-8-9-11-9-7-6-9-7-6-6. 7-9-11-6-4-11-6-8-1Ø-8 7-9-7-7-1Ø-8-9-8	39-43-4Ø-4Ø-42-35-41-43 37-36-42-44-44-42-4Ø-42 35-41-38-38-44-42-44-35 38-42-4Ø-41-4Ø
2	1Ø	8-8-5-5-1Ø-8-7-6-6-8-5 6-8-8-5-5-5-7-12-7-7-7 4-6-6-4-6-8-8-7	27-31-34-22-27-27-32-29 19-18-31-34-3Ø-26-29-35- 32-21-31-32-27-25-25-34 33-35-29-37-29-28
4	2Ø	12-6-8-7-8-9-7-7-8-8-8 8-12-7-8-8-8-5-9-6-5-9 9-6-7-8-7-8-6	18-23-18-18-19-16-2Ø-22 24-21-19-21-25-24-19-21 16-13-18-16-19-25-25-23 2Ø-17-22-22-15-18
7	5Ø	12-6-8-9-7-8-1Ø-1Ø-9-8 8-6-12-5-9-8-6-8-1Ø-7 6-8-8-7-6-5-6-9-1Ø-7	15-12-12-12-11-9-13-11 11-1Ø-12-9-12-7-12-9-7 6-16-9-8-13-11-8-6-9-13 7-9-6
1Ø	1ØØ	3-3-6-7-4-7-6-2-7-7-3 6-3-4-4-6-4-7-4-3-6-5 5-4-3-8-5-3-2-6	3-1-3-5-3-3-2-1-5-3-1-1 1-4-2-2-2-6-3-4-3-1-3-1 1-7-2-2-2-3
		Z= 5.Ø cm	
Ø	1Ø	5-1Ø-7-6-8-7-7-5-6-1Ø 7-5-8-6-3-7-12-4-8-6 1Ø-8-5-5-6-7-6-9-8-8	25-25-24-3Ø-29-11-26-21 28-15-3Ø-25-2Ø-24-27-19 3Ø-27-1Ø-18-21-17-31-31 25-26-17-19-19-29-14-31 28
2	2Ø	9-17-14-11-7-1Ø-13-5 8-9-11-5-1Ø-7-13-1Ø-6 1Ø-8-16-11-1Ø-9-4-14	13-17-15-23-22-17-17-27 11-26-25-3Ø-9-9-12-16-19 11-16-25-22-26-17-2Ø-23 13-16-22-28-23-12-16-14 21
5	2Ø	1Ø-9-5-9-6-4-11-6-9-7 6-8-13-8-6-11-12-6-1Ø 1Ø-8-6-6-6-8-6-9-6-5 8-7-2-5-7-6	23-18-13-1Ø-1Ø-1Ø-15-19 21-22-6-1Ø-12-19-14-11-17 9-18-13-21-13-8-15-11-17 12-12-6-11-17-9-11-18-16
8	2Ø	6-5-7-5-3-3-4-7-8-5-3 6-3-2-5-5-4-4-9-4-5-3 5-4-8-2-3-5-2-7-5-6-3 5-4	5-2Ø-18-5-9-14-16-9-11-8 8-18-14-12-3-7-8-8-19-11 6-8-4-3-6-13-11-15-18-7 8-12-8-1Ø-8
11	5Ø	6-2-5-8-6-6-4-1Ø-6-12 8-12-6-7-5-1Ø-6-8-5-4 5-7-9-1Ø-1-9-8-6-1Ø-5 1Ø-5-5-1Ø-9	6-2-9-14-8-7-6-11-12-9-8 11-5-13-6-9-4-5-4-3-3-13 8-8-1-1Ø-1Ø-7-1Ø-6-13-2-6 7-8
14	5Ø	Ø-6-4-3-4-1-4-4-5-6-3 4-3-5-6-6-2-3-6-3-1-1 3-3-4-Ø-3-1-4-4-5-6-5 1-2	Ø-1Ø-2-3-4-5-6-9-8-6-4-2 2-2-3-8-4-6-6-7-3-1-7-7-6 Ø-2-2-4-5-5-3-4-2-4

z = 10.0cm

0 20	6-3-4-3-8-5-6-5-9-4-3 4-6-6-4-3-3-4-6-8-5-6 3-8-5-6-6-5-4-3	14-16-18-5-15-13-16-14-19 13-13-7-9-12-20-6-6-12-10 16-14-16-13-12-12-12-9-14 10-12-10
2 20	6-4-5-4-4-4-7-5-4-6-3 5-3-6-1-6-4-7-7-3-5-4 5-6-4-6-4-4-3-4-6-5-5 3	11-11-18-12-8-12-4-7-13-12 12-9-6-15-11-11-10-11-9-13 8-12-11-8-11-7-7-11-10-5- 11-8-8-13-10
6 20	6-3-7-3-4-3-4-2-3-5-2 3-5-4-6-2-2-2-4-4-5-5 3-4-6-2-4-3-2-5	10-15-9-12-8-3-11-5-6-8-6 8-15-6-7-5-9-2-10-8-13-9- 5-9-7-10-9-10-9-7
10 50	11-4-11-5-9-9-4-7-8-5 4-7-8-9-6-10-10-5-9-6 5-9-7-10-7-8-7-8-4-9	8-3-5-59-7-3-4-6-4-4-4-10 5-5-9-11-6-8-5-5-9-7-4-4 5-6-8-5-7
14 50	9-8-0-7-8-5-4-2-4-5-3 4-2-11-6-5-2-7-5-0-4 5-5-3-5-4-5-3-4-7	8-5-0-7-5-7-52-3-7-7-2-1 8-4-4-6-3-3-0-3-5-7-3-0 6-2-5-4-7
18 50	2 3-5-1-1-6-4-0-3-0-1 7-2-3-2-4-2-1-4-3-3-1 2-4-0-4-3-2-3-5	1-1-3-5-3-4-2-0-3-0-2-3 1-2-3-5-4-0-3-4-3-2-
20 100	6-0-1-5-6-4-4-1-5-1-6 3-4-4-3-0-3-3-3-3-4-5 4-2-1-3-2-6-4-2	3-0-0-3-2-1-4-2-4-2-4 1-3-1-1-0-1-1-2-2-2-3 2-2-0-1-3-1-1-4

continued.....

FLOW RETE = 18.6Ø NL/MIN

Z = Ø.5 CM

Ø	1Ø	9-1Ø-9-8-8-7-1Ø-8-5-8-8-7-5 1Ø-7-11-8-6-5-6-8-9-4	45-45-46-47-45-47-44-48-47-48 49-47-49-47-47-46-45-47-49-48
2.1	1Ø	8-4-6-8-4-5-5-8-5-8-5-1Ø-6 6-8-6-9-7-6-9-6-7-6-6-6-6 6-7-5-6-5-8-9	43-44-45-44-46-45-44-43-45-42 45-44-44-44-46-4Ø-45-43-45-42 45-44-44-44-46-4Ø-45-43-46-46 44-45-43-43-43-44-41-45-43-43
4.1	2Ø	9-12-8-12-12-11-6-12-8-1Ø 11-11-9-1Ø-1Ø-1Ø-11-1Ø-12 1Ø-11-9-9-1Ø-11-13	18-22-2Ø-2Ø-18-24-17-14-27-23-17 19-24-2Ø-19-18-22-21-17-16-22-18 21-17-23
5.8	2Ø	7-5-7-7-7-5-5-7-7-9-9-6-7 7-6-7-8-5-1Ø-5-8-6-8-7-9 1Ø-6-9-11-8-8-8-8-6-8-5	12-12-13-15-14-8-9-13-16-19-12 13-13-15-11-13-12-9-11-13-11-12 13-11-14-12-8-13-11-14-11-14-18 1Ø-11-9
6.68	2Ø	4-4-4-5-5-5-5-4-4-2-2-2 5-5-4-4-2-5-2-3-3-4-3-4 5-3-4	6-4-3-9-7-12-3-7-5-11-2-6-9-7-7 4-7-3-7-5-8-6-6-9-7-6-4-6

Z= 2.Ø Cm

Ø	1Ø	4-11-6-9-9-9-6-11-9-7-8 7-9-8-6-13-6-9-12-5-9-1Ø 8-12-9-7-8-12-11	4Ø-41-43-39-4Ø-39-43-42-4Ø-43-41 41-42-38-41-42-39-39-43-39-4Ø-39 41-42-43-4Ø-39-42-39-41-42-39-41 42-43-39-43
2.8	2Ø	8-1Ø-7-9-12-9-12-11-8-8 11-6-8-8-9-11-9-8-9-6-8 7-12-1Ø-8-9-9	24-27-29-28-26-23-3Ø-28-21-25-23 23-26-29-29-28-26-26-28-26-24-27 29-29-28-24-26
6.7	5Ø	1Ø-8-8-13-12-8-9-1Ø-12 7-1Ø-7-8-11-9-8-8-8-9 9-8-7-6-1Ø-8-7-6-8-8-8 8-5-1Ø-8-1Ø-6-8-1Ø	17-12-12-13-13-12-13-15-16-1Ø 1Ø-9-14-14-13-13-1Ø-18-11-13-16 1Ø-13-11-1Ø-18-13-12-1Ø-9-12-12 9-14-12-13-14-9-14
9.3	1ØØ	7-3-5-3-4-4-7-5-5-6-7 5-4-5-4-6-5-5-5-6-5-5 5-6-7-3-7-5-6-7-7-5-6 4-6-5	7-4-3-6-4-7-5-4-3-6-4-5-3-5-3-5 3-6-4-4-5-5-3-4-6-2-5-4-4-7-6-4 6-3-6-5

Z= 5.Ø Cm

Ø	2Ø	13-14-14-13-13-13-16-15 13-11-12-12-9-14-11-11 9-9-11-9-11-13-14-13-11 13-1Ø-13-11-12-14-13-12 1Ø-9-14	26-28-25-26-27-25-23-25-26-24-27 22-21-23-24-27-24-26-24-23-27-25 23-24-25-26-24-28-23-25-27-23-28 21
4.1	2Ø	9-12-6-1Ø-1Ø-7-11-11-13 14-11-1Ø-11-1Ø-11-9-13 1Ø-11-9-9-11-13-13-9-9 8-9-1Ø-9-12-1Ø-15-13-14 11	22-18-21-2Ø-21-21-26-26-17-19-17 23-22-16-14-2Ø-16-23-18-2Ø-14-21 17-17-25-15-21-2Ø-19-19-19-17-17 18-2Ø
7.9	2Ø	8-6-6-6-5-5-6-1Ø-6-8-6 8-9-6-6-4-1Ø-5-7-5-7-6 5-9-4-6-1Ø-9-6-9-9-6-7	19-14-17-19-17-16-14-13-19-19-12 13-19-14-12-2Ø-14-13-15-12-16-21 19-19-1Ø-18-14-17-13-17-14-15-9
12.Ø	5Ø	6-5-9-8-6-9-7-6-6-6-9 4-6-7-8-5-4-8-6-7-7-4 5-6-3-5-6	1Ø-11-1Ø-1Ø-12-8-8-11-8-12-13-11 9-1Ø-13-8-8-11-1Ø-9-8-11-1Ø-9-8 11-1Ø-9-8-8-1Ø-11
17.1	1ØØ	1Ø-6-5-5-4-4-3-2-5-6 5-4-5-4-8-3-1-4-5-9 4-8-3-3-7-4-5-7-8-3-4	9-5-5-7-3-3-3-1-3-7-4-4-4-7-8-4 1-4-4-8-5-6-1-3-3-3-5-6-7-4-4

Z = 1Ø Cm

Ø	2Ø	7-8-6-8-8-2-8-5-8-1Ø-3 5-4-6-7-5-6-7-6-5-5-5 8-4-6-7-5-8-6-5-6-9-5 4-6-6-9-3-5-6-5-7-4-6 8 4-8-6-7-5-7	14-13-14-2Ø-16-15-14-12-11-13-14 16-9-12-12-13-11-14-14-8-14-16 19-11-15-14-13-14-17-11-12-15-1Ø 13-11-14-13-11-12-11-11-8-15-16 17-12-1Ø-1Ø-12
5.1	2Ø	4-4-6-3-4-5-4-2-8-5-4 3-8-7-6-4-7-4-2-3-4-1 3-2-3-5-2-2-7-5-5-4-9 Ø-1-5-2-6-5-5-2-2-3-2 4-6	1Ø-12-13-1Ø-11-1Ø-14-8-22-11-13 1Ø-12-11-15-9-8-1Ø-11-7-11-11-8 1Ø-8-9-9-1Ø-9-9-18-8-1Ø-11-1Ø-12 7-11-1Ø-6-9-1Ø-9-7-11-9-8
1Ø.1	5Ø	15-5-12-9-3-2-3-3-1Ø 11-6-7-5-4-8-9-7-5-5 2-5-12-4-4-4-3-7-4-5 8-1Ø-7-5-8-7-8-7-3-12 1Ø-2-2-6-9-4	8-7-5-7-9-4-8-9-7-7-9-6-4-6-9-5 4-7-8-8-5-8-5-9-7-9-6-9-5-7-6-1Ø 7-5-5-7-8-5-4-9-7-9-9-8-7-8-9-7-8 6-8-9
15.1	1ØØ	6-Ø-3-5-4-1-6-5-3-8-5 8-5-4-9-6-9-8-6-5-5-7	3-3-5-8-6-2-5-5-6-6-8-8-5-8-7-4 8-7-4-4-4-7-6-4-4-5-3-4-4-3-5-4

continued . . . . .

		3-7-6-8-8-6-5-4-7-3-5 6-6-10-9-3-5-6-7-5-5-4	3-6-6-8-8-4-5-5-5-4-7-4
20.1	100	3-3-4-3-3-3-2-4-2-2-2 5-1-1-0-4-2-0-1-2-4-3 4-1	2-2-2-3-2-1-4-1-2-1-4-5-4-2-2-2- 2-3-3-1-3-2-3-1

FLOW RATE — NOZZLE DIAMETER : 0.12 Cm
= 2.30 NL/Min.
Z = 0.50 Cm

==========

0	10	10-8-11-9-8-9-11-10-9-8-9 11-12-9-8-11-8-8-9-12-8-11 9-12-8-9-9-11-8-9-10-9-9-11 10	45-45-45-46-45-45-45-45-44-45-45 46-46-45-45-45-45-44-45-45-45-45 45-45
1.6	10	8-9-9-8-10-6-9-9-7-8-8-9-6 7-8-9-9-8-7-8	25-26-25-24-21-24-25-27-25-26- 24-25-24-24-26-24-25-24-26-25
3.0	20	8-8-8-8-10-7-8-9-7-8-8-6-9 8-9-7-9-8-9-8	16-13-14-13-18-15-15-16-13-14- 15-16-14-15-18-15-14-13-15-14
4.3	50	4-4-3-4-5-6-2-4-4-4-3-3-6 7-3-4-5-4-3-4	5-2-3-4-3-2-3-1-3-2-2-4-3-2-4-3 5-2-2-3
6.1	100	6-7-7-5-5-4-6-5-3-4-7-5-6-4-6 4-5-7-5-6-4-6-4-5-7-5-6	2-2-2-2-0-1-2-2-2-2-2-0-1-2- 2-0-2-2-2-1

Z =2.0 Cm

0	20	13-13-12-13-12-13-11-14-14-12 12-13-11-14-11-11-12-11-11-13 12-11-13-12-14-11-12-13-11-13 12-12-14-12-13-12-14-11-13	24-21-25-18-19-19-25-22-24-19 19-20-22-21-20-21-25-21-19-18 21-24-22-21-19-21-24-18-20-19 24-21-19-22-24
2.3	20	10-7-9-5-10-9-9-9-9-10-11-7-10 12-6-9-10-12-8-8-8-10-10	18-13-14-15-15-13-18-16-13- 15-12-21-19-19-11-13-11-12- 15-14-17-16-15
4.3	50	13-8-14-10-9-10-8-9-10-7-8-8 10-12-12-10-13-11-12	12-9-10-11-8-6-9-8-7-11-11-9 7-9-8-11-12-8-9
9.2	100	4-6-6-1-0-3-4-5-4-4-7-4-1-5 7-6-5-4-5-5	1-4-1-0-0-2-1-2-2-3-7-4-0-1-3 2-2-2-3-0

Z = 5.0 CM

Ø	2Ø	9-8-6-8-7-9-8-6-6-7-9-7-6-8 8-5-7-6-8-7-9-9-8-6-7-7-8-9 6-1Ø-5	13-16-12-13-1Ø-11-12-17-8-13 16-12-12-12-12-14-12-13-1Ø-12 14-13-14-12-13-12-1Ø-13
3.3	5Ø	14-16-13-17-16-14-16-13-14 15-1Ø-1Ø-12-12-13-16-14-1Ø 13-14	1Ø-1Ø-11-9-1Ø-8-9-11-8-11-8-7 11-8-1Ø-8-11-8-1Ø-8
7.3	5Ø	7-5-4-11-5-11-7-6-8-4-8-3-8 1Ø-11-8-11-2-9-8-7-6-1Ø-8	7-5-4-8-3-8-4-3-3-2-5-3-6-7-6 6-8-3-8-5-5-4-5-4
11.Ø	1ØØ	8-1-9-12-4-2-4-7-5-4-1Ø-7-4 8-6-7-4-8-6-3	4-1-4-3-Ø-Ø-1-1-2-1-4-3-2-4-4 3-2-2-3-1

Z=1Ø.Ø CM

Ø	5Ø	11-4-7-8-8-3-4-6-3-5-46-7-5 5-6-4-5-5-5-5-4-3-6-6-6	9-4-8-7-6-2-3-5-4-7-3-6-7-7-5 5-4-3-5-5-5-7-5-7-5-7
5.3	5Ø	7-3-5-4-4-Ø-8-5-4-7-4-3-6-4 4-1-3-6-7-5-4-5-5-5-4-3-5	7-3-8-4-4-Ø-7-3-3-4-3-2-5-3-1 2-4-3-2-2-4-2-3-3-5-2-2
1Ø.3	1ØØ	6-7-7-8-11-5-3-3-4-8-9-5-6 5-4-5-8-2-5-4-7	4-3-3-2-4-2-1-Ø-1-1-3-4-2-1-2 2-3-2-Ø-2-2-2
17.7	2ØØ	5-4-4-2-6-5-8-7-2-1Ø-2-2-7-1 2-6-3-5-4	Ø.5-1-1-Ø-Ø-Ø-1-1-Ø-2-Ø-1-2 Ø.5-Ø-Ø-Ø-Ø-Ø.5

FLOW RATE=3.25NL/MIN
Z=Ø.5CM

Ø	1Ø	9-7-8-9-8-7-9-9-8-8-7-8-8-9 9-8-9-8-8-9-8-9-8-7-8-9-8-7 8-9-8-7-8-8-9-8-9	46-46-47-46-46-43-46-46-45-46-48 46-47-46-45-47-46-46-47-46-46-45 45-46-46-48-46-46-46-47-45-45-46
1.6	1Ø	6-6-6-6-7-6-7-6-7-7-9-8-8-6 7-8-9-7-8-6-8-6-8-7-8-7-8-7 7-8-6-7-6	28-27-25-26-25-3Ø-27-27-29-29-26 27-26-28-26-26-29-28-26-24-28-27 25-28-25-27-27-24-27-24-28-26-24
3.Ø	2Ø	7-6-8-7-8-7-7-8-8-7-7-7-9-8 6-9-7-9 9-8-7-9-7-8-7-7-8-8 7-8-9-6-7	17-14-16-13-14-15-16-15-15-13-18 15-17-17-15-17-16-2Ø-16-17-13-13 18-17-17-15-16-18-16-16-17-16-17
4.3	5Ø	9-9-8-9-7-9-9-5-8-6-6-9-9-7 6-8-7-9-9-8-6-7-9-8-5-9-8-8 7-7-8-7-9	6-5-4-6-3-4-4-5-4-4-4-8-4-5-6-4 4-6-5-6-5-8-4-5-4-6-5-5-4-6-6-4 4
6.1	1ØØ	5-2-6-5-4-7-3-7-5-2-3-Ø-5-6 4-2-7-4-3-Ø-7-4-3-4-7-5-3-6 4-3-5-3-3	2-1-3-2-1-3-2-3-1-Ø-2-Ø-2-1-3-Ø 2-2-1-3-Ø-3-2-1-2-3-1-1-2-1-3-Ø 1

Z=2.Ø CM

Ø	2Ø	12-11-11-11-11-11-13-1Ø-11 12-9-12-11-1Ø-14-12-1Ø-11 11-1Ø-11-9-13-12-1Ø-11-12 1Ø-11-1Ø-11-1Ø-11	26-22-21-26-23-22-22-25-21-25-24 22-22-21-23-24-25-22-24-23-21-23 21-24-21-24-22-22-22-21-24-21-26
2.3	2Ø	11-7-6-6-1Ø-9-9-1Ø-7-7-6-9 9-7-1Ø-9-9-11-7-9-1Ø-9-9-7	23-18-23-2Ø-18-19-19-2Ø-19-14-19 19-21-19-23-21-19-23-22
4.3	5Ø	9-9-6-9-8-8-9-7-8-7-1Ø-9-1Ø 11-9-8-9-9-8-9-11-9-8	15-16-12-14-13-12-12-11-14-14-16 16-13-14-13-12-13-15-13-12-16-12 14
6.3	5Ø	8-1Ø-8-7-8-7-9-7-8-1Ø-8-7-7	9-12-8-9-9-14-11-1Ø-13-12-9-11-1Ø

continued . . . .

		7-6-8-7-4-8-6-8-8-6	11-11-12-8-6-13-12-11-11-11
9.2	1ØØ	4-5-7-7-3-6-4-9-4-5-4-5-8-5	3-2-6-6-3-5-3-6-2-2-4-5-6-4-2-2-2
		6-5-5-4-4-2-6-	2-2-1-4
		Z=5.Ø CM	
Ø	2Ø	7-9-8-7-9-8-1Ø-6-7-14-9-8-9	15-16-11-14-16-16-16-13-12-16-11-16
		8-8-9-8-11-1Ø-1Ø-8-7-9-11-8	14-15-1514-15-17-13-16-16-14-16-14
		9-7-1Ø-8-9-8-11-9	16-14-14-17-15-13-13-14-13-16
3.3	5Ø	12-8-16-12-14-16-13-11-9-13	11-1Ø-12-1Ø-13-13-12-11-1Ø-11-1Ø-9
		12-14-1Ø-12-1Ø	12-9-11-1Ø
7.3	5Ø	1Ø-7-13-9-8-8-9-8-9-5-12-7	8-7-7-8-9-8-6-7-6-6-1Ø-6-7-7-6-8-1Ø
		9-12-9-1Ø-9-7-8-9	6-6-6
11.Ø	1ØØ	7-1Ø-4-8-8-7-6-8-2-9-1-5	4-3-3-3-2-2-3-5-2-2-1-3-5-2-5
		6-6-8	
		Z = 1Ø CM	
Ø	2Ø	8-1Ø-11-8-5-12-5-8-6-7-8	8-8-7-11-6-1Ø-6-9-6-9-11-7-1Ø-6
		8-11-8-8-1Ø-4-5-6-9-8-12	7-8-7-6-6-8-6-9-7-11-6-8-6-11-7
		7-9-1Ø-9-5-7-8-11-7-8-7	6-8-1Ø-6
5.3	5Ø	9-6-3-6-2-7-5-4-2-4-5-7	7-6-5-7-4-6-7-6-5-3-5-8-5-7-7-8
		5-7-7-6-5-4-4-6	4-3-4-4-6
1Ø.3	1ØØ	9-9-12-9-8-7-8-6-12-6-7	3-5-3-4-3-3-3-2-4-2-3-3-3-2-2.5-
		6-7-6-5-9-5-1Ø-8-6	4-3-4-4-3
17.7	1ØØ	4-5-4-2-3-3-6-5-1-1-Ø-7	2-2-3-2-1-1-2-3.5-1-1-Ø-4-4-1-2
		4-2-4-8-Ø-3-1	3-Ø-2-
		FLOW RATE = 4.6Ø NL/MIN Z = Ø.5 CM	
Ø	1Ø	8-7-8-6-8-8-8-7-8-1Ø-7-8	46-47-45-46-47-47-47-46-47-47
		8-8-9-8-7-8-9-7-	47-45-46-47-47-46-
1.6	1Ø	8-6-7-8-11-12-8-1Ø-9-9-1Ø	26-27-28-26-26-27-27-26-28-28-28
		1Ø-8-9-8-8-9-11-8-7	28-25-28-26-27-28-27-28-26-27
3.Ø	2Ø	9-7-8-8-8-7-8-1Ø-1Ø-1Ø-9	18-17-14-19-2Ø-18-19-17-15-19-16
		8-1Ø-9-9-9-1Ø-9-1Ø-8	22-19-17-18-2Ø-18-17-2Ø-17
4.3	5Ø	8-8-9-8-12-9-6-8-6-8-8-6	1Ø-8-9-7-8-9-8-8-8-7-6-7-8-1Ø-8
		9-1Ø-1Ø-8-9-9-8-9-	7-7-9-8-9
6.1	1ØØ	7-6-8-9-9-8-11-11-11-8-8	5-4-3-3-2-2-3-2-3-2-1-2-3-3-3-3
		8-8-9-8-7-9-8-1Ø-9	1-5-4-3-
		Z=2.Ø CM	
Ø	2Ø	12-12-13-12-13-11-1Ø-13-14	25-27-27-26-29-28-26-26-3Ø-27-26
		14-12-11-12-12-13-11-12-11	3Ø-26-25-29-26-27-25-3Ø-27-26-25
		13-11-12-14-13-12-13-13-12	28-27-3Ø-26-27-26-28-29-27-25-27
		11-14-1Ø-11-13-13	
2.3	2Ø	9-9-11-9-11-1Ø-1Ø-8-8-1Ø-11	22-23-22-23-23-24-25-21-25-23-23
		1Ø-11-9-9-1Ø-11-1Ø-12-11	24-22-23-22-23-23-24-23-24
4.3	5Ø	11-9-11-11-11-14-1Ø-11-13	15-17-14-16-16-16-18-16-14-17-16
		14-1Ø-11-13-9-11-13-1Ø-11	16-14-16-14-15-17-14-16-17
		12-1Ø	
6.3	5Ø	7-6-8-7-7-1Ø-8-8-8-8-9-8-8	12-12-14-14-9-12-9-1Ø-13-9-11-12
		8-9-1Ø-8-7-8-9	13-11-13-12-13-1Ø-11-12

9.2	100	7-9-5-8-5-7-9-7-6-6-4-5-6 7-11-5-7-6-6-7	4-5-4-3-3-5-3-4-2-4-4-5-3-3-6-44 3-5-3

Z= 5.0 CM

0	20	7-9-10-8-9-11-9-11-8-9-11 11-9-6-10-7-8-9-7-9-7-10 9-11-9-11-9-7-7-10-11-8-7	15-19-17-12-16-19-14-16-15-20-18 18-17-15-14-17-14-20-16-17-20-15 17-19-20-17-20-14-14-16-15-13-16
3.3	50	12-12-14-14-17-10-8-13-11 9-14-12-15-12-8-14-15-14 17-12-9-11-13-17-12-13-12 12-14-17-13	14-11-13-11-14-10-9-10-12-11-11 13-11-11-13-11-11-13-12-10-14-13 12-13-11-11-14-13-12-12-11
7.3	50	8-11-10-11-15-11-8-9-12-11 6-11-8-15-12-11-13-9-10-9	10-9-9-9-8-7-9-10-8-8-7-9-8-11-10 9-7-9-10-9
11.0	50	7-8-7-4-6 8-3-4-6-10-6-6 7-4-4-3-7-10-7-5	3-2-4-4-6-3-4-3-5-4-3-5-3-5-4-5 5-4-5-3-5-4

Z= 10.0 CM

0	20	5-4-8-4-4-3-5-5-5-6-7-4-4 5-4-5-4-5-6-7-4-8-4-2-4-6 4-5-4-6-4-5-5	10-11-10-6-8-7-9-10-11-8-13-8-12 11-9-14-9-13-9-11-6-10-8-12-9-11 9-8-10-11-10-11-8
5.3	50	5-5-5-7-8-5-5-4-4-7-7-5-3 5-3-5-6-5-5-6	8-6-6-7-6-5-5-6-8-5-6-7-5-5-6-5 6-6-6-6
10.3	100	7-8-9-7-6-9-11-7-6-5-3-6 6-5-5-6-8-10-9-7	4-3-4-3-5-5-5-3-3-4-4-3-3-3-4-4 4-5-4-4
17.7	100	4-6-2-5-4-3-6-6-5-5-4-4 5-5-3-6-4-4-4-5	2-2-1-3-1-3-2-3-3-3-3-2-2-1-3-3 2-3-2-3

12.2	100	4-3-6-3-5-4-5-5-4-5-3-4-7 5-5-3-4-3-5-7-5-2-7-5-6-5 5-5-3 3-2-3-4	1-2-3-4-0-3-5-3-2-5-2-4-1-2-3 3-0-5-4-4-4-5-3-3-2-4-3-3-3-2 4-2-3
15.3	100	3-2-3-3-2-1-2-4-2-5-2-3-2 7-4-4-6-4-7-3-2-6-3-2-4-2 4-4-5-3-3-3-4	2-0-1-2-1-1-1-2-3-3-0-1-1-3 2-3-2-2-2-3-2-2-1-0-3-2-1-3 1-2-0-1-1

Table 4 : Local Mean Gas Hold-up and Bubble Frequency

System: Air/water
Nozzle Diameter: 0.24 cms.
Gas Injection Rate: 9.32 NL/min.

Z = 0.5 cms

r (mm)	Chart speed ms/div.	Number of waves developed per 10 divisions on oscilloscope screen	Number of divisions for which gas is present at the tip of sensor probe per 50 divisions	Local average bubble frequency ($\bar{f}$)	Local average gas hold-up ($\bar{\varepsilon}$)
1	2	3	4	5	6
0	20	8.4	30.5	42.0	0.61
2.3	20	7.3	23.5	36.5	0.47
5.1	50	10.625	13.35	21.25	0.267
7.5	100	5.65	1.65	5.65	0.03
		Z = 2.0 cms			
0	20	9.53	25.7	47.65	0.514
3.0	20	6.9	20.2	34.5	0.404
6.6	50	7.875	10.5	15.75	0.21
8.6	100	4.63	2.8	4.63	0.056
		Z = 5.0 cms			
0	20	8.4	13.5	42.0	0.27
4.1	50	11.5	11.5	23.0	0.23
8.1	50	3.1	6.56	6.20	0.131
12.1	100	5.2	5.9	5.20	0.118
14.7	100	3.6	2.96	3.60	0.0592
		Z = 10.0 cms			
0	50	6.1	5.74	12.2	0.115
5.1	50	4.775	4.80	9.55	0.096
10.1	100	8.65	3.25	8.65	0.065
15.1	100	6.15	2.80	6.15	0.056
20.1	100	2.68	1.24	2.68	0.0248

Table 4 (Continued):

Gas Injection Rate: 13.20 NL/min.

Z = 0.5 cms.

1	2	3	4	5	6
0	10	8.7	47.4	87.0	0.948
1.0	10	7.75	44.5	77.5	0.89
2.0	10	7.22	30.0	72.2	0.60
4.0	20	7.54	19.6	37.7	0.392
7.0	20	3.228	6.57	16.14	0.131
7.84	20	1.34	2.40	6.70	0.048

Z = 2.0 cms.

0	10	7.9	40.2	79.0	0.804
2	10	6.62	28.97	66.2	0.579
4	20	7.64	19.92	38.2	0.398
7	50	7.975	10.1	15.95	0.202
10	100	4.72	2.8	4.72	0.056

Z = 5.0 cms.

0	10	6.97	23.6	69.7	0.472
2.0	20	10.04	18.37	50.2	0.367
5.0	20	7.45	13.92	37.25	0.278
8.0	20	4.7	10.02	23.5	0.20
11.0	50	7.025	7.52	14.05	0.150
14.0	50	3.45	4.37	6.90	0.0874

Z = 10 cms.

0	20	5.08	12.03	25.4	0.24
2	20	4.7	10.25	23.5	0.205
6	20	3.76	8.38	18.8	0.167
10	50	7.35	6.05	14.7	0.121
14	50	4.475	4.28	8.95	0.0856
18	50	2.70	2.5	5.4	0.05
20	100	3.25	1.85	3.24	0.037

Continued.....

Table 4 (Continued):

Gas Injection Rate: 18.6 NL/min.

Z = 0.5 cm.

1	2	3	4	5	6
0	10	7.65	47.0	76.5	0.94
2.1	10	6.18	43.9	61.8	0.878
4.1	20	10.26	19.9	51.3	0.398
5.8	20	7.25	12.4	36.25	0.248
6.68	20	3.884	6.28	19.42	0.1256
		Z = 2.0 cms.			
0	10	6.32	40.8	63.2	0.816
2.8	20	9.02	26.4	45.1	0.528
6.7	50	8.55	12.5	17.1	0.250
9.3	100	5.2	4.6	5.2	0.092
		Z= 5.0 cms.			
0	20	12.1	24.8	60.5	0.496
4.1	20	10.64	19.0	53.2	0.38
7.9	20	6.64	15.5	33.2	0.31
12.0	50	6.2	9.9	12.4	0.198
17.1	100	4.96	4.5	4.96	0.09
		Z = 10.0 cms.			
0	20	6.06	12.96	30.3	0.26
5.1	20	4.02	9.6	20.1	0.196
10.1	50	6.4	7.1	12.8	0.142
15.1	100	5.5	5.2	5.5	0.104
20.0	100	2.36	2.4	2.36	0.048

Continued.....

Table 4 (Continued):

Nozzle Diameter: 0.12 cms.
Flow Rate: 2.30 NL/min.

Z = 0.5 cms.

1	2	3	4	5	6
0	10	9.5	45	95	0.90
1.6	10	8.0	24.8	80	0.496
3.0	20	8.1	14.7	40.5	0.294
4.3	50	4.125	3.0	8.25	0.06
6.1	100	5.38	1.54	5.38	0.031
		Z = 2.0 cms.			
0	20	12.4	21.0	62.0	0.42
2.3	20	9.04	15.0	45.2	0.30
4.3	50	10.2	9.2	20.4	0.184
9.2	100	4.31	2.0	4.31	0.04
		Z = 5.0 cms.			
0	20	7.16	12.5	35.8	0.25
3.3	50	13.6	9.33	27.3	0.186
7.3	50	2.54	5.08	14.75	0.101
11.0	100	2.25	2.25	5.95	0.045
		Z = 10.0 cms.			
0	50	5.4	5.42	10.8	0.108
5.3	50	4.48	3.37	8.96	0.067
10.3	100	5.68	2.1	5.68	0.042
17.7	200	4.60	0.5	2.30	0.01

Continued.....

Flow Rate = 3.25 NL/min.

Z= 0.5 cm.

1	2	3	4	5	6
0	[illegible]	8.2	4.6	82	0.92
1.6	[illegible]	7.04	25.6	70.4	0.512
3.0	[illegible]	7.58	15.2	37.9	0.304
4.3	[illegible]	7.70	4.8	15.4	0.916
6.1	[illegible]	4.15	1.7	4.15	0.034
		Z = 2.0 cms.			
0	[illegible]	11.0	22.8	55.0	0.456
2.3	[illegible]	8.46	19.9	42.3	0.398
4.3	[illegible]	8.7	13.4	17.4	0.268
6.3	[illegible]	7.475	10.56	14.95	0.211
9.2	[illegible]	5.14	3.7	5.14	0.074
		Z = 5.0 cms.			
0	[illegible]	8.75	14.6	43.75	0.292
3.3	[illegible]	12.10	10.9	24.2	0.218
7.3	[illegible]	8.90	7.2	17.8	0.144
11.0	[illegible]	6.33	3.0	6.33	0.06
		Z = 10 cms.			
0	[illegible]	8.04	7.8	40.2	0.156
5.3	[illegible]	5.4	5.23	10.8	0.104
10.3	[illegible]	8.5	3.7	8.5	0.074
17.7	[illegible]	3.44	1.92	3.44	0.038

Continued.....

Table 4 (Continued):

Flow Rate = 4.60 NL/min.

Z = 0.5cm.

0	10	7.85	46.5	78.5	0.93
1.6	10	8.8	27.0	88.0	0.54
3.0	20	8.82	18.0	44.1	0.36
4.3	50	8.435	8.06	16.87	0.162
6.1	100	8.61	2.84	8.61	0.057

Z= 2.0 cms.

0	20	12.22	24.8	61.1	0.496
2.3	20	9.92	23.1	49.6	0.462
4.3	50	11.25	15.7	22.5	0.314
6.3	50	8.05	11.6	16.1	0.232
9.2	100	6.62	3.8	6.62	0.076

Z = 5.0 cms.

0	20	8.90	16.5	44.5	0.33
3.3	50	11.25	11.8	22.5	0.236
7.3	50	10.5	8.8	21.0	0.176
11.0	50	6.15	4.04	12.3	0.081

Z = 10.0 cms.

0	20	4.88	9.76	24.4	0.195
5.3	50	4.95	6.0	9.9	0.120
10.3	100	7.0	3.83	7.0	0.076
17.7	100	4.5	2.37	4.5	0.047

Continued.....

System: Argon/Mercury
Nozzle Diameter = 0.08 cm.
Gas Injection Rate: 2.0 NL/min.

Z = 0.5 cm.

1	2	3	4	5	6
0	20	3.12	18.0	15.6	0.36
2.8	20	3.00	16.0	15.0	0.32
5.8	50	5.15	12.2	10.3	0.244
11.2	100	3.07	3.15	3.07	0.063

Z = 2.0 cms.

0	50	5.86	9.90	11.72	0.198
4.0	50	5.38	7.63	10.76	0.152
8.2	50	4.21	6.6	8.42	0.132
12.8	100	2.78	2.7	2.78	0.054

Z = 4.0 cms.

0	20	1.98	7.33	9.9	0.146
4.0	20	1.90	5.33	9.5	0.106
8.0	50	3.845	4.84	7.69	0.097
12.0	100	4.1	2.9	4.1	0.058
15.3	200	3.46	1.61	1.73	0.032

Table 5 : Properties of the Plume as a Function of Axial Distance

Experimental variables	Z (mm)	$\bar{\epsilon}_{max}$	$r_{p,\bar{\epsilon}}$ (mm)	$\bar{\epsilon}_{av.}$	$r_{\bar{\epsilon}\ max/2}$	$\bar{f}_{max}$	$r_{p.\bar{f}}$ (mm)	$r_{\bar{f}_{max}}$
System:Air/ water	5	0.61	7.8	0.222	4.5	42	8.5	5.2
d_o=0.24 cm	20	0.514	10.4	0.152	5.4	47.6	9.6	5.0
$\dot{Q}$=9.32 NL/min.	50	0.27	17.4	0.10	8.4	42	15.4	4.4
	100	0.115	26.0	0.0357	12.0	12.2	23.2	15.0
$\dot{Q}$=13.20 NL/min.	5	0.948	8.20	0.262	3.0	87	8.5	3.6
	20	0.804	10.8	0.20	3.9	79	10.2	3.9
	50	0.472	18.4	0.136	6.8	69.7	16.4	4.6
	100	0.24	27.0	0.061	10.0	25.4	23.6	10.0
$\dot{Q}$=18.6 NL/min.	5	0.94	8.4	0.29	3.7	76.5	9.0	5.5
	20	0.816	11.6	0.23	4.3	63.2	10.6	4.7
	50	0.496	20.2	0.199	9.4	60.5	18.2	8.6
	100	0.26	27.6	0.0787	11.0	30.3	24.0	8.4
d_o = 0.12 cm.	5	0.90	5.0	0.215	1.9	95	7.2	2.6
$\dot{Q}$ = 2.30 NL/min.	20	0.42	11.0	0.096	3.8	62	9.8	3.4
	50	0.25	14.2	0.0486	6.0	35.8	12.8	6.2
	100	0.108	20.0	0.0386	9.0	10.8	22.2	11.0
$\dot{Q}$ = 3.25 NL/min.	5	0.92	5.4	0.254	2.0	82	6.6	3.0
	20	0.456	11.5	0.144	5.2	55	10.2	3.4
	50	0.292	15.0	0.081	6.6	43.7	13.2	6.2
	100	0.156	22.4	0.063	9.0	40.2	22.4	7.0

Table 5 (Continued):

Experimental variables	Z (mm)	$\bar{\epsilon}_{max}$	$r_{p,\bar{\epsilon}}$ (mm)	$\bar{\epsilon}_{av.}$	$r_{\bar{\epsilon}\ max/2}$	$\bar{f}_{max}$	$r_{p,\bar{f}}$ (mm)	$r_{\bar{f}_{max}}$
Q=4.60 NL/min.	5	0.93	5.8	0.306	2.1	78.5	7.6	3.0
	20	0.496	12.2	0.185	5.6	61.1	10.4	3.8
	50	0.33	17.2	0.1047	7.2	44.5	15.2	5.8
	100	0.195	24.0	0.080	8.6	24.4	22.6	5.4
System:	5	0.36	12.8	-	8.0	15.5	-	7.8
Argon/ Mercury								
d_o=0.08 cm.	20	0.198	15.2	-	10.8	11.8	-	10.4
$\dot{Q}$ =2.0 NL/min.	40	0.146	18.0	-	11.0	10.0	-	11.2

Table 6. The Calculated Values of u_g, u_B, u_l and V_l

System: Air/water

Experimental variables	Z (mm)	u_g (m/sec)	u_B (m/sec)	u_l (m/sec)	$V_l \times 10^{-3}$ (m^3/sec)	$V_l' \times 10^{-3}$ (m^3/sec)
d_o=0.12 cm	5	1.87	0.44	1.30	0.0969	0.0863
$\dot{Q}$ = 2.30 NL/min.	20	1.22	0.335	0.85	0.251	0.199
	50	1.0866	0.281	0.791	0.546	0.342
	100	0.79	0.25	0.53	0.64	0.49
d_o=0.12 cm	5	1.737	0.448	1.135	0.1039	0.1154
$\dot{Q}$ =3.25 NL/min.	20	0.946	0.346	0.541	0.184	0.256
	50	0.78	0.293	0.461	0.362	0.4215
	100	0.565	0.258	0.289	0.411	0.635
d_o=0.12 cm.	5	1.725	0.466	1.052	0.1060	0.145
$\dot{Q}$ =460 NL/min.	20	0.961	0.363	0.47	0.173	0.314
	50	0.761	0.31	0.414	0.356	0.524
	100	0.53	0.268	0.238	0.396	0.8047

Continued.....

Table 6 : (Continued):

Experimental variables	Z (mm)	u_g (m/sec)	u_B (m/sec)	u_l (m/sec)	$V_l \times 10^{-3}$ (m^3/sec)	$V'_l \times 10^{-3}$ (m^3/sec)
d_o=0.24 cm.	5	4.3	0.53	3.61	0.457	0.199
$\dot{Q}$ =9.32 NL/min.	20	2.6	0.43	2.08	0.695	0.36
	50	1.65	0.36	1.25	1.057	0.656
	100	2.00	0.30	1.681	3.45	1.139
d_o=0.24 cm	5	4.17	0.548	3.42	0.507	0.259
$\dot{Q}$ =13.2 NL/min.	20	2.35	0.455	1.781	0.66	0.459
	50	1.55	0.381	1.108	0.99	0.79
	100	1.57	0.321	1.228	2.64	1.349
d_o=0.24 cm	5	4.7	0.575	3.89	0.626	0.28
$\dot{Q}$ = 18.6 NL/min.	20	2.53	0.477	1.91	0.78	0.50
	50	1.377	0.404	0.87	0.79	0.84
	100	1.634	0.342	1.26	2.79	1.397